

DUKE POWER COMPANY
OCONEE NUCLEAR STATION
RELOAD DESIGN METHODOLOGY

Technical Report

NFS-1001A

DECEMBER 1999

REVISION 5

Abstract

This Technical Report describes Duke Power Company's Reload Design Methodology for the Oconee Nuclear Station. Included in this report are descriptions of Fuel Design, Fuel Cycle Design, Fuel Mechanical Performance, Maneuvering Analysis, Thermal-Hydraulic Design, Technical Specifications Review and Development, Accident Analysis Review, and the Development of Core Physics Parameters. Where significant portions of these descriptions are provided in other NRC approved reports, the descriptions have been incorporated by reference.

Table of Contents

1. Introduction
2. Fuel and Core Component Design
 - 2.1 Fuel Design
 - 2.2 Core Component Design
3. Fuel Cycle Design
 - 3.1 Preliminary Fuel Cycle Design
 - 3.1.1 Overview of Nuclear Calculation System
 - 3.1.2 Calculations and Results of PFCD
 - 3.2 Final Fuel Cycle Design
 - 3.2.1 Fuel Shuffle Optimization and Cycle Depletion
 - 3.2.2 Rod Worth Calculations
 - 3.2.3 Power Distribution Calculations
 - 3.2.4 Fuel Burnup Calculations
 - 3.2.5 Reactivity Coefficients and Deficits
 - 3.2.6 Boron Related Parameters
 - 3.2.7 Xenon Worth
 - 3.2.8 Kinetics Parameters
4. Fuel Rod Mechanical and Thermal Performance Analysis
5. Maneuvering Analysis
 - 5.1 Fuel Cycle Depletion
 - 5.2 Power Maneuver
 - 5.3 Control Rod Scans
 - 5.4 Margin Analysis
6. Thermal-Hydraulic Analysis
7. Technical Specifications Review and Development
 - 7.1 Technical Specifications Review
 - 7.2 Development of Core Safety Limits
 - 7.2.1 Determination of Core Safety P-T Limits
 - 7.2.2 Determination of Core Power-Power Imbalance Limits
 - 7.3 Development of Limiting Safety System Settings
 - 7.3.1 Determination of RPS P-T Trip Setpoints
 - 7.3.2 Determination of RPS Power-Flow-Imbalance Trip Setpoints
 - 7.4 Development of Limiting Conditions for Operation
 - 7.4.1 Determination of LOCA-Limited Power Distribution Limits
 - 7.4.2 Determination of Control Rod Position Limits Based on Shutdown Margin Criterion

7.4.3 Determination of Control Rod Position Limits Based on Ejected Rod Worth Criterion

- 8. Accident Analysis Review
 - 8.1 Introduction
 - 8.2 Overview of Accident Analysis Review

- 9. Development of Core Physics Parameters
 - 9.1 Startup Test Predictions
 - 9.1.1 Critical Boron Concentrations and Boron Worths
 - 9.1.2 Xenon Worths
 - 9.1.3 Rod Worths
 - 9.1.4 Reactivity Coefficients
 - 9.1.5 Power Distributions
 - 9.1.6 Kinetics Parameters
 - 9.2 Physics Test Manual

- 10. References

- Appendix A Deleted

- Appendix B List of Revisions

- Amendment 1 Responses to Requests for Additional Information

- Amendment 2 NRC Safety Evaluation Report

- Supplement 1 Deleted

- Supplement 2 Deleted

List of Tables

7-1 Reactor Protection System Trip Functions (Typical Values)

List of Figures

- 1-1 Relationship of Reload Methodology Topical Reports
- 1-2 Elements of Reload Design
- 7-1 Steady State Pressure Temperature Core Protective Safety Limit
- 7-2 Margin to Center Fuel Melt/Clad Strain LHR Versus Core Offset
- 7-3 Core Protective Safety Limits
- 7-4 Determination of RPS P-T Trip Setpoints
- 7-5 Protective System Maximum Allowable Setpoints
- 7-6 Rod Position Limits for 4 Pump Operation
- 7-7 Power Imbalance Limits for 4 Pump Operation
- 7-8 Part Length Rod Position Limits
- 8-1 Accident Analysis Review Process

1. Introduction

The design of a commercial light water reactor is such that the reactor core is loaded with a specified number of fuel assemblies which are generally identical in design but different in the amount of fissile material content. In the initial core the fuel assemblies differ in the initial enrichment of the fuel, and in subsequent fuel cycles they differ in the amount of the burnup of the fuel as well. The refueling of a reactor consists of removing part of the core (a certain number of irradiated fuel assemblies, the number and identity of which are determined by a fuel management scheme) and loading an equal number of fresh and possibly previously burned fuel assemblies called the "reload batch". In general, after refueling the neutronic, thermal-hydraulic, safety, and operating parameters of the core would be different from the previous fuel cycle. The design analyses required to determine the mechanical design, enrichment and number of assemblies of the reload batch as well as the core loading pattern, the nuclear and thermal-hydraulic characteristics of the reloaded core, and the safety analyses demonstrating the safe operation of the reloaded reactor is called reload design.

This report describes the various aspects of the reload design. In the following paragraphs, a brief overview of the major elements of the reload design process and the reload design criteria are provided. Subsequent sections provide detailed discussion including descriptions of design methods, analytical formulation, and calculation procedures of the major reload design tasks used for Oconee reload design. Where other approved reports provide these descriptions they have been incorporated by reference. Figure 1-1 provides a pictorial relationship of referenced topical reports to the overall reload design methodology.

The reload design is essentially a series of analytical exercises with the objective to design the reload core in such a manner that the reactor can be operated to a specified power level for a specified number of days within the acceptable safety criteria. It consists of the development of the basic specifications of the reload batch (mechanical characteristics of the fuel assembly, fuel, rod and associated structures, fuel enrichment, pellet dimensions, shape and enrichment, fuel stack length, fill gas pressure, number of assemblies, uranium loading, etc.). It sets forth the number and identity of each residual fuel assembly, selects the location of each fuel assembly and control rod in the core for the new fuel cycle, establishes the core characteristics, operating limits, and protection system setpoints. It also demonstrates that the operation of the reactor during the new fuel cycle will be within safety considerations already evaluated and approved or provides new safety analyses to demonstrate conformance to applicable safety criteria.

In arriving at the final reload design, the designer tries to meet the requirements imposed by the operational considerations, fuel economics considerations and safety considerations. These requirements are called reload design criteria and are as follows:

1. The mechanical design of the reload fuel will be compatible with the residual fuel.
2. Initial core excess reactivity will be sufficient to enable operation for the desired length of the cycle including any planned power coastdowns.
3. The fuel assemblies to be discharged at the end of the fuel cycle will attain optimum burnup so that maximum energy extraction consistent with the fuel mechanical integrity criteria is achieved.
4. Values of important core parameters (moderator temperature coefficient, Doppler coefficient, ejected rod worth, boron worth, total control rod group worth, maximum linear heat rate of the fuel pin at various elevations in the core, and shutdown margin) are predicted to be conservative with respect to the values assumed in the safety analysis of various postulated accidents. Where they are not conservative acceptable reanalysis of applicable accidents is performed.
5. Fuel management will produce fuel rod powers and burnups that do not exceed the mechanical and thermal-hydraulic criteria.
6. The power distributions within the reactor core for all permissible core conditions that could exist during the operation of the cycle will not exceed the thermal design criteria of the fuel nor the LOCA limited peak linear heat rates.
7. Technical Specification limits of specified core parameters and of core protection system trip setpoints after allowance for appropriate measurement tolerances should have adequate margin from nominal values of these parameters during operational conditions throughout the cycle such that sufficient operating flexibility is retained for the fuel cycle.

The reload design process is comprised of the coordinated effort of designers and analysts from many areas, each of which generates specified information in a sequential and sometimes iterative manner to develop the final reload design, meeting the design criteria. The major elements of the reload design process may include (1) fuel design, (2) fuel cycle design, (3) fuel mechanical performance analysis, (4) maneuvering analysis, (5) thermal-hydraulic analysis, (6) safety analysis, (7) Core Operating Limits Report (COLR) and Technical Specification development, (8) reload report development, and (9) generation of core physics parameters.

The fuel design element includes the following activities: (1) specifying the fuel design to be supplied by the vendor, and (2) communicating fuel design changes to appropriate groups.

The fuel cycle design establishes the number and enrichment of the reload batch fuel assemblies, specifies the number and identity of residual fuel assemblies, and determines the arrangement (location and orientation) of the fuel assemblies and the locations of control rods and their grouping in such a manner that the specified criterion on energy production and certain specified criteria on fuel burnup, power distribution and control rod worth requirements are satisfied.

Fuel mechanical analyses include: internal fuel rod pressure, clad collapse, clad strain, clad stress, clad corrosion, and centerline fuel melt. NRC approved methods are used to perform these analyses. Depending on the available margin, these analyses are performed on either a generic or cycle specific basis. To verify the applicability of these analyses, the analysis assumptions are compared to the fuel design and power history for the core design.

The maneuvering analysis involves detailed power distribution evaluation in three dimensions by simulating various anticipated and postulated design conditions and is performed to confirm that the fuel cycle design provides adequate protection to safety limits. The data generated in the maneuvering analysis are used to confirm that the power distributions are acceptable with respect to thermal limits, given permissible assumptions on control rod position, axial imbalance, and Xenon distribution.

Thermal-hydraulic analyses establish the maximum permissible power distributions for various coolant flows, coolant temperatures, and core pressures. The maneuvering analysis uses these power distributions to ensure that the plant operating limits are set to maintain the required DNB margin. These analyses are based on NRC approved methods. Depending on the available margin, these analyses are performed on a generic or specific basis. The analysis assumptions are compared to cycle design parameters to verify the applicability of the thermal-hydraulic analyses.

The accident analyses are reviewed to ensure that important core safety parameters predicted for the reload cycle are bounded by the values used in the existing accident analysis, and where necessary, appropriate accidents are reanalyzed.

The results of the maneuvering analysis in conjunction with the results of thermal and thermal-hydraulic analyses, as appropriate, are used to generate the cycle specific Core Operating Limits Report. These analyses are also used to either confirm that the existing Technical Specifications continue to be valid for the reload cycle or to generate new Technical Specifications limits.

The next phase of the reload design is the integration and documentation of the results of previous phases into a report called the reload report. This report is generated whenever the reload design results in proposed Technical Specification changes. It includes a description of the reload core, the fuel design, results of nuclear, thermal, thermal-hydraulic, and fuel mechanical analysis, and a review of the accident analysis.

A number of physics parameters pertinent to the reload cycle are calculated to confirm that important core parameters for the reload cycle are bounded by the values used in the accident analyses. Other physics parameters are calculated to ensure that the limits utilized in the maneuvering analysis are applicable. Finally, others are calculated to enable an orderly and safe startup of the cycle, to perform startup testing, and to perform core follow calculations. The calculations performed to support startup and operation of the plant typically form the last step in the reload design process.

In the following sections each of the major phases of the reload design process is discussed in more detail. Figure 1-2 shows a flow chart of the various phases.

Figure 1-1

Relationship of Reload Methodology Topical Reports

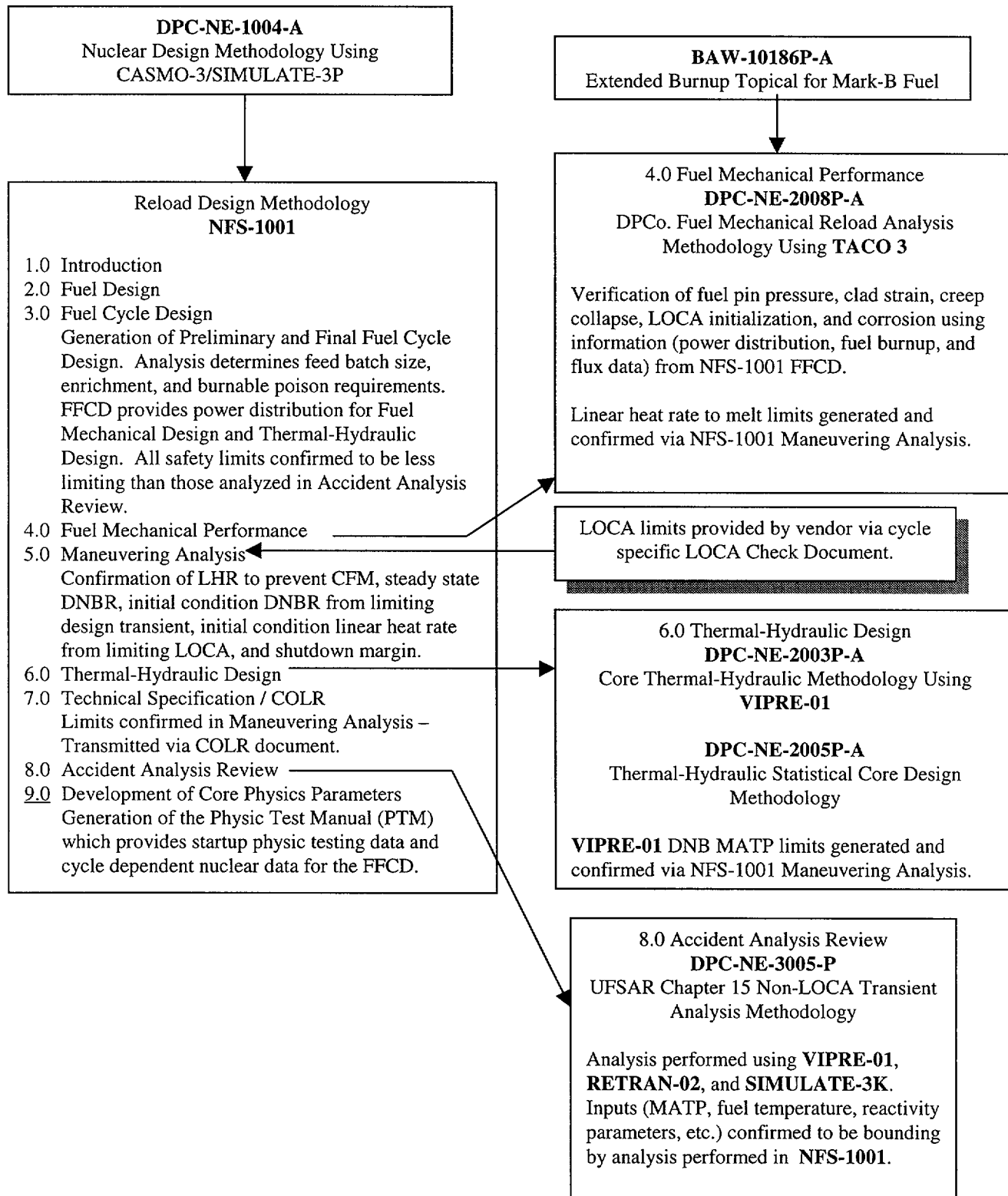
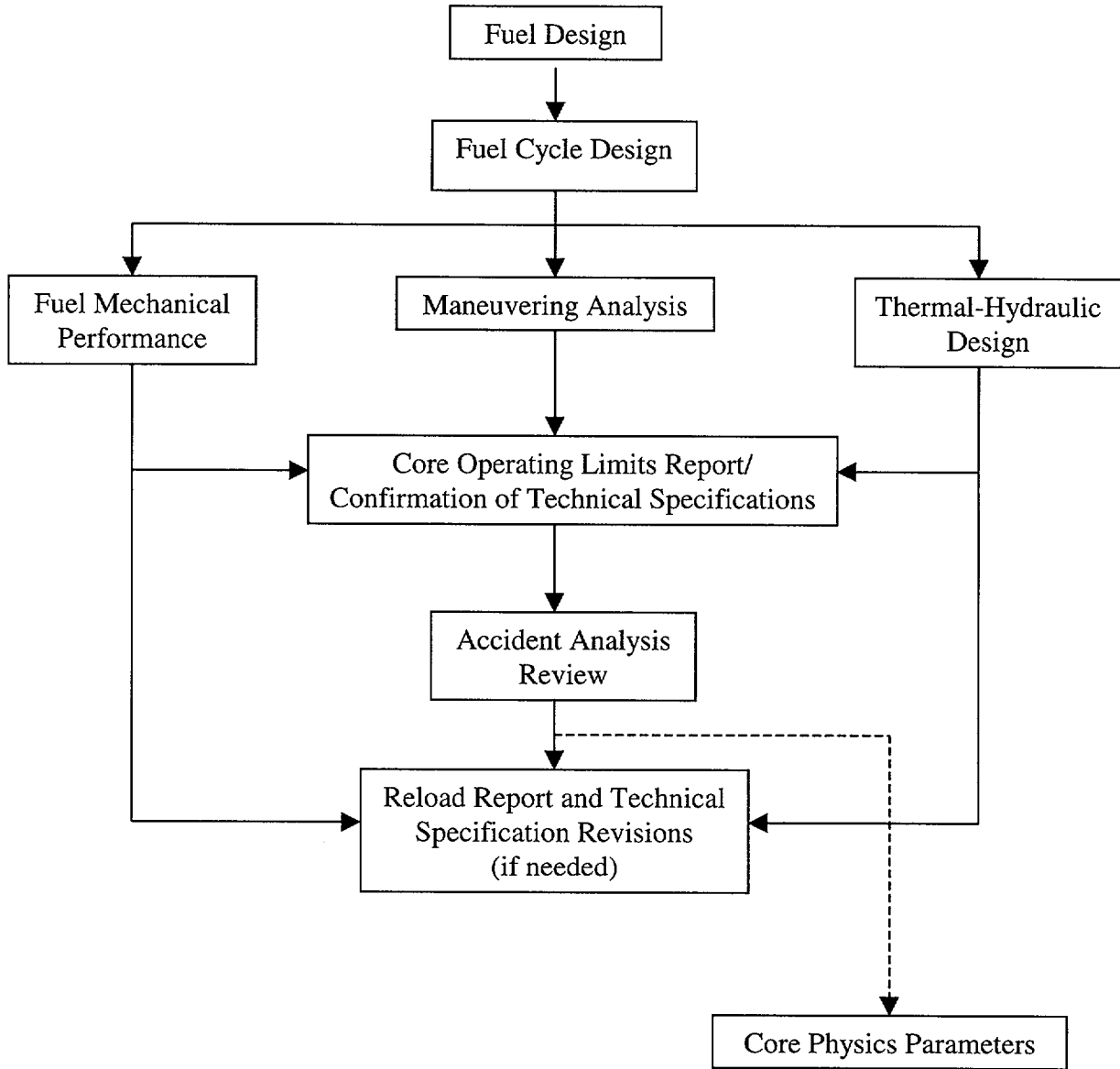


Figure 1-2

Elements of Reload Design



2. Fuel and Core Component Design

2.1 Fuel Design

Fuel designs are consistent with Technical Specification 4.2.1. The fuel designs are described in Chapter 4.0 of the Updated Final Safety Analysis Report (UFSAR, Reference 1).

2.2 Core Component Design

Core Component designs are consistent with Technical Specification 4.2.2. The component designs are described in Chapter 4.0 of the UFSAR.

3. Fuel Cycle Design

3.1 Preliminary Fuel Cycle Design

The purpose of the preliminary fuel cycle design (PFCD) is to determine the number and enrichment of the fresh and possibly burned assemblies to be inserted during the next refueling. A preliminary fuel shuffling scheme is developed and check calculations on certain key parameters are performed.

The input required for the PFCD consists of general ground rules and design bases developed from cycle energy, contract, and operating requirements. The output of the PFCD is the number and enrichment of the feed assemblies.

3.1.1 Overview of Nuclear Calculation System

The nuclear calculation system enables the nuclear designer to numerically model and simulate the nuclear reactor core. The current system in use at Duke Power is described in Reference 2. Additional detail or flexibility may be added to the model, provided the uncertainties specified in Reference 2 are demonstrated to remain conservative.

3.1.2 Calculations and Results of PFCD

Once the calculation models are prepared for the cycle of interest, the nuclear designer chooses a feed enrichment, number of assemblies, and preliminary loading pattern for the reload core. Calculations are performed to verify cycle lifetime and power peaking. The process is iterated until the number and enrichment of feed assemblies as well as a preliminary shuffle scheme has been determined which yield the desired cycle lifetime and a reasonable power distribution.

The preliminary number and enrichment of the feed assemblies must typically be determined eighteen months prior to reactor shutdown for refueling to assure that an adequate quantity of separative work is available. Changes to these preliminary estimates are normally possible up to twelve months prior to reactor shutdown. It is necessary that the results of the PFCD be complete in time to support the fuel order.

3.2 Final Fuel Cycle Design

Having determined the preliminary number and enrichment of the fuel assemblies during the PFCD, the final fuel cycle design (FFCD) concentrates on optimizing the placement of fresh and burned assemblies, control rod groupings, and burnable poison assemblies (if any) to result in an acceptable fuel cycle design. If not already performed during the PFCD, cladding corrosion calculations are performed to ensure licensing limits are met (References 7 and 8). The fuel cycle design is finalized based upon design criteria intended to ensure that the results of the subsequent calculations

are acceptable. If unacceptable results are obtained, the fuel cycle design may be revised to obtain a design that produces acceptable results. When appropriate, the calculations performed to support the PFCD are incorporated into the FFCD.

During the reload design process, nuclear calculations are performed to generate physics parameters as needed for input to fuel mechanical performance, thermal and thermal-hydraulic performance, maneuvering analysis, and accidents and transients analyzed during the safety analysis. The fuel cycle design must meet all design criteria with appropriate reductions to account for calculation uncertainties.

3.2.1 Fuel Shuffle Optimization and Cycle Depletion

Beginning of cycle (BOC) power distribution calculations are performed starting with the fuel shuffle scheme developed in the PFCD and modifying that scheme in an attempt to minimize the power peaking. This is accomplished by either an automated search, or a trial and error type search, until an acceptable BOC power distribution results. The cycle is then typically depleted using steps corresponding to 0, 4, 12, 25, 50, 100, 150...EFPD to verify that power peaking versus burnup remains acceptable. The shuffling variations may include re-arranging the location of the burned and fresh fuel assemblies, groupings of control rods (groups 5, 6, 7) and rotation of the spent fuel assemblies. These calculations are typically performed assuming quarter core symmetry.

The shuffle pattern determined by optimizing the power distribution may later need to be modified based upon results obtained in the remaining nuclear calculations.

3.2.2 Rod Worth Calculations

Control rods serve several functions in the Oconee reactor. The primary function is to provide adequate shutdown capability during normal and accident conditions. They are also used to maintain criticality during power maneuvers and to compensate for reactivity loss due to fuel depletion. Since the presence of control rods influences both power distributions and criticality, it is necessary in many calculations to evaluate not only the reactivity effect but also the perturbation that a given rod configuration has on the power distribution.

Oconee is typically designed and operated in a "all rods out" (feed and bleed) mode. In this mode the majority of the cycle is depleted with control rod groups 1-6 fully withdrawn and group 7 inserted enough to provide reactivity and imbalance control.

Most calculations of control rod worth are used in the safety analysis of the reload core. The calculations discussed in subsequent sections include the following :

1. Choice of Control Rod Groupings and Worths
2. Shutdown Margin

3. Ejected Rod Worth
4. Dropped Rod Worth

3.2.2.1 Control Rod Groupings and Worths

Control rod locations in Oconee are fixed, however, the rods in a particular group may vary from cycle to cycle. The control rod groupings are determined by nuclear calculations to evaluate the effects that a particular ejected rod grouping has on power distribution, group worth, dropped rod worth, and ejected rod worth. The worth of each regulating bank (5, 6, 7) is calculated as needed to verify the values utilized in the applicable accident analyses. The total rod worth (all rods in less the worst stuck rod) is used in the shutdown margin calculation.

The groupings chosen during the FFCD are confirmed during the maneuvering analysis.

3.2.2.2 Shutdown Margin

Shutdown margin calculations are performed as described in Reference 3. Additionally, conservatism is applied to these calculations to account for control rod poison depletion and a 10% calculated rod worth uncertainty. These calculations are performed to verify all Technical Specification requirements and accident analyses input assumptions are valid for the particular fuel cycle design. If the shutdown margin is inadequate, rod position limits are adjusted, a new control rod grouping is developed, or the fuel cycle design is revised.

3.2.2.3 Ejected Rod Worth

Ejected rod worth calculations are performed as described in Reference 3. Additionally, conservatism is applied to these calculations to account for a 15% calculated rod worth uncertainty. These calculations are performed to verify all Technical Specification requirements and accident analyses input assumptions are valid for the particular fuel cycle design. If the ejected rod worth exceeds the limit, rod position limits are adjusted, a new control rod grouping is developed, or the fuel cycle design is revised.

3.2.2.4 Dropped Rod

Dropped rod worth calculations are performed as described in Reference 3. Additionally, conservatism is applied to these calculations to account for a 15% calculated rod worth uncertainty. These calculations are performed to verify all Technical Specification requirements and accident analyses input assumptions are valid for the particular fuel cycle design. If the dropped rod worth exceeds the limit, rod position limits are adjusted, a new control rod grouping is developed, or the fuel cycle design is revised.

3.2.3 Power Distribution Calculations

For Oconee, emphasis in the FFCD is on radial power distributions both on an assembly and local rod basis. Power distributions are calculated using the calculation methods described in Reference 2. Thermal and thermal-hydraulic analyses have been performed on the Oconee reactors which indicate typical radial pin peaks that will result in acceptable DNB and Center Fuel Melt (CFM) margins. These margins are calculated and confirmed during the maneuvering analyses as described in Section 5.

3.2.4 Fuel Burnup Calculations

Current design criteria include limitations on fuel burnup. These limitations may be required as a result of calculations of internal fuel rod pressure, fuel rod growth, cladding corrosion, or licensing limitations. Fuel burnup calculations are performed using the calculation methods described in Reference 2. Both assembly average and local fuel rod burnups may be calculated using these methods.

3.2.5 Reactivity Coefficients and Deficits

Reactivity coefficients define the reactivity insertion for small changes in reactor parameters such as moderator temperature, fuel temperature, and power level. These parameters are input to safety analysis and used in modeling the reactor response during accidents and transients. Whereas reactivity coefficients represent reactivity effects over small changes in reactor parameters, reactivity deficits usually apply to reactivity inserted from larger changes typical of HFP to HZP. An example of a reactivity deficit is the power deficit from HFP to HZP. A different way of looking at the terms is that the coefficient when integrated over a given range yields the deficit, or the coefficient is the partial derivative of reactivity with respect to one specific parameter.

Typically, a nominal case is established at some reference condition. Then one parameter of interest is varied up and/or down by a fixed amount in another calculation and the resulting change in core reactivity divided by the parameter change yields the reactivity coefficient.

3.2.5.1 Doppler Coefficient

The Doppler Coefficient or Fuel Temperature Coefficient (FTC) is the change in core reactivity produced by a small change in fuel temperature. The major component of the Doppler coefficient arises from the behavior of the Uranium-238 and Plutonium-240 resonance absorption cross sections. As the fuel temperature increases, the resonances broaden increasing the chance that a neutron will be absorbed and thus decreasing the core reactivity.

3.2.5.2 Moderator Temperature Coefficient

The Moderator Temperature Coefficient (MTC) is the change in reactivity produced by a small change in moderator temperature. In Oconee the average core moderator temperature is increased as power is escalated from 0 to 15% HFP. At and above 15% HFP the average moderator temperature is held constant at 580 °F. However, for accident and transient analyses it is necessary to know the moderator temperature coefficient at HFP and also at HZP.

3.2.5.3 Temperature Coefficient

The fractional change in reactivity due to a small change in core temperatures is defined as the core temperature coefficient of reactivity. This is equal to the sum of the moderator and Doppler temperature coefficients and may be explicitly calculated at HZP for isothermal conditions (TFUEL = TMOD) by varying both the fuel and moderator temperatures from the average moderator temperature at HZP. Similarly the temperature coefficient at HFP may be explicitly calculated by varying the moderator and fuel temperatures from their averages at HFP.

3.2.5.4 Power Coefficient and Power Deficit

The power coefficient of reactivity is the core reactivity change resulting from an incremental change in core power level. The power deficit is usually the total reactivity change associated with a power level change from HZP to HFP.

The power coefficient is defined by the following equation:

$$\alpha_p = \frac{k_{\text{eff}}^1 - k_{\text{eff}}^2}{P_1 - P_2} \cdot \frac{k_{\text{eff}}^1 * k_{\text{eff}}^2}{k_{\text{eff}}^1 - k_{\text{eff}}^2}$$

where : k^1 is k effective for the core at power P_1 (%)

k^2 is k effective for the core at power P_2 (%).

Neglecting second order effects this equation is equivalent to the following :

$$\alpha_p = \text{MTC} \frac{\Delta\text{TMOD}}{\Delta P} + \text{FTC} \frac{\Delta\text{TFUEL}}{\Delta P}$$

where MTC is the moderator temperature coefficient and FTC is the fuel temperature coefficient (Doppler coefficient).

In Oconee the core average moderator temperature is constant at approximately 580 °F above 15% HFP. Therefore, for power levels above 15% HFP the power coefficient can be reduced to just the fuel temperature contribution or

$$\alpha_p = \text{FTC} \frac{\Delta T_{\text{FUEL}}}{\Delta P}$$

Since the power coefficient should include flux redistribution effects resulting from axial variations in burnup and isotopics as well as non-uniform fuel temperature distributions it should be performed using a 3-D simulator with thermal-hydraulic feedback.

A typical power coefficient calculation for HFP would proceed in the following manner. The HFP case is run and the core k-effective is calculated (k_{eff}^1). Then a second is run with the core power level reduced 5% while holding everything else constant. The k-effective from this case (k_{eff}^2), along with the results from the reference case are used to calculate the power coefficient :

$$\alpha_p = \frac{k_{\text{eff}}^1 - k_{\text{eff}}^2}{k_{\text{eff}}^1 * k_{\text{eff}}^2} = \frac{\Delta \rho}{\% \text{ Power}}$$

The power deficit may be used in the shutdown margin calculation (see Section 3.2.2.2) and is the reactivity change from HZP to HFP. This calculation should be performed in three dimensions to satisfactorily model the axial flux redistribution. These calculations are usually performed at least two times during the cycle burnup.

The HFP and HZP cases typically should have the equilibrium xenon concentration corresponding to HFP. The power deficit is calculated from the following equation :

$$\text{Power Deficit} = \frac{k_{\text{eff}}^1 - k_{\text{eff}}^2}{k_{\text{eff}}^1 * k_{\text{eff}}^2} * 100 = \% \Delta \rho$$

where k_{eff}^1 is core k-effective at HZP and k_{eff}^2 is core k-effective at HFP.

3.2.5.5 Miscellaneous Coefficients

For reload design, certain coefficients of reactivity may not be routinely calculated. These include moderator density coefficient, moderator pressure coefficient, and moderator void coefficient.

3.2.6 Boron Related Parameters

Critical boron concentrations are calculated at a variety of conditions as described in Reference 3.

3.2.7 Xenon Worth

The HFP equilibrium xenon worth may be calculated at BOC (4 EFPD) and at EOC. These values are compared to previous cycle values when a reload report is generated.

Calculations are performed for HFP equilibrium xenon conditions and for no xenon conditions. The difference in reactivities between the equilibrium and no xenon cases is the xenon worth.

3.2.8 Kinetics Parameters

The kinetics behavior of the nuclear reactor is often described in terms of solutions to the Inhour equation for six effective groups of delayed neutrons. Transient and accident analyses often involve kinetic modeling of the reactor core. The rate of change in power from a given reactivity insertion can be calculated by solving the kinetics equations if the six group effective delayed neutron fractions, the six group precursor decay constants, and the prompt neutron lifetime are known.

The computer codes used to calculate these parameters are described in references 2 and 3. This information is needed for validation of the accident analyses and startup physics testing. The sum of the six group β^I -effective, β -effective, for the new reload cycle is compared to that of the previous cycle when a reload report is generated.

4. Fuel Rod Mechanical and Thermal Performance Analysis

The methods for analyzing fuel rod internal pressure, centerline fuel melt, clad strain, and cladding creep collapse are contained in DPC-NE-2008P-A (Reference 4). The methods for analyzing clad stress and fatigue are consistent with the Framatome Cogema Fuels (FCF) methodology of BAW-10186P-A (Reference 7), as identified via letter to the NRC (Reference 9). The method for analyzing clad corrosion is also consistent with the FCF methodology of BAW-10186P-A (Reference 7), as identified via letter from the NRC (Reference 8).

5. Maneuvering Analysis

The purpose of a maneuvering analysis is to generate three-dimensional power distributions and imbalances for a variety of rod positions, xenon distributions, and power levels. The maneuvering analysis can be divided into four discrete phases. The first is the fuel cycle depletion performed to establish a nominal fuel depletion history. The second step is the performance of various power maneuvers that conservatively characterize the effect of maldistributed xenon on the power distribution. The third phase is to perform control rod and Axial Power Shaping Rod (APSR) scans at the most severe times during the power transient. Each of these phases involves the running of multiple cases and generating three-dimensional power distributions, rod positions, and imbalance for each case. Finally, this data is processed by computer programs which calculate CFM, clad strain, DNBR, and LOCA margin to be used to set COLR (see Section 7) limits on rod position, axial offset versus power level, and reactor protective system setpoints.

5.1 Fuel Cycle Depletion

If appropriate restart files from the cycle depletion performed during the FFCD are not available, then the fuel cycle depletion is performed as the first step of the maneuvering analysis. The depletion is typically performed in steps of 0, 4, 12, 25, 50, 100, 150 ... EFPD. The xenon, power, and exposure data for these cases are saved for use in later analyses.

5.2 Power Maneuver

The effect of non-equilibrium xenon conditions on the power distribution is quantified by modeling various bounding power maneuvers. These power maneuvers are initiated from the most limiting cycle burnups determined based on the nominal cycle depletion. In general, the power maneuvers selected produce three-dimensional xenon distributions which result in a variety of core axial offset conditions. These xenon distributions are saved for use as input to the control rod scan cases explained below.

5.3 Control Rod Scans

A sequence of cases which are used to model various limiting combinations of full and part length control rod positions are referred to as control rod scans. A set of control rod scans is performed at a variety of xenon conditions from the power maneuvers and/or nominal depletion to evaluate the combined effect of limiting burnup, severely maldistributed xenon, and mispositioned control rods on power peaking. Three-dimensional power and exposure data for each case are saved for input to the calculation of margin to CFM, clad strain, DNB, and LOCA limits.

5.4 Margin Analysis

Each three-dimensional power distribution is converted into four margin distributions. Margin is defined as the percent difference between the predicted power and the value of power at the design criteria limits. The design criteria are CFM, clad strain, steady-state DNB, transient DNB initial conditions, and LOCA initial conditions. The minimum margin and core power axial offset are determined for each margin distribution.

A file is saved which relates each minimum margin and core offset to the appropriate control rod positions and power level. This data is used to develop the relationship between the margin to a design criterion, core offset, control rod position, and power level. These relationships are used to determine the limits on core offset and control rod position that are required to preserve the various design criteria.

6. Thermal-Hydraulic Analysis

Thermal-Hydraulic analyses are performed to establish maximum permissible power distribution limits to maintain the required margin to Departure from Nucleate Boiling at various coolant flows, temperatures, and pressures. The methods for performing the Thermal-Hydraulic analyses are described in DPC-NE-2003P-A (Reference 5) and DPC-NE-2005P-A (Reference 6). Additionally, the treatment of the rod bow penalty is discussed in BAW-10186P-A (Reference 9). This topical concluded that the rod bow penalty is insignificant and unnecessary for the DNB analysis. The general criteria for thermal-hydraulic performance is that no core damage due to critical heat flux take place during steady state operations or during anticipated transients. The need to perform the thermal-hydraulic analyses in conjunction with a reload arises when there is a change in the fuel design, a change in the input assumptions or the original analysis, or a change in the regulatory criteria.

7. Technical Specifications Review and Development

7.1 Technical Specifications Review

One of the license conditions applicable to the operation of a power reactor is that the reactor facility should be operated in accordance with the Technical Specifications. Technical Specifications are criteria for safe operation of the reactor and are established from applicable design evaluations, safety analyses, and other considerations. Included in the Technical Specifications are safety limits, limiting system settings, limiting conditions for operation, surveillance requirements, identification of design features, and identification of administrative controls.

The Technical Specifications on core safety limits, certain limiting safety system settings, and certain limiting conditions for operations are established on the basis of, among other things, the nuclear and thermal-hydraulic characteristics of the core and applicable accident analyses. Since the nuclear and thermal-hydraulic behavior of the core and accident analyses may be affected by the reload design, the Technical Specifications (and their bases), particularly the sections pertaining to core safety limits, limiting safety system settings, limiting conditions for operation, surveillance requirements, and reactor design features are reviewed to confirm their continued validity for the reload cycle. Modifications of the Technical Specifications are made as necessary to ensure safety of operation and/or to improve flexibility in operation. Technical Specifications affected by a typical reload design include (i) core safety limits, (ii) limiting safety system settings based on core safety limits and fuel design limits, and (iii) limiting conditions for operation based on LOCA analysis and initial conditions for the limiting DNB transient. Many of these specifications that were historically included in the Technical Specification have been relocated to the cyclic Core Operating Limits Report (COLR). If changes required by the reload design are limited to specifications in the COLR, then generation of a reload report and NRC approval of the changes are not required. The following subsections describe the manner in which these Technical Specification and COLR limits are developed.

7.2 Development of Core Safety Limits

The core safety limits define limits on the values of pertinent core parameters such that if normal operation is within these limits, the integrity of the fuel cladding is maintained. Fuel cladding integrity can be assured (within permissible tolerances) by maintaining the minimum DNBR in the core at or above the design limit and by limiting the maximum linear heat rate in the core to less than or equal to the center fuel melt and cladding strain LHR limits. In order to achieve this condition, values of pertinent core parameters, which correspond to the minimum DNBR at the design limit and/or the linear heat rate at the center fuel melt or cladding strain LHR limits are calculated, and these values form the core safety limits. Core safety limits are specified on core pressure-core outlet temperature combinations (P-T limits) and on reactor power-power imbalance combinations. In calculating these limits it is assumed

that all other pertinent variables are at their design limits (maximum or minimum, as appropriate).

7.2.1 Determination of Core Safety P-T Limits

The P-T limits are based entirely on the DNBR criterion, and they represent the values of core outlet pressure--vessel outlet temperature combinations for which a minimum DNBR at the design limit is predicted when other pertinent parameters are at their respective design limits. The thermal-hydraulic analysis defines the values of core outlet pressure as a function of vessel outlet temperature for which a minimum DNBR at the design limit is predicted for the maximum design conditions during 4-pump and 3-pump modes of operation. The core safety limit is obtained by superimposing the P-T curves corresponding to 4-pump and 3-pump modes of operation and by drawing the enveloping curve. A typical P-T safety limit is shown in Figure 7-1.

7.2.2 Determination of Core Safety Power-Power Imbalance Limits

The core safety power-power imbalance limits define the values of reactor power as a function of axial imbalance such that a minimum DNBR equal to the design limit and/or a linear heat rate equal to the center fuel melt/clad strain limits is predicted when other pertinent parameters (RCS flow, pressure and temperature, and hot channel factors) are at their design limits.

These limits indirectly represent the limits on the DNBR criterion-limited power peaks and the center fuel melt/clad strain criterion-limited power peaks. Since power peaking is not directly measurable by the RPS, the DNBR criterion-limited power peaks and the center fuel melt/clad strain criterion-limited power peaks are separately correlated to RPS measurable reactor power and power imbalance, and limits are then established on reactor power-power imbalance combinations to satisfy the DNBR and center fuel melt/clad strain criteria. The power-power imbalance limits separately established for the DNBR and center fuel melt/clad strain criteria are then superimposed and the resulting most limiting power-power imbalance envelope forms the core safety limit.

7.2.2.1 Calculation of Power-Power Imbalance Limits for Center Fuel Melt/Clad Strain Criterion

The power-power imbalance limits based on the center fuel melt/clad strain criteria are determined by a synthesis of the results of the fuel thermal analysis and the results of the maneuvering analysis.

The fuel thermal analysis establishes the maximum permissible linear heat rate in the core to prevent center fuel melting. The fuel mechanical analysis establishes the maximum permissible linear heat rate in the core to prevent exceeding the cladding strain limits. A conservative overlay of these maximum permissible linear heat rates is

used to generate what will be referred to as the center fuel melt linear heat rate limit (CFMLHR), the allowable total peaking factor is established by the relation:

$$\text{MAPF} = \frac{\text{CFMLHR}}{\text{LHR} \times \text{FOP}}$$

where LHR is the average full power linear heat rate in the core and FOP is the power level expressed as a fraction of rated power.

The maneuvering analysis (Section 5) establishes the maximum calculated total peaking factors for various core conditions, (power levels, xenon conditions, control rod positions and burnups). These calculated maximum total peaking factors are increased by several conservative factors to obtain the worst case expected total peaking factor corresponding to each condition. The individual conservative factors are as follows :

1. Nuclear uncertainty factor as specified in Reference 2.
2. Spacer grid effect factor of 1.026, which is only applicable when utilizing assemblies with Inconel intermediate spacer grids.
3. Engineering hot channel factor of 1.014
4. Densification power spike factor which varies with axial location of the peak in the core. For current fuel designs a factor of 1.08 is utilized.

The nuclear uncertainty factor accounts for the uncertainty in the calculated peak due to the limitations of the analytical models and the spacer grid effect factor accounts for the flux distortion caused by Inconel spacer grids (no spacer grid effect factor is required for Zircalloy spacer grids). The engineering hot channel factor accounts for the manufacturing tolerances of critical fuel rod design parameters (pellet enrichment, pellet density, pellet diameter, etc.). The densification power spike factor accounts for the local flux enhancement resulting from gaps in the fuel column induced by fuel densification. Although fuel assembly bowing is considered to have the potential for enhancing the power peaks, no explicit allowance is required for assembly bow on the basis that the other conservatism factors (nuclear uncertainty factor, engineering hot channel factor, and densification power spike factor) are adequate to offset the effect of the assembly bow power spike factor without an additional allowance. A burnup dependent peaking penalty consistent with topical reports BAW-10147P-A (Reference 10) and BAW-10186P-A (Reference 7) is applied to account for the potential power peaking enhancement due to fuel rod bow.

The worst case expected maximum total peaking factors calculated in this manner for different power levels are compared to the respective allowable total peaking factors, and the central fuel melt margin for each condition can be determined. The margin at a particular power level is given by:

$$\text{Margin (\%)} = \frac{\text{allowable total peak} - \text{worst case expected maximum total peak}}{\text{allowable total peak}} \times 100$$

Core conditions which correspond to non-negative margins are acceptable conditions, and core conditions which correspond to negative margins cannot be permitted. In order to preclude core conditions with negative margins, limits should be established on acceptable values of power peaking conditions for each power level, and corresponding reactor trip setpoints should be established so as to trip the reactor when conditions approach unacceptable values. Since power peaking cannot directly be measured by the RPS, power peaks are first correlated with the RPS-measurable axial offset for each power level. The outputs of the maneuvering calculations include the maximum total peaking factor in the core, its location and the corresponding core axial offset. In order to determine the axial offset limits that correspond to an acceptable margin for a particular power level, the margin for each calculated maximum total peak for that power level is plotted against the corresponding axial offset. These plots define a relationship between core offset and margin. The value of offset at the zero margin intercept defines the offset limit for that particular set of reactor conditions. Figure 7-2 provides an example of the analysis for the 100% FP case.

In practice, detailed calculations typically are performed for the 100% FP case. Limits for other power levels may be determined by conservatively extrapolating the 100% FP limits to other power levels by using the power feedback effect on peaking factors and by validating these limits by comparison with results of a limited number of maneuvering calculations at these power levels. Offset limits are typically established for power levels of 110% FP and 100% FP.

7.2.2.2 Calculation of Power-Power Imbalance Limits for DNBR Criterion

The power-power imbalance limits based on the DNBR criterion are determined by a synthesis of the results of the thermal-hydraulic analysis and the results of the maneuvering analysis.

The thermal-hydraulic analysis establishes the maximum allowable total peaking factors as a function of core elevation for various axial flux shapes to prevent violation of the DNBR criterion. The maneuvering analysis generates the power distribution in the core (including the maximum total peaking factor and the associated axial peaking factor for each fuel assembly, typically in a 1/4-core representation, and the core axial offset) for various design conditions and for various times in the cycle. For each power distribution, the calculated maximum total peaking factors of each of the assemblies is increased by the radial nuclear uncertainty factor and the resulting adjusted peak is compared to the allowable peaking factor for that axial peaking factor and axial peak location. Application of the radial nuclear uncertainty is not necessary when the allowable peaking factor is determined using the statistical core design methodology described in Reference 6 (which accounts for the radial nuclear

uncertainty in developing the allowable peaking factor). The DNBR margin is then obtained as:

$$\text{DNBR Margin (\%)} = \frac{\text{allowable total peak} - \text{adjusted maximum total peak}}{\text{allowable total peak}} \times 100$$

For each calculated power distribution, the DNBR margin is calculated for each assembly, and then the minimum DNBR margin in the core for each power distribution is determined.

In order to determine the axial offset limits that correspond to the acceptable DNBR margin, the minimum DNBR margins are plotted for each calculated power distribution against the corresponding axial offset and the maximum allowable positive and negative offset limits are determined in a manner similar to that used to establish the center fuel melt limited offset limits. In this case also, offset limits are typically established for power levels of 110% FP and 100% FP at full flow conditions.

7.2.2.3 Calculation of the Core Safety Limits on Power-Power Imbalance

The core safety limits on power-power imbalance are the most limiting values of the center fuel melt /clad strain power imbalance limits and the DNBR power imbalance limits for each power level. To determine the core safety limits, first the limiting offsets at the various power levels are determined by superimposing the DNBR and center fuel melt/clad strain offset limits at each power level. The following example uses representative numbers to illustrate the procedure.

Power Level % FP	CFM/clad strain Offset Limits %		DNBR Offset Limits %		Limiting Offset %	
	-ve	+ve	-ve	+ve	-ve	+ve
110	30.8	30.8	35	33	30.8	30.8
100	48	48	55	50	48	48

The limiting offsets at each power level are converted to imbalance limits using the relation :

$$\text{Power imbalance} = \text{axial offset} \times \text{fraction of full power.}$$

The resulting imbalance limits are plotted on a power-power imbalance graph. Representative limits are shown in Figure 7-3. The following additional steps are required to complete the procedure of determining the core safety limits on power-power imbalance :

1. Draw a horizontal straight line corresponding to the maximum power level analyzed.
2. From points where this line intersects the imbalance limit envelope, draw two straight lines, one on the positive imbalance side and one on the negative imbalance side, that conservatively envelop the imbalance points.

These three straight lines define the power-power imbalance limits for 4-pump operation.

The power-power imbalance limits for 3-pump operation can be determined by reducing the thermal power associated with each break point of the 4-pump curve to the values of the maximum allowable core thermal power for 3-pump operation and by drawing straight lines parallel to the 4-pump envelope through the points defined by the 3-pump thermal power and the 4-pump imbalance limits. The maximum thermal power for the 3-pump mode is obtained by multiplying the 3-pump flow by the flux-flow trip setpoint and adding the allowance for calibration and instrumentation error for power measurement to the product.

7.3 Development of Limiting Safety System Settings

The reactor protection system contains several trip functions designed to prevent the process variables from exceeding the safety limits, to ensure that the fuel design limits (minimum DNBR and center fuel melt/clad strain LHR limits) are not exceeded during conditions of normal operation and anticipated transients, and to enable reactor shutdown during accident condition. These trip functions, their intended purpose, and their setpoints are shown in Table 7-1. The trip setpoints are established by reducing the safety limits or other design analysis limits by appropriate error adjustment factors, which account for any uncertainty in the measurement of that variable and the calibration and instrumentation errors.

In general, the trip setpoints requiring modification for a reload cycle are the P-T trip setpoints and the power-flow-imbalance trip setpoints as a result of a change in the core safety limits and/or a change in the flux/flow trip setpoints.

7.3.1 Determination of RPS P-T Trip Setpoints

The P-T trip function defines values of RCS pressure as a function of RC outlet temperature at which the RPS should trip and provides protection of the P-T core safety limits.

The P-T trip setpoints are derived by error-adjusting the P-T core safety limits and by considering the high RCS pressure, low RCS pressure, and high RC outlet temperature trip setpoints. Error adjustment is performed on the RCS pressure (to account for the difference in pressure between the core outlet and the point of measurement and to

account for the error in the measurement of pressure by the RPS) and the RC outlet temperature (to account for the error in temperature measurement by the RPS). The P-T trip setpoints are to be modified whenever the P-T core safety limits are changed, P-T error adjustment factors are changed, the high RC outlet temperature trip setpoints are changed, or the low RCS pressure trip setpoint is changed.

In order to determine the P-T trip setpoints, first the locus of pressure-temperature points constrained by the high RCS pressure trip setpoint (2355 psig), the high RCS temperature trip setpoint (618 °F), and the low RCS pressure trip setpoint (1800 psig) are identified on the Core Safety P-T Limit curve, as shown in Figure 7-4. Referring to Figure 7-4, the lines AB, BC, and DE respectively represent the locus of P-T points constrained by the high RCS pressure trip, the high RCS temperature trip, and the low RCS pressure trip setpoints. Next, the pressure-temperature points C and D are adjusted for the difference between the core pressure and the RCS pressure at the measurement location and for the errors in the temperature and pressure measurements by the RPS. Referring to Figure 7-4, C' and D' are the error adjusted points, and the straight line C'D' joining these points defines the locus of RPS P-T trip setpoints.

7.3.2 Determination of RPS Power-Flow-Imbalance Trip Setpoints

The power-flow-imbalance trip setpoints define the values of reactor power at which RPS trip should occur whenever the combinations of power, flow and their uncertainties produce limiting values which result in the design minimum DNBR during a flow transient and whenever the combination of power, imbalance, and their uncertainties correspond to the core safety limits on power-imbalance. This trip function is established by considering maximum allowable power-to-flow ratio and by considering the maximum allowable values of power as a function of imbalance. The maximum allowable power-to-flow ratio is constrained by the requirement that the minimum DNBR, in the event of a limiting flow transient, is equal to or greater than the design limit. Thus the power-flow-imbalance trip setpoints ensure core protection during transients involving a flow reduction (by the power-to-flow trip portion of the trip function) and during conditions involving adverse power distributions (by the power-imbalance trip portions of the trip function).

In order to determine the power-flow-imbalance trip setpoints, first the maximum allowable power-to-flow ratio is to be obtained. The maximum allowable power-to-flow ratio (also called the flux / flow trip setpoint) is obtained by reducing the calculated flux / flow ratio by an error adjustment factor, which takes into account the noise in the RPS flow signal and other electronic errors in the RPS flow instrumentation. Next, the core safety power-imbalance limits are error-adjusted both on the power level limit and the imbalance limit. The error adjustment factor for power level includes an allowance for the neutron flux error (uncertainty in correlating the RPS measured neutron flux to reactor power), an allowance for the calorimetric error, and an allowance for any setpoint error. The error adjustment factor for imbalance accounts for the uncertainty in the measurement of axial imbalance by the

out-of-core detector system, and it is a function of the imbalance limit and the power level. To establish the RPS power-flow-imbalance trip setpoints the error adjusted power and imbalance are plotted on a figure with imbalance as the horizontal axis and power as the vertical axis. The envelope is obtained by the straight lines passing through pairs of these points and the horizontal straight line drawn passing through the point representing the maximum power level analyzed for the 4-pump case or the maximum power allowed by the flux/flow trip setpoint. A representative flux / flow / imbalance trip function envelope is given in Figure 7-5.

7.4 Development of Limiting Conditions for Operation

The limiting conditions of operation generally requiring modification in conjunction with a reload cycle are the power distribution limits, shutdown margin-limited control rod insertion limits, and the ejected rod worth-limited control rod insertion limits.

The power distribution limits are limits on pertinent core parameters (such as control rod positions, axial imbalance, quadrant power tilt, and xenon conditions which influence the power distribution in the core) such that the power distributions in the core during normal operation are within the values assumed in the safety analysis for the limiting loss of coolant accident and the limiting DNB transient. These power distribution limits are determined by a conservative overlay of the LOCA limited power distribution limits and the operational DNB power distribution limits. The operational DNB power distribution limits are developed in a manner equivalent to that described in Section 7.2.2.2 but for the most limiting condition 2 transient statepoint.

The shutdown margin-limited control rod insertion limits are limits on the maximum allowable control rod insertions satisfying the shutdown margin criterion, and the ejected rod worth-limited control rod insertion limits are limits on the maximum allowable control rod insertions satisfying the ejected rod worth criterion.

7.4.1 Determination of LOCA-Limited Power Distribution Limits

The ECCS analysis establishes acceptable values of the linear heat rate in the core such that the performance of the Emergency Core Cooling System conforms to the requirements 10CFR50.46 and Appendix K. The values of the allowable linear heat rates are established by the currently applicable ECCS evaluation model for Oconee. The maximum operating linear heat rates at the designated core elevations should be maintained at or below the allowable values. The maximum operating linear heat rate is a function of the power level and the maximum operating peaking factor. Thus, for a given power level the maximum operating linear heat rate varies with the maximum operating peaking factor. Therefore, for a given power level the maximum operating linear heat rates can be maintained within the allowable linear heat rates by maintaining the maximum operating power peaks at the designated axial locations

within the allowable peaking factor. The allowable peaking factor at axial location z for the power level FOP is given by :

$$\text{APF (FOP, } z) = \frac{\text{ALHR}(z)}{\text{LHR} \times \text{FOP}}$$

where APF (FOP, z) is the allowable peaking factor at elevation z for power levels equal to or less than FOP, ALHR (z) is the allowable linear heat rate at axial location z , and LHR is the densified average linear heat rate at 100% FP.

The power peaking factor in the core changes with fuel burnup, axial imbalance, full length control rod position, and part length control rod position. In addition, the peaking factor is influenced by the existence of any quadrant power tilt and non-equilibrium xenon conditions. Therefore, allowable ranges of these core operation parameters would have to be established in order that the maximum operating peaking factors at the designated axial locations be within the allowable values. Although the fuel densification phenomenon has the potential for enhancing power peaks, no explicit allowance is required for power spikes associated with this phenomenon in the LOCA power distribution limits on the basis that the densification power spikes do not enhance the local heat flux.

The effect of a positive quadrant power tilt on the peaking factors is quantified either on a cycle-specific basis as a function of assembly location and burnup statepoints, or by application of a conservative generic factor. These cycle-specific 'tilt factors' typically range from 0.8% to 1.4% increase in peaking factor (depending on the assembly location) per percent positive quadrant tilt. The conservative tilt factor may be as high as 1.5% increase in peaking factor per percent positive quadrant tilt. Technical specifications permit reactor operation with a positive quadrant tilt as specified in the COLR. A tilt limit of 5.0% would typically amount to a 4.0% to 7.0% increase in peaking factor when using the cycle-specific tilt factors, or a 7.5% increase in peaking factor when using the conservative generic factor. Therefore, the allowable peaking factor would have to be reduced by 4.0% to 7.0%, or by 7.5%, whichever is applicable, to account for the permitted quadrant tilt condition.

The effect of non-equilibrium xenon conditions on peaking factors is quantified by the analysis of the power peaking factors occurring during various power maneuvers. Power redistribution caused by transient xenon in the power maneuver leads to peaking and offsets being explicitly accounted for in the setting of LOCA limits.

The remaining core parameters which influence the maximum operating power peaks are the full-length control rod position, part length control rod position, axial imbalance, and core burnup. The permissible values of these quantities are to be determined such that resulting power peaks, after accounting for any uncertainties, would be within the maximum allowable power peaks. The maneuvering analysis establishes the relationship of operating peaking factors at various axial locations with

the core imbalance and control rod positions. The maneuvering analysis calculations include part length control rod scans inducing a range of values of core axial offset for different full length control rod positions. The calculations are performed for various power levels and for the full range of core burnups. The calculations yield the values of the maximum peaking factor at the different axial planes corresponding to various full-length control rod positions, various axial offsets, and for different part length rod positions, and these calculations also yield the variations of the maximum peaking factor with axial offset. The calculated maximum peaks at each axial plane are increased by the nuclear uncertainty factor as identified in Reference 2, the spacer grid effect factor (if the reload design utilizes fuel with Inconel intermediate spacer grids), the power level uncertainty factor and the engineering hot channel factor to obtain the worst case operating peaking factors.

To determine the allowable values of full-length and part-length control rod positions and the axial offsets, first an operating range for the full-length control rod position is chosen and then the ranges of axial offsets and part-length control rod positions for which the worst case operating peaking factors at the designated axial planes are less than or equal to their respective allowable values are determined. If the resulting ranges of axial offset and part-length control rod position are acceptable from the standpoint of operational flexibility, the assumed full-length control rod position ranges and the calculated range of axial offset and part-length control rod position are taken as their operating limits. If, however, the resulting ranges of axial offsets and part-length control positions are unacceptable from the standpoint of operational flexibility, a more restrictive full-length control rod bank position is selected and the corresponding axial offset and part-length control rod position limits established.

Since the core peaking factors do not remain constant throughout the entire fuel cycle, the operating limits on control rod positions and axial offsets should be based on the composite results of calculations for representative times in the cycle. In order to provide maximum operating flexibility, the operating limits on control rod positions and axial offsets may be established for different cycle burnup intervals (e.g., BOC - 100 EFPD, 100 EFPD - 250 EFPD and 250 EFPD-EOC). The operating limits applicable to each burnup interval are generated on the basis of the results of maneuvering calculations corresponding to the beginning and end of each burnup interval. (For each burnup interval, the control rod grouping and the nominal position of the regulating control rod groups are the same).

Calculations of axial offset limits, part length control rod position limits, and full length control rod position limits are performed for various power levels (typically for 100% FP, 90% FP, and 80% FP). The offset limits at each power level are converted to imbalance limits by multiplying the offset limits by the applicable power fraction. Typical operating limits established in this manner are shown in Figures 7-6 through 7-8.

7.4.2 Determination of Control Rod Position Limits Based on Shutdown Margin Criterion

The criterion on shutdown margin is that a minimum of 1% $\Delta k/k$ shutdown margin should be available at all times. The shutdown margin decreases with increasing power and also with increasing inserted rod worth. Therefore, associated with each power level, there is a maximum allowable full length control rod insertion limit which corresponds to a minimum shutdown margin of 1% $\Delta k/k$. Shutdown margin limited rod insertion limits are determined by evaluating the shutdown margins at different power levels (typically at 102% FP, 50% FP, and 15% FP). Since shutdown margins change with cycle burnup, shutdown margin limited rod insertion limits may be calculated for different burnup intervals of the fuel cycle or at the most limiting burnup for the cycle. Typical shutdown margin limited rod insertion limits are identified in Figure 7-6.

7.4.3 Determination of Control Rod Position Limits Based on Ejected Rod Worth Criterion

The criterion on the ejected rod worth is that its value shall not exceed the value assumed in the UFSAR rod ejection analysis. The ejected rod worth is a function of, among other things, the inserted control rod group worth and the cycle burnup (through changes in power distribution). For a fixed burnup the ejected rod worth changes with control rod insertion; therefore limits on the allowable control rod insertion should be placed at various power levels so that the ejected rod worth criterion is satisfied. In order to determine the ejected rod worth limited control rod position limits the ejected rod worths are calculated corresponding to the most limiting of the shutdown margin and LOCA-limited full length rod insertion limits for different power levels. The calculated ejected rod worths are increased by a 15% calculated rod worth uncertainty and compared to the allowable values. If the adjusted calculated ejected rod worths are within the allowable values, no further calculations are needed; otherwise, the control rod insertion limit is changed to the value that corresponds to acceptable ejected rod worths. When the ECCS-limited and ejected rod worth limited rod insertion limits are more limiting than the shutdown margin limited insertion limits, the ECCS and ejected rod worth limited rod insertion limits are combined by superposition into a single rod insertion limit.

Table 7-1

Reactor Protection System Trip Functions (Typical Values)

Reactor Trip	Monitored Parameter	Trip Setpoint During 4-Pump Operation	Purpose of Trip
Overpower trip	Neutron flux	105.5 %FP	To provide core protection during transients involving uncontrolled power increase.
Power-flow-imbalance trip	Neutron flux, RC flow and power imbalance	Flux/Flow setpoint provided in cyclic COLR	To provide core protection during transients involving a flow reduction and during core conditions involving excessive power peaking.
RCS pressure-temperature trip	RCS pressure and RC outlet temperature	Function of RC outlet temperature	To provide core protection during transients involving a reduction in pressure or a reduction in core heat removal.
Low RCS pressure trip	RCS pressure	1800 psig	To provide core protection during transients involving a pressure reduction.
RC pump monitor trip	Neutron flux and pump contact monitor voltage	Loss of two pumps above 2% FP	To provide core protection during loss of RC pumps.
High RCS pressure trip	RCS pressure	2355 psig	To provide protection of RCS pressure boundary from excessive pressures.
High RCS temperature trip	RC outlet temp.	618 °F	To prevent excessive temperature in the RCS.
High RC pressure Trip	RB pressure	4 psig	To ensure reactor shutdown during a LOCA and SLB inside containment.

Figure 7-1

Steady State Pressure Temperature Core Protective Safety Limit

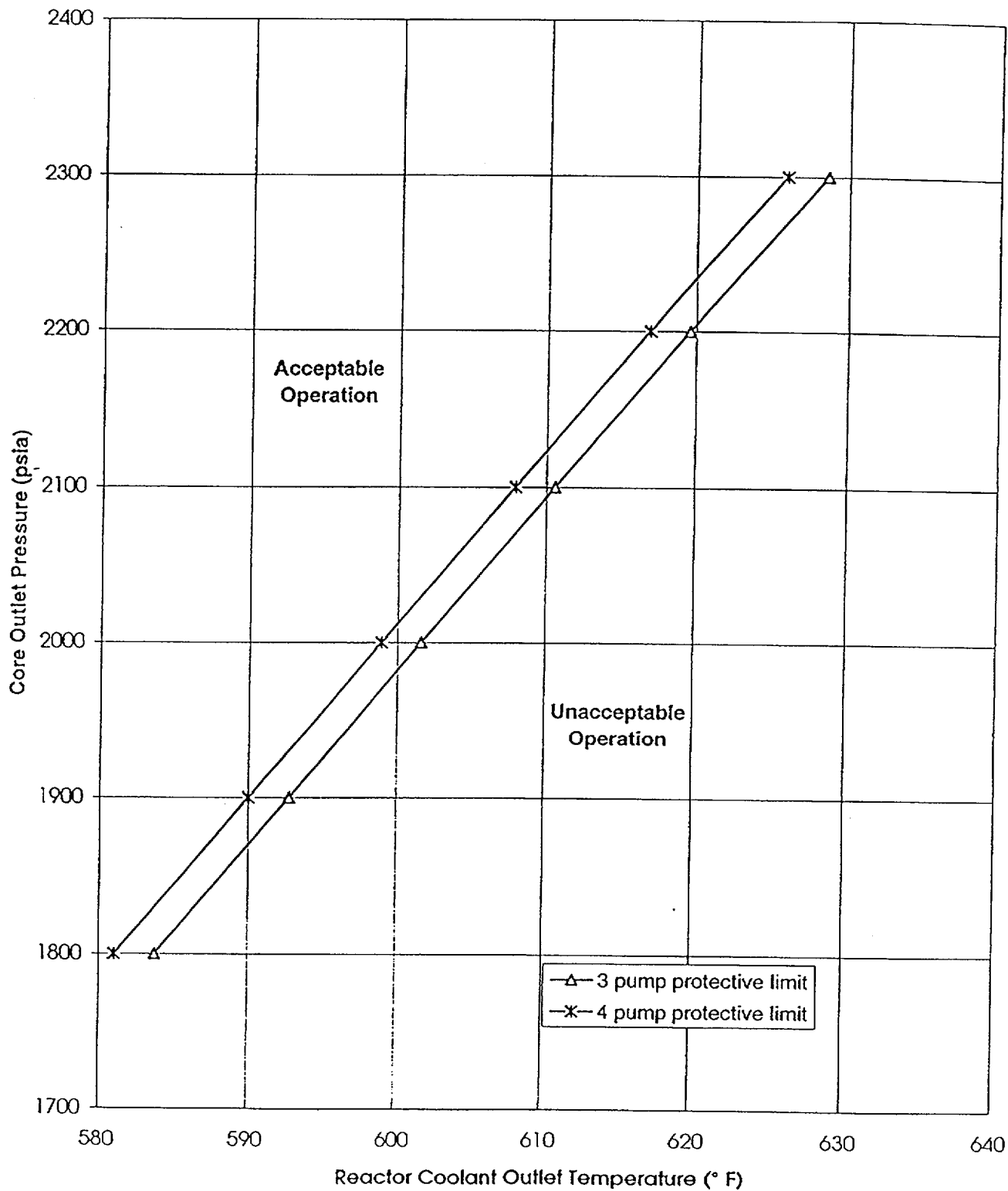


Figure 7-2

Margin to Center Fuel Melt/Clad Strain LHR Versus Core Offset

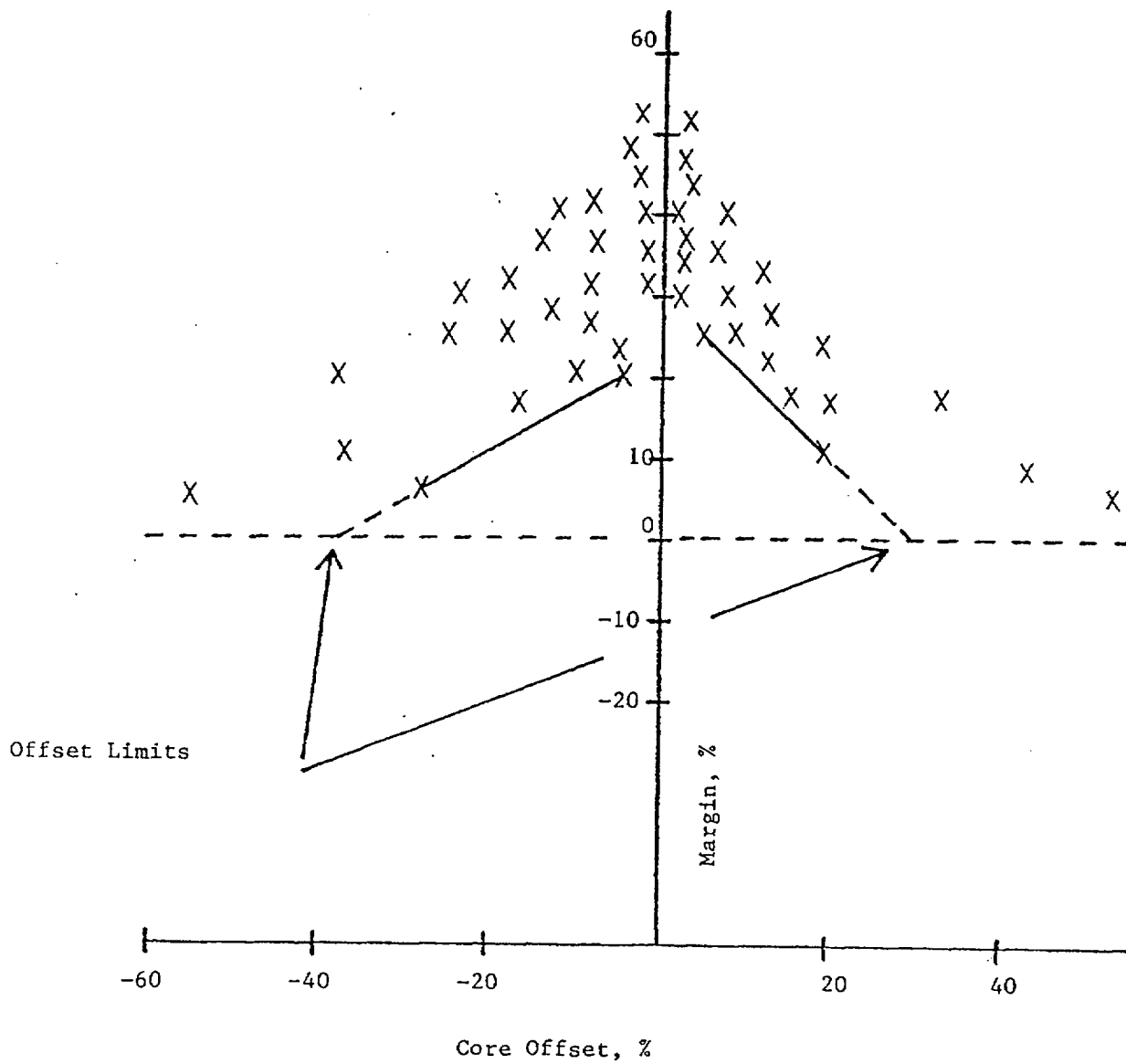


Figure 7-3

Core Protective Safety Limits

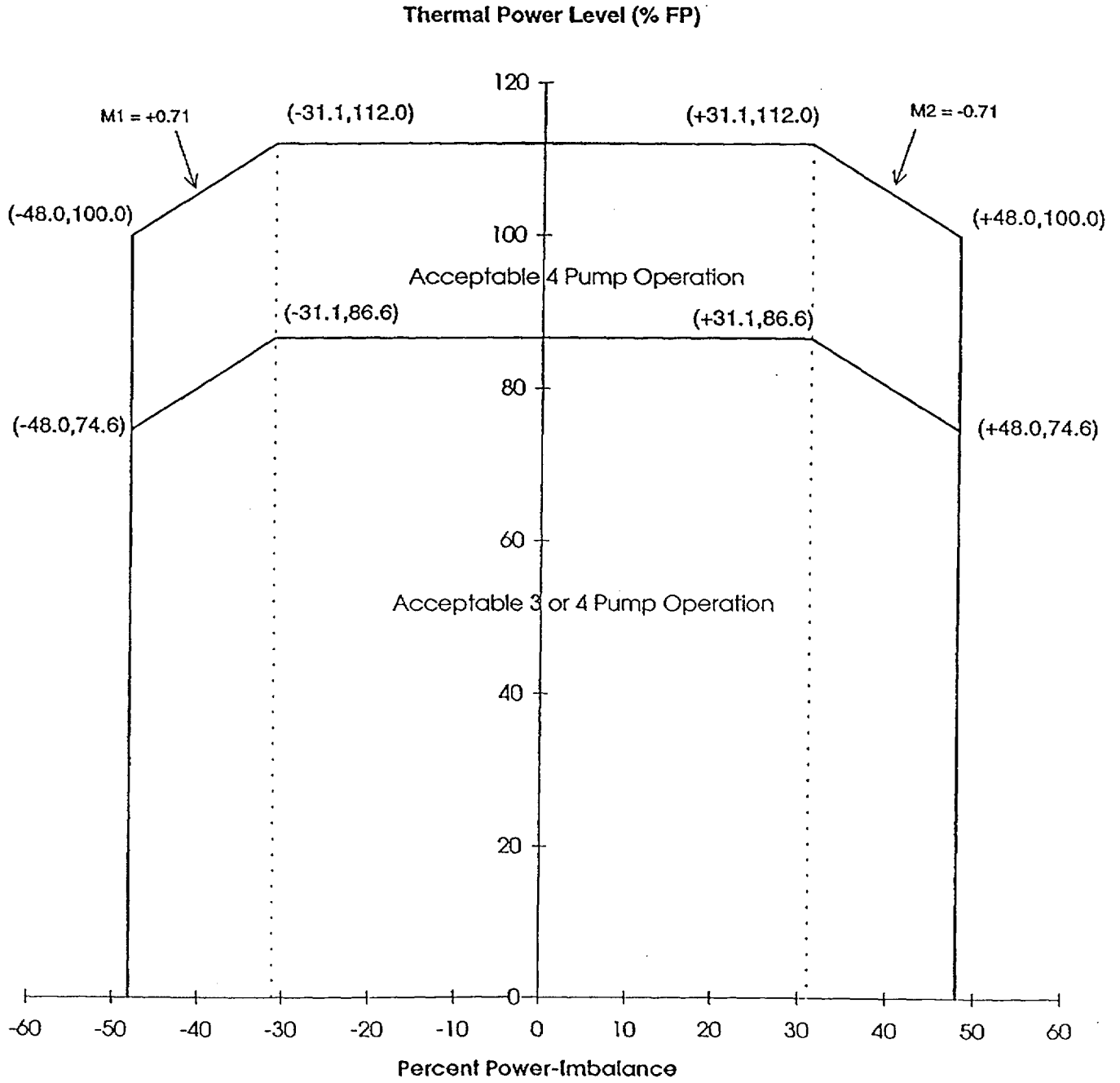


Figure 7-4

Determination of RPS P-T Trip Setpoints

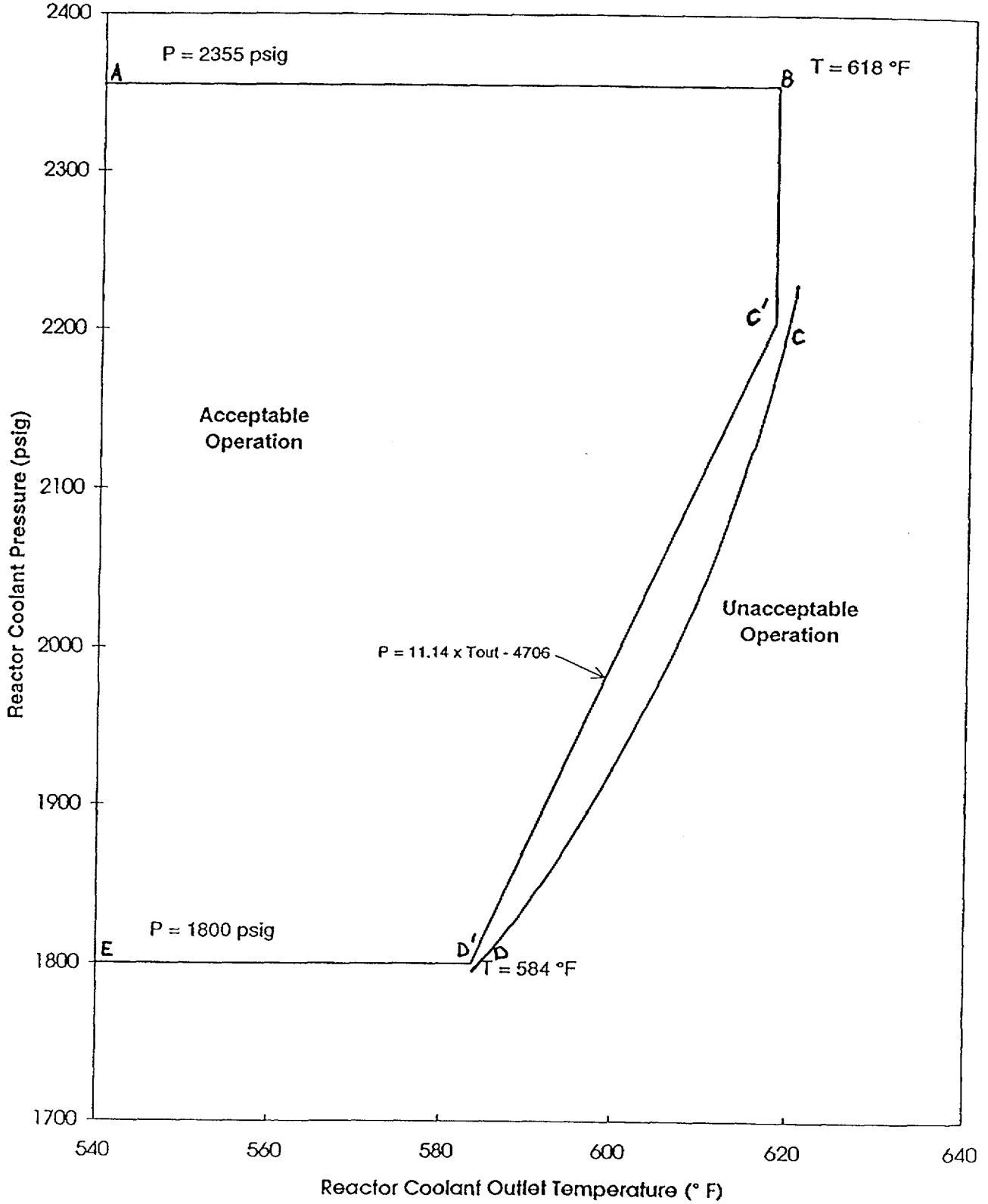
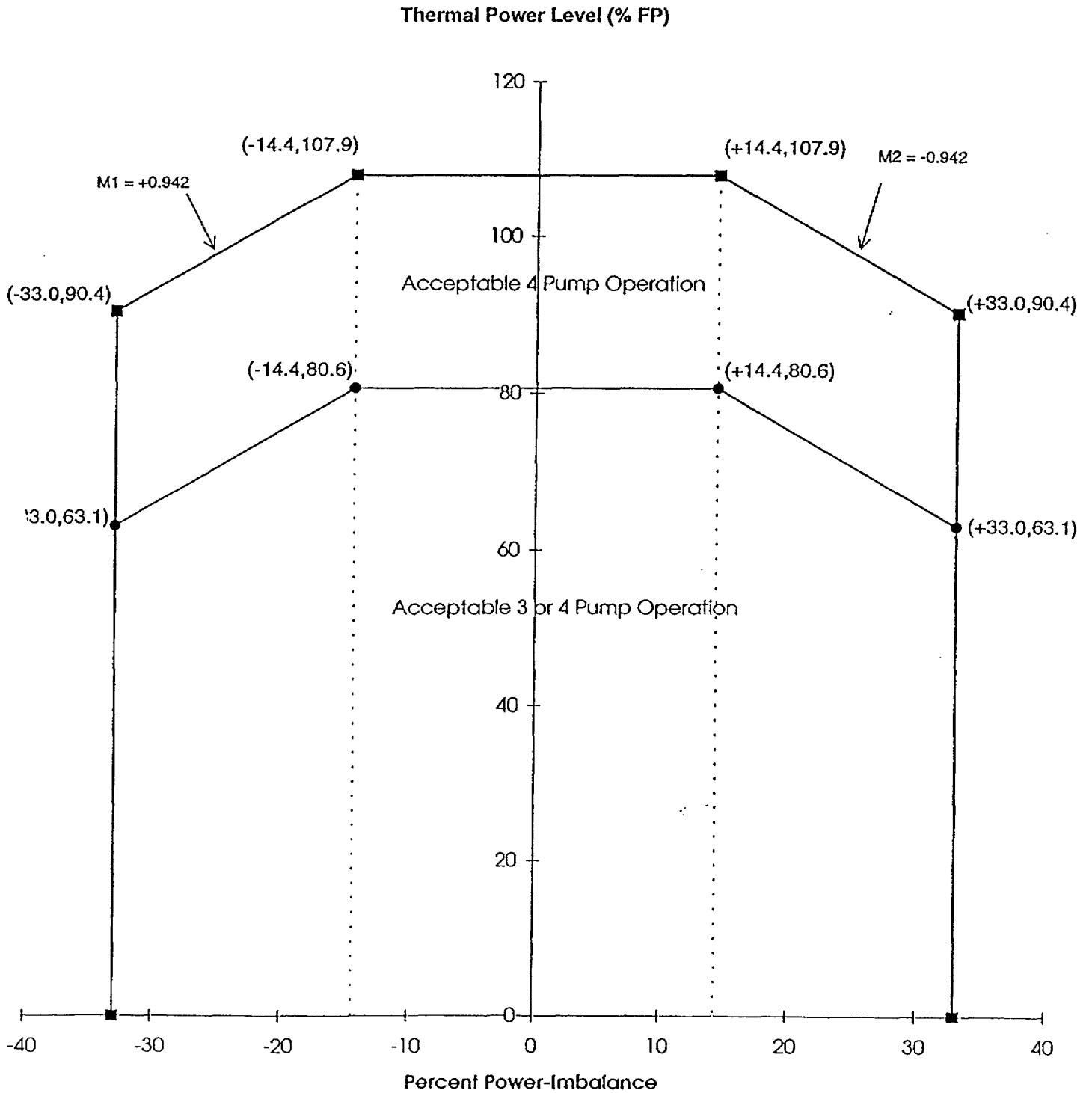


Figure 7-5

Protective System Maximum Allowable Setpoints



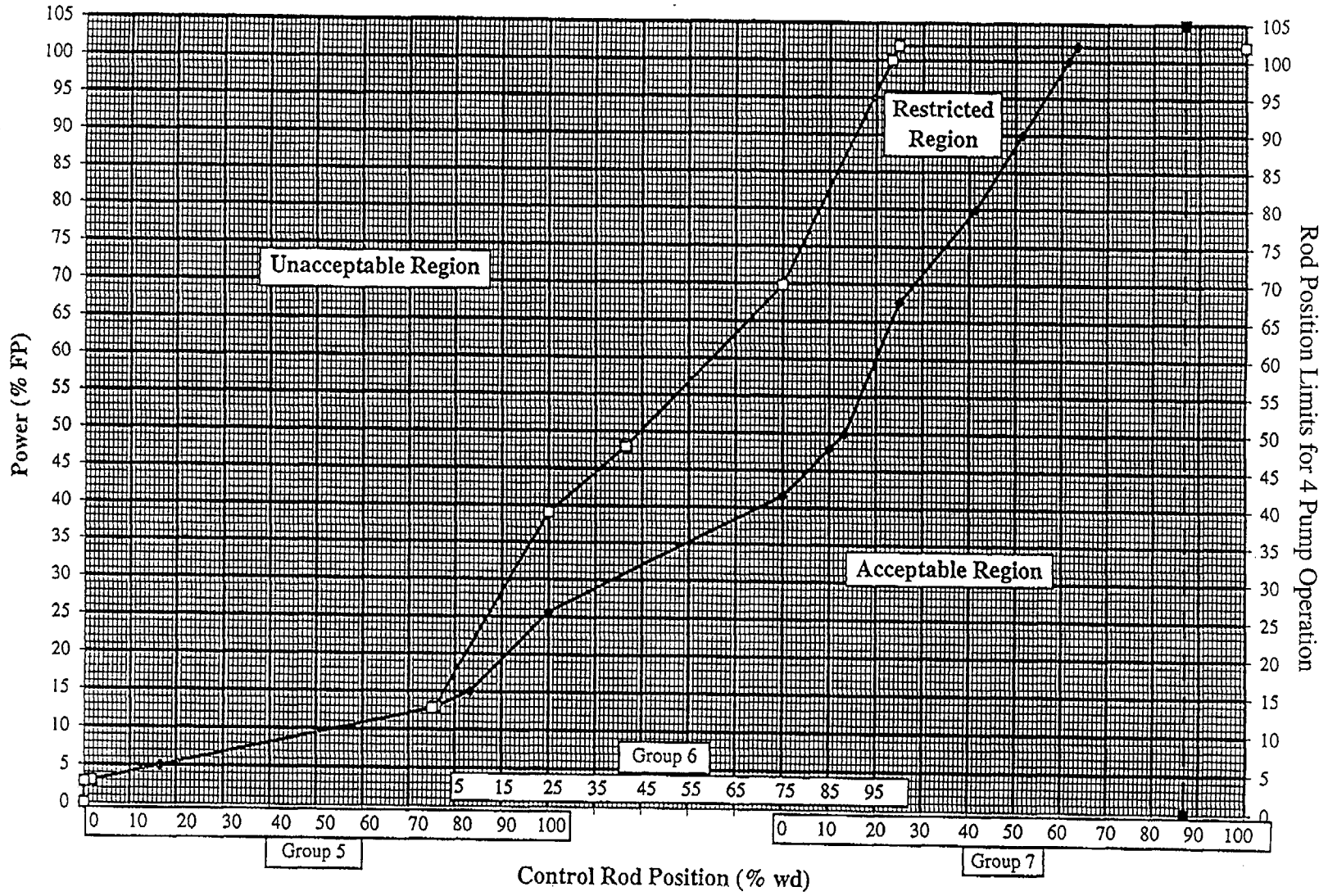


Figure 7-6

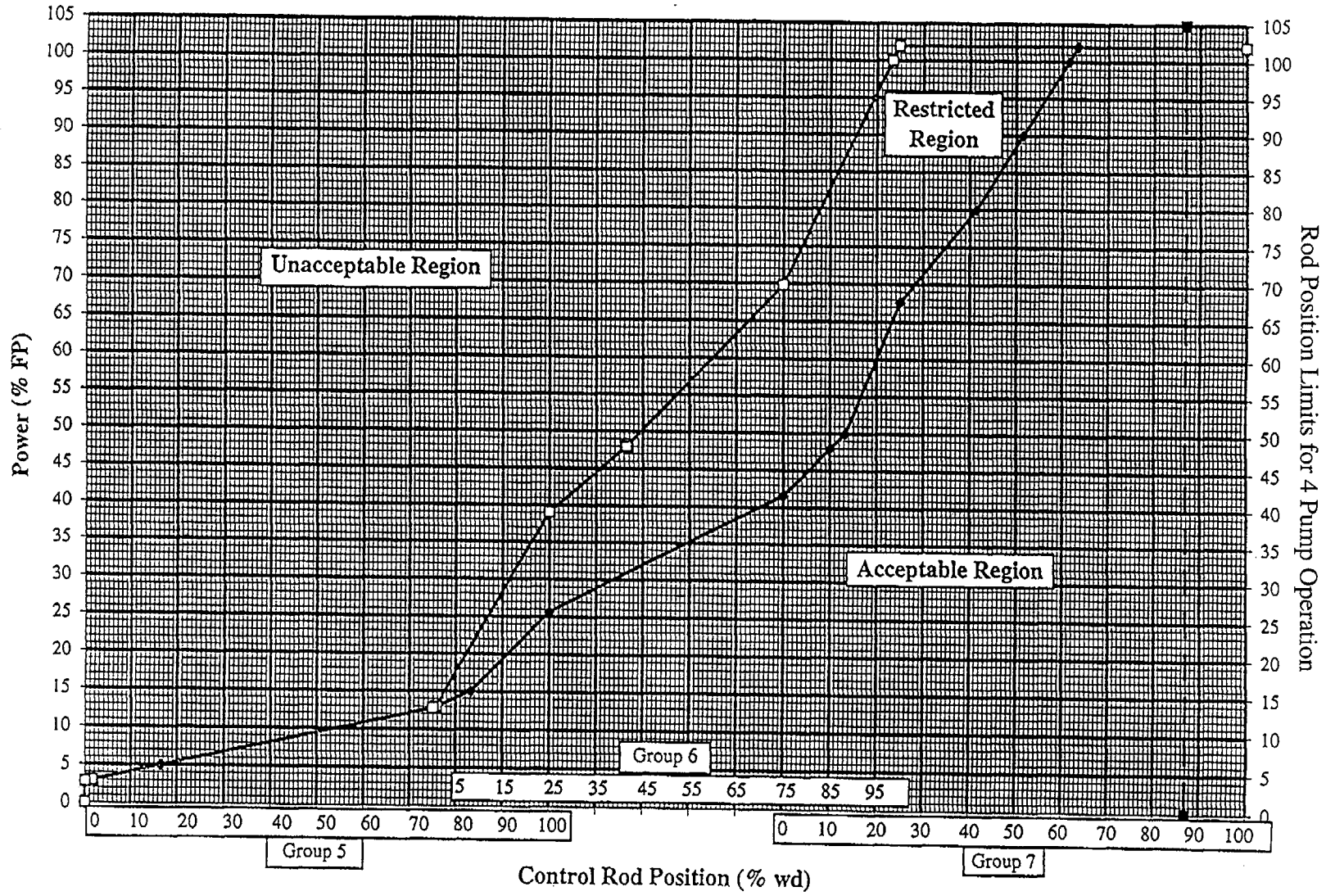


Figure 7-6

Figure 7-7

Power Imbalance Limits for 4 Pump Operation

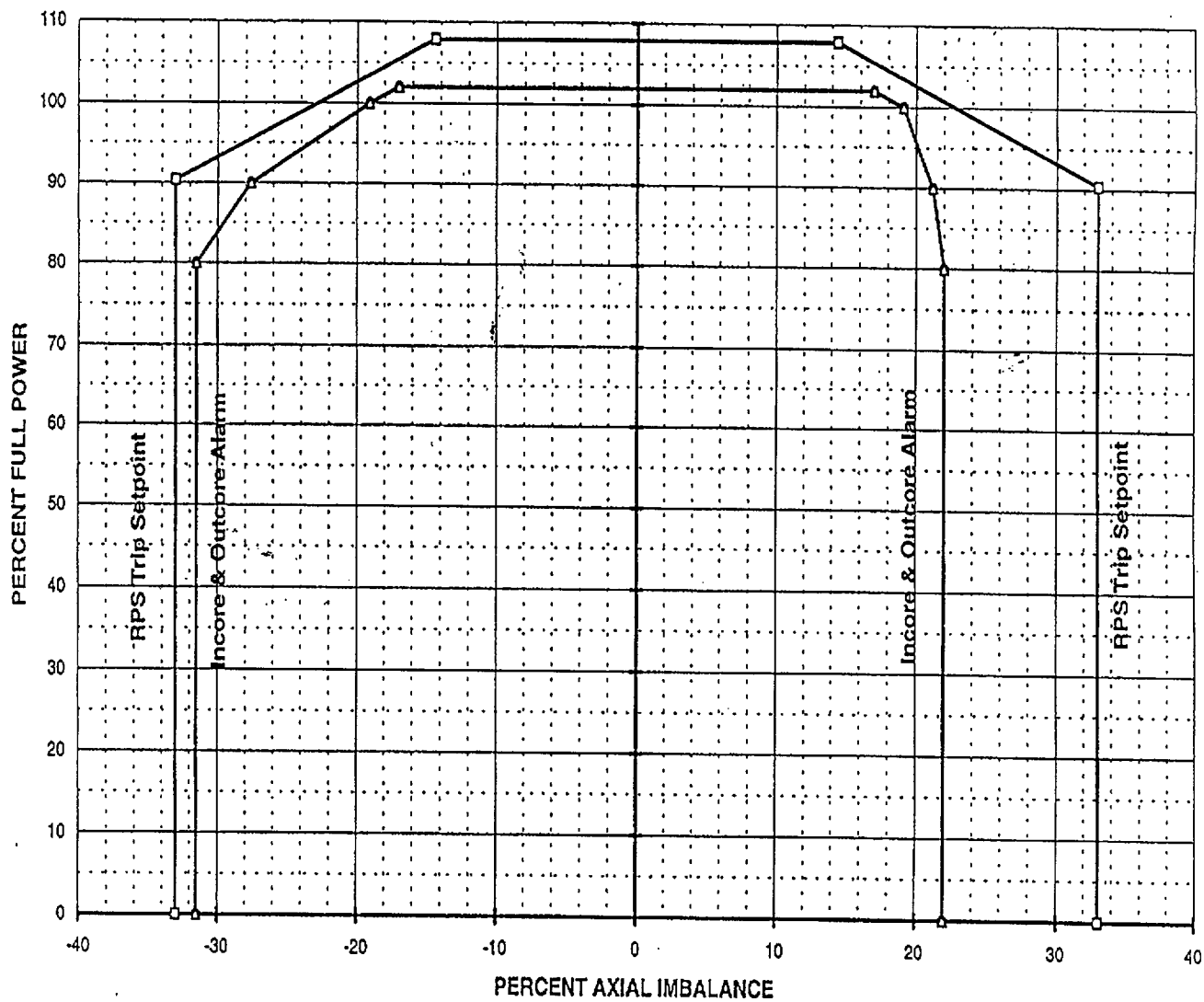


Figure 7-8

Part Length Rod Position Limits

Part Length Rod Position is Unrestricted

Recommended Steady State Operating Band
30% – 40% Withdrawn

8. Accident Analysis Review

8.1 Introduction

A major aspect of the safety consideration of a reactor is the analysis of postulated accidents. These safety analyses enable one to confirm that the reactor system is designed to mitigate such events and that the resulting consequences of such events are acceptable. The most important considerations affecting the calculated consequences of the various postulated accidents are (a) the values of plant parameters assumed in the analysis, (b) the performance characteristics of the mitigating systems assumed in the analysis, and (c) the analytical models used. In general, the accident analyses documented in the UFSAR(Reference 1) are based on values of plant parameters that correspond to bounding conditions, are based on conservative performance characteristics of the mitigating systems, and were performed utilizing generally accepted analytical methodology. Beginning with Oconee Unit 2 Cycle 18 the non-LOCA accident analysis methodology of DPC-NE-3005 (Reference 3) will be used. The LOCA analysis methodology described in UFSAR Section 15.14 will also be used.

The primary goal of safety analysis during the reload design process is to ensure the continued safe operation of the facility with the refueled core. The reference safety analyses and facility Technical Specifications establish the bases and conditions for safe operation of the core. An equivalent level of safety for the refueled core is established when it is determined that the reload design satisfies the analysis bases and conditions. In particular, the accident analyses contained in the licensing basis safety analyses remain valid if a reload design predicts steady-state and transient parameters that lie within the ranges of the values assumed in the reference analyses. Thus, reload safety analysis consists of verifying that the core physics, fuel performance, thermal-hydraulic, and mechanical design parameters for the reload design are bounded by the licensing basis analysis values.

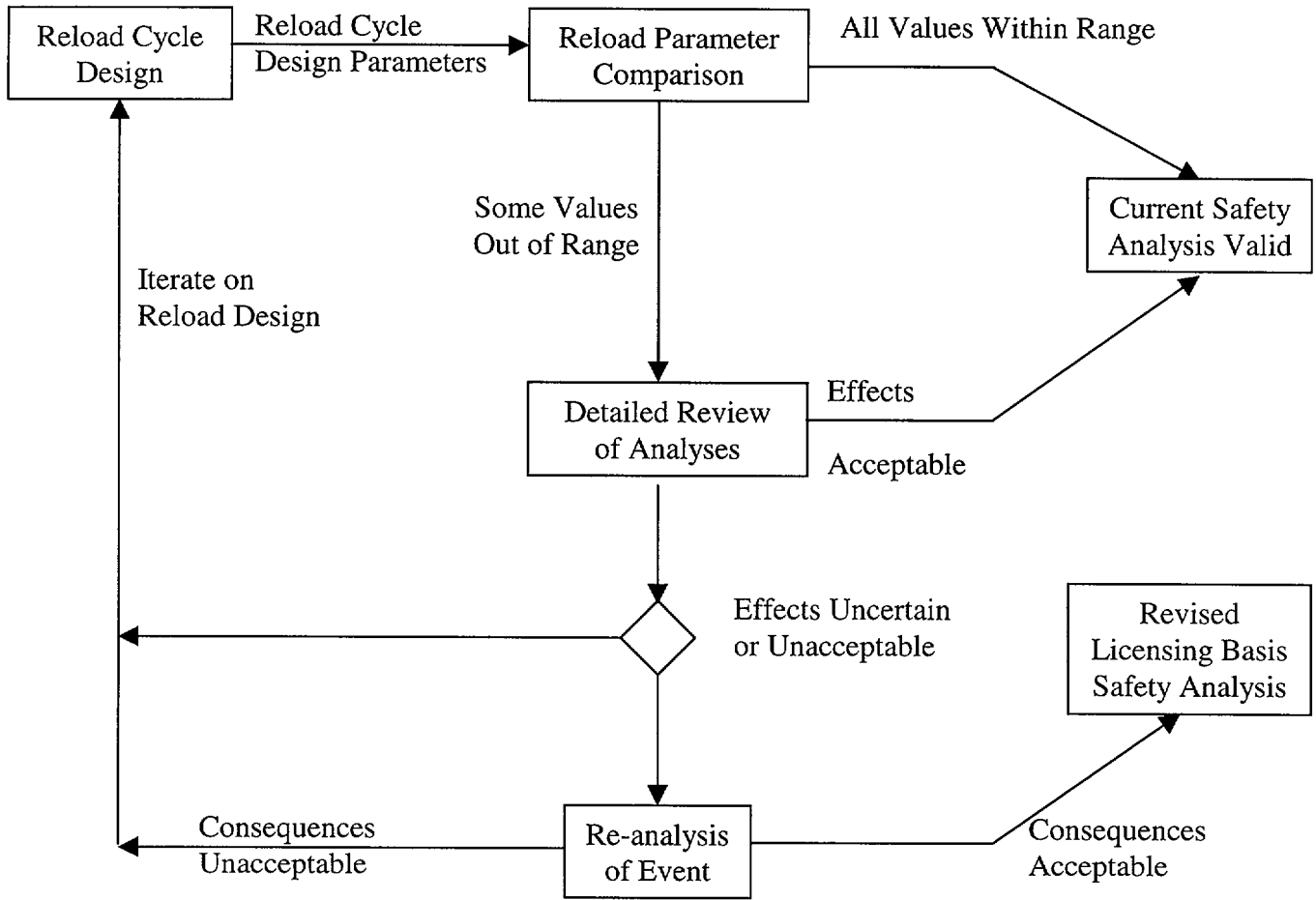
8.2 Overview of Accident Analysis Review

The role of accident analysis review in typical Oconee reload design consists of a systematic review of the reference analysis of all postulated accidents. In this review each accident is examined by comparing the values of important plant parameters and RPS trip functions and trip setpoints assumed in the reference accident analysis to the corresponding values predicted for the fuel cycle under consideration. The safety parameters of interest for the reload cycle are obtained from appropriate nuclear design, thermal-hydraulic design, and fuel performance analyses. If the safety analysis review confirms that all pertinent plant parameters and RPS trip functions and trip setpoints for the reload cycle are conservative with respect to their values assumed in the accident analyses, it is concluded that the reference accident analyses continue to be valid for the fuel cycle, and therefore in these situations no reanalyses of accidents are performed. If, however, one or more plant parameters or RPS trip functions or trip

setpoints assumed in the reference accident analyses are found to be non-conservative for the fuel cycle, a reanalysis of affected accidents is performed. This process is shown schematically in Figure 8-1.

Figure 8-1

Accident Analysis Review Process



9. Development of Core Physics Parameters

Upon completion of the reload design, a variety of physics parameters have been generated primarily for HFP and some HZP conditions. The purpose of this stage of developing core physics parameters is to provide additional calculations to supplement those already performed. The results of these calculations are used for startup test predictions and core physics parameters throughout the cycle. Changes to the startup test procedures, plant operations, or particular core designs may change the physics parameters that are required. The following descriptions are typical of current requirements.

9.1 Startup Test Predictions

After each refueling, the reactor undergoes a startup test program aimed at verifying that the reactor core is correctly loaded, control rods are in the correct locations and are functioning properly, and to verify reactor behavior is accurately predicted by the nuclear models which were used in generating the data used in the plant's safety analysis.

9.1.1 Critical Boron Concentrations and Boron Worths

Critical boron concentrations and boron worths are typically calculated at a variety of rod configurations, at HZP and HFP, as a function of boron concentration, at different xenon concentrations, and at different times in the fuel cycle. The calculation model is capable of critical boron searches and when critical boron concentrations are desired is usually run in this mode. An acceptable alternative, however, is to not search on critical boron but to correct the input boron concentration to the critical boron concentration using a calculated boron worth and the calculated reactivity.

Both HFP and HZP critical boron calculations are normally performed for startup physics tests. Soluble boron worths are usually calculated at HFP and HZP for startup physics tests. The boron worths are usually calculated by running two similar cases except that the soluble boron concentration is varied. The differential boron worth is calculated by subtracting the reactivities and dividing by the boron difference. Differential boron worths are usually quoted in $\% \Delta \rho / 100 \text{ PPM}$ or in $\text{PPM} / \% \Delta \rho$ (the latter is sometimes referred to as the inverse boron worth).

Critical boron concentration is calculated as a function of cycle burnup. These predictions may be provided in tabular form.

Differential boron worth may be calculated as a function of boron concentration and also as a function of cycle burnup. These predictions may also be provided in tabular form.

9.1.2 Xenon Worths

Xenon worth is calculated as a function of cycle burnup. The nominal HFP depletion cases with equilibrium xenon are used as input to a second set of cases where the xenon concentration is set to zero. The difference in reactivities between the equilibrium xenon and no xenon cases equals the equilibrium xenon worth at HFP. The results may be provided in tabular form.

9.1.3 Rod Worths

9.1.3.1 Group Worths

The worth of groups 1 to 8 and the integral rod worth curves for groups 5-7 are calculated at BOC HZP for use in the zero power physics testing. The rod groups are sequentially inserted or withdrawn from the calculation assuming no control rod overlap. The group worth is the difference in reactivity between the fully inserted case and the fully withdrawn case.

At HFP equilibrium xenon, near BOC, the above rod worths are calculated in a similar manner except that when calculating the integral rod worth curves a control rod overlap of 25% and HFP conditions are used.

At HZP, group 8 rod scans are performed where group 8 is stepped in small increments into or out of the core. The HZP results are used to provide tables of rod worth versus position.

9.1.3.2 Stuck Rod Worth

The maximum worth of a single control rod stuck out of the reactor core at HZP is calculated during the reload design. Site engineers use this in the reactivity balance procedures to guarantee shutdown margin. If the stuck rod worth is to be measured during the startup test program, then a recalculation of the worth is performed simulating the test conditions. This worth would then be provided as a startup test prediction.

9.1.3.3 Dropped Rod Worth

The maximum worth of a single control rod dropped into the reactor core is calculated during the reload design. If this parameter is to be measured during the startup test program, then a recalculation of the worth is performed simulating the test conditions. This worth would then be provided as a startup test prediction.

9.1.3.4 Ejected Rod Worth

The maximum ejected rod worth is calculated during the reload design. If this parameter is to be measured during the startup test program, then a recalculation of the

worth is performed simulating the test conditions. This worth would then be provided as a startup test prediction.

9.1.4 Reactivity Coefficients

At HZP the isothermal temperature coefficient is measured as described in the Oconee Startup Physics Testing Program. The calculations used for predicting the isothermal temperature coefficient should be run in a manner consistent with the test method and provide any associated correction factors.

The Doppler or fuel temperature coefficient at HZP can be calculated by varying the fuel temperature while maintaining the moderator temperature constant at 532°F. The resulting reactivity change divided by the change in fuel temperature is the Doppler coefficient at HZP.

The predicted moderator coefficient may be calculated by subtracting the Doppler coefficient from the isothermal coefficient and is compared to the measured moderator coefficient obtained by subtracting the predicted Doppler coefficient from the measured isothermal coefficient. Alternately, the moderator temperature coefficient can be explicitly calculated.

9.1.5 Power Distributions

Power distributions, both assembly radial and total peaking factors, are measured at various power levels for Oconee reload startups. Calculations are run at power levels and conditions similar to the measured conditions to provide predicted power distributions to compare to measurements.

9.1.6 Kinetics Parameters

Kinetics parameters are calculated using the methodology and codes as discussed in section 3.2.8. These parameters include the six group β effective and λ , total β effective, and reactivity versus positive and negative doubling times.

9.2 Physics Test Manual

The purpose of the physics test manual is to document the predicted behavior of the reactor core as a function of burnup and power level. It is intended to be used for operator guidance and the site engineer. This report includes startup test predictions and sufficient information to calculate reactivity balance throughout the cycle. Parameters typically required throughout the cycle include power deficits, boron worths, control rod worths as a function of burnup and shutdown boron concentrations. Any additional calculations are performed as needed.

10. References

1. Oconee Nuclear Station, Units 1, 2, and 3, Updated Final Safety Analysis Report, Docket Nos. 50-269, -270, and -287.
2. Nuclear Design Methodology Using CASMO-3/SIMULATE-3P, DPC-NE-1004A, Revision 0, Duke Power Company, November 1992.
3. UFSAR Chapter 15 Transient Analysis Methodology, DPC-NE-3005-PA, Revision 1, Duke Power Company, June 1999.
4. Fuel Mechanical Reload Analysis Methodology using TACO3, DPC-NE-2008P-A, Revision 0, Duke Power Company, April 1995.
5. Oconee Nuclear Station Core Thermal-Hydraulic Methodology using VIPRE-01, DPC-NE-2003P-A, Revision 0, Duke Power Company, October 1989.
6. Thermal-Hydraulic Statistical Core Design Methodology, DPC-NE-2005P-A, Revision 1, Duke Power Company, November 1996.
7. Extended Burnup Evaluation, BAW-10186P-A, Framatome Cogema Fuels, June 1997 (SER dated January 25, 1999).
8. Letter from D. L. LaBarge (NRC) to W. R. McCollum, Jr. (ONS), Use of Framatome Cogema Fuels Topical Report on High Burnup – Oconee Nuclear Station, Units 1, 2, and 3 (TAC Nos. MA0405, MA0406, MA0407), Docket Nos. 50-269, 50-270, and 50-287; March 1999.
9. Letter from M. S. Tuckman to Document Control Desk, Duke Energy Corporation's Use Of FCF's Extended Burnup Evaluation Topical Report, BAW-10186P-A, August 1999.
10. Fuel Rod Bowing in Babcock and Wilcox Fuel Designs, BAW-10147P-A, Revision 1, Babcock and Wilcox Co., May 1983.

Appendix A

Appendix A - Deleted

Appendix B

List of Revisions

<u>Revision</u>	<u>Date Issued</u>
1	May 1980
2	January 1981
3	April 1981
4	June 1981
5	December 1999

Amendment 1

Responses to Requests for Additional Information

OS801.01

DUKE POWER COMPANY

POWER BUILDING

422 SOUTH CHURCH STREET, CHARLOTTE, N. C. 28242

WILLIAM O. PARKER, JR.
VICE PRESIDENT
STEAM PRODUCTION

November 13, 1980

TELEPHONE: AREA 704
373-4063

Mr. Harold R. Denton, Director
Office of Nuclear Reactor Regulation
U. S. Nuclear Regulatory Commission
Washington, D. C. 20555

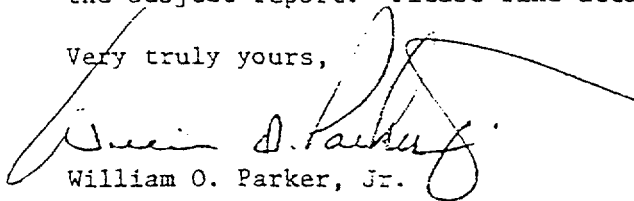
Attention: Mr. R. W. Reid, Chief
Operating Reactors Branch No. 4

Subject: Oconee Nuclear Station
Docket Nos. 50-269, -270, -287
Oconee Reload Design Methodology Technical Report

Dear Sir:

Your letter of October 16, 1980 requested additional information concerning the subject report. Please find attached the requested information.

Very truly yours,



William O. Parker, Jr.

.FTP:scs
Attached

bcc: P. M. Abraham
K. S. Canady
R. H. Clark
R. L. Gill
N. A. Rutherford
L. H. Flores

H. T. Snead
S. T. Rose
G. B. Swindlehurst
J. L. Jones
Master File OS-801.01
Section File OS-801.01

4/84

ATTACHMENT

DUKE POWER COMPANY
OCONEE NUCLEAR STATION

OCONEE RELOAD DESIGN METHODOLOGY
TECHNICAL REPORT

RESPONSES TO NRC QUESTIONS
OF
OCTOBER 16, 1980

Q. 1. Paragraph 3.2.5. Reactivity Coefficients and Deficits.

The described procedure for the calculation of the reactivity deficits involves PDQ07 or EPRI-NODE. However, it is not clear whether for widely different states the reactivity difference due to the spectral component is also included. The same comment applies to the differential boron worth calculation.

- A. 1. The lattice code EPRI-CELL does change cross section libraries as a function of moderator temperature. These cross sections are then used in PDQ07 Version 2 for both color set calculations, which lead to input for EPRI-NODE, and for quarter core calculations. Therefore, the spectral component is included in the calculations of reactivity coefficients and reactivity deficits.

The effects of soluble boron on the flux spectrum is accounted for in two ways. First the soluble boron concentration input to the EPRI-CELL fuel depletion is varied from 1200 ppm at BOL to 400 ppm at 6000 MWD/MTU and is held constant at this concentration for the rest of the depletion. Second, the non-fuel cross sections (eg. control rod guide tubes, reflector, etc.) are generated as a function of soluble boron concentration.

Q. 2. Table 3-1, Shutdown Margin Calculation.

Give a description of the manner in which the "Worth reduction due to burnup of poison material" has been calculated.

- A. 2. CPM has been used to generate a curve of control rod reactivity reduction ($\% \Delta \rho$) as a function of fuel burnup at HFP Nominal conditions. This is changed to a $\%$ reduction in control rod worth versus burnup. For rodded fuel cycles the control rod bank that is inserted is conservatively assumed to have been inserted for the whole cycle. For unrodded (feed & bleed) cycles the lead regulating bank is conservatively assumed to have been inserted 20% for the whole cycle. Knowing the worth of the rod groups, the integral rod worth curve, and the accumulated burnup that each has seen, the burnup penalty can be calculated.

Q. 3. Paragraph 3.2.8, Kinetics Parameters.

Present a more detailed description of the DELAY code. Provide the source of the code, e.g., Duke Power Company.

A. 3. The DELAY code has been written by Duke Power Company. The following four pages have been extracted from the DELAY code manual and describe the theory, equations, and data sources for the code.

1.0 INTRODUCTION

DELAY is a utility type code which calculates the six group delayed neutron β 's, λ 's and also reduces them by a group independent effectiveness value. In addition to this, DELAY calculates the prompt neutron lifetime and then solves the In-hour equation to correlate reactivity insertion and doubling time.

Input for DELAY is available from two dimensional quarter core PDQ calculations and EPRI-CELL fuel depletion calculations.

2.0 THEORY

2.1.1 β_i , λ_i and β_i^{eff} Calculation

β_i is defined as the fraction of fission neutrons produced that appear as delayed neutrons of delayed group i . λ_i is defined as the effective decay constant for the precursors that produce delayed neutrons in delayed group i . These quantities are defined by the following equations:

$$(1) \quad \beta_i = \frac{\sum_{jg} \beta_{ijg} \nu_{jg} \Sigma_{jg}^F \phi_{jg}}{\sum_{jg} \beta_{ijg} \nu_{jg} \Sigma_{jg}^F \phi_{jg}}$$

and

$$(2) \quad \lambda_i = \frac{\sum_{jg} \lambda_{ijg} C_{ijg}}{\sum_{jg} \lambda_{ijg} C_{ijg}}$$

where

$(\nu \Sigma^F)_{jg}$ is the neutron production rate, C denotes the concentration of delayed neutron precursors, and the subscripts i, j, g refer to the delayed neutron group, fissioning isotope, and incident neutron energy group respectively.

The concentration of delayed neutron precursors is related to the fission rate by

$$(3) \quad \lambda_{ijg} C_{ijg} = k \beta_{ijg} \nu_{ijg} \Sigma_{ijg}^F \phi_{ijg}$$

Using equation 3, the solution to equations (1) and (2) becomes:

$$(4a) \quad \beta_i = \frac{\sum_{jg} \beta_{ijg} \nu_{jg} \Sigma_{jg}^F \phi_{jg}}{\sum_{jg} \beta_{ijg} \nu_{jg} \Sigma_{jg}^F \phi_{jg}}$$

$$(4b) \quad \beta_i^{effective} = \beta_i \cdot \text{EFFECTIVENESS FACTOR}$$

$$(5) \quad \lambda_i = \frac{\beta_i}{\frac{\sum_{jg} (\beta_{ijg} \nu_{jg} \Sigma_{jg}^F \phi_{jg}) / \lambda_{ijg} C_{ijg}}{\sum_{jg} \lambda_{ijg} C_{ijg}}}$$

where

$$(6) \quad P_{jg} = \frac{v_{jg} \Sigma_{jg}^F \phi_{jg}}{\sum_{jg} v_{jg} \Sigma_{jg}^F \phi_{jg}}$$

is the fraction of the total neutron production rate arising from fissions of isotope j by incident neutrons of group g . Equation (6) is solved using integrated fission rate data from POQ calculations. Suggested effectiveness factors are 0.961 for Ocone and 0.97 for McGuire.

2.1.2 Delayed Neutron Data

Tomlinson's values of delayed neutron parameters have been chosen for DELAY. The values have been reproduced here as Table 1 for documentation purposes and have been used in DELAY.

2.2 Prompt Neutron Lifetime

The prompt neutron lifetime, λ^* is defined

$$(7) \quad \lambda^* = \frac{1}{V_1 \Sigma_{T1}} + \frac{k_2}{V_2 \Sigma_{T2}}$$

where

$$(8) \quad \Sigma_{T1} = \frac{v \Sigma_{F1}}{k_1}$$

$$(9) \quad \Sigma_{T2} = \frac{\Sigma_{R1}}{\Sigma_{T1}} \frac{v \Sigma_{F2}}{k_2}$$

$$(10) \quad V_i = \frac{\sigma_a^{B-10} \text{ at } 2200 \text{ m/sec}}{\sigma_a^{B-10}} \times 220000 \frac{\text{cm}}{\text{sec}} / \frac{\text{m}}{\text{sec}}$$

The parameters and their units are defined in Table 2.

2.3 Reactivity Calculation

The In-hour equation has been simplified to include only the asymptotic reactor period. The form programmed into DELAY is the following:

$$\rho = \frac{\lambda^*}{\tau} + \sum_{i=1}^6 \frac{\beta_i \text{ effective}}{1 + \lambda_i \tau}$$

where τ = asymptotic reactor period
 ρ = reactivity

TABLE 1

Delayed Neutron Data
From Tomlinson AERE-R-6993

Fast Fission

Isotope	Group	λ (sec^{-1})		Relative Abundance		Absol. Gp. Yield (n/100F)	
			\pm S.D.		\pm S.D.		\pm S.D.
U235	1	.0127	.0003	.038	.004	.063	.007
	2	.0317	.0012	.213	.007	.351	.016
	3	.115	.004	.188	.024	.310	.042
	4	.311	.012	.407	.010	.672	.034
	5	1.40	.012	.128	.012	.211	.022
	6	3.87	.548	.026	.004	.043	.007
U238	1	.0132	.0004	.013	.001	.058	.007
	2	.0321	.0009	.137	.003	.502	.037
	3	.139	.007	.162	.030	.712	.129
	4	.358	.021	.388	.018	1.708	.120
	5	1.41	.099	.225	.019	.989	.089
	6	4.02	.317	.075	.007	.330	.036
Pu239	1	.0129	.0003	.038	.004	.024	.003
	2	.0311	.0007	.280	.006	.179	.013
	3	.134	.004	.216	.027	.138	.019
	4	.331	.018	.328	.015	.210	.018
	5	1.26	.171	.103	.013	.066	.010
	6	3.21	.378	.035	.007	.022	.004
Pu240	1	.0129	.0006	.028	.004	.022	.004
	2	.0313	.0007	.273	.006	.238	.024
	3	.135	.016	.192	.079	.162	.065
	4	.333	.046	.350	.030	.315	.040
	5	1.36	.304	.128	.027	.119	.027
	6	4.04	1.16	.029	.009	.024	.007
Pu242 [†]	1	.0129		.004		.006	
	2	.0295		.195		.31	
	3	.131		.162		.26	
	4	.338		.411		.56	
	5	1.39		.213		.35	
	6	3.55		.010		.016	

TABLE 2

Parameters for Prompt Neutron Lifetime Calculation

Parameter	Description	Units	Source
k_1	$k_{\text{effective}}$, fast group	none	PDQ
k_2	$k_{\text{effective}}$, thermal group	none	PDQ
Σ_R	Removal cross section to thermal group	cm^{-1}	PDQ flux weighted edit fuel only
$\nu\Sigma_{F1}$	Neutron production cross section in fast group	cm^{-1}	PDQ flux weighted edit fuel only
$\nu\Sigma_{F2}$	Neutron production cross section in thermal group	cm^{-1}	PDQ flux weighted edit fuel only
Σ_{T1}	Total cross section fast group	cm^{-1}	equation 8
Σ_{T2}	Total cross section in thermal group	cm^{-1}	equation 9
v_1	Neutron velocity, fast group	cm/sec	equation 10
v_2	Neutron velocity, thermal group	cm/sec	equation 10
$\sigma_{B10}(2200\text{m})$	Thermal cross section at 2200 m/sec for B_{10} ($3.84\text{E}+3$)	barns	Chart of the Nuclides
σ_{ai}	Average boron cross section for group i	barns	PDQ
λ^*	Prompt neutron lifetime	sec	equation 7

Q. 4. Paragraph 3.3.2. Start-up Accident

Give the variation of the total (and its components) reactivity for the start-up accident for the first 10 seconds after the accident initiation, (these would complement Fig. 14-1 and 14-2 of the Oconee FSAR Rev 16).

- A. 4. The variation of the total reactivity during a start-up accident is the sum of three reactivity effects. The withdrawal of the control rod banks adds positive reactivity which causes the neutron power level to increase and raise the average core temperature. The increase in fuel temperature causes a negative reactivity feedback due to the negative Doppler coefficient. The increase in power level increases heat transfer from the fuel to the coolant, resulting in an increase in moderator temperature. This causes a positive reactivity feedback since a positive beginning of cycle moderator coefficient is assumed. The transient response is primarily determined by the rate of positive reactivity addition from the withdrawal of rods, and the Doppler feedback which slows or terminates the nuclear excursion. The moderator feedback has a smaller effect.

The reactivity response of the startup accident simulation performed by B&W and used in the original FSAR analysis is not available. In order to respond to the question, the variation of the total reactivity and its components were back-calculated from the results presented in FSAR Figures 14-1 and 14-2, utilizing the analysis assumptions specified in the FSAR. Using this method, the trends of the parameters of interest can be determined with a reasonable degree of accuracy. Figures 4-1 and 4-2 show the variation of the reactivity consistent with FSAR Figures 14-1 and 14-2 respectively. It should be noted that these figures do not represent the first 10 seconds of the transients, considering that the initial conditions are $10E-9$ rated power and 1% k/k subcritical. Figures 4-1 and 4-2 illustrate the time interval of greatest interest during the transient, Figure 4-1 is the same scale as Figure 14-1, and Figure 4-2 is the first one second of the response in Figure 14-2. For both transients the reactivity addition for the first 10 seconds following initiation of rod withdrawal would only cause a reduction in the subcriticality margin.

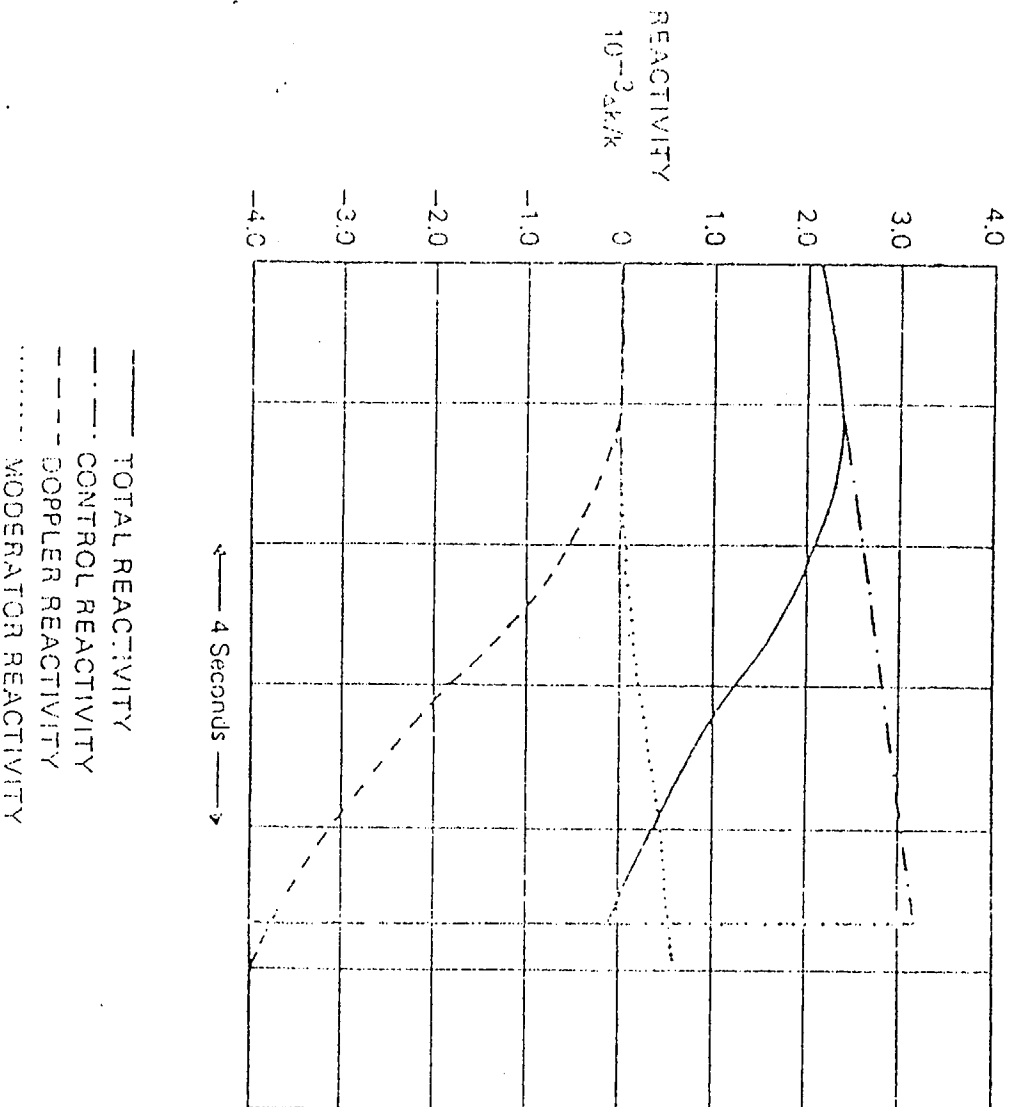


Figure 4-1. (FSAR Figure 14-1)

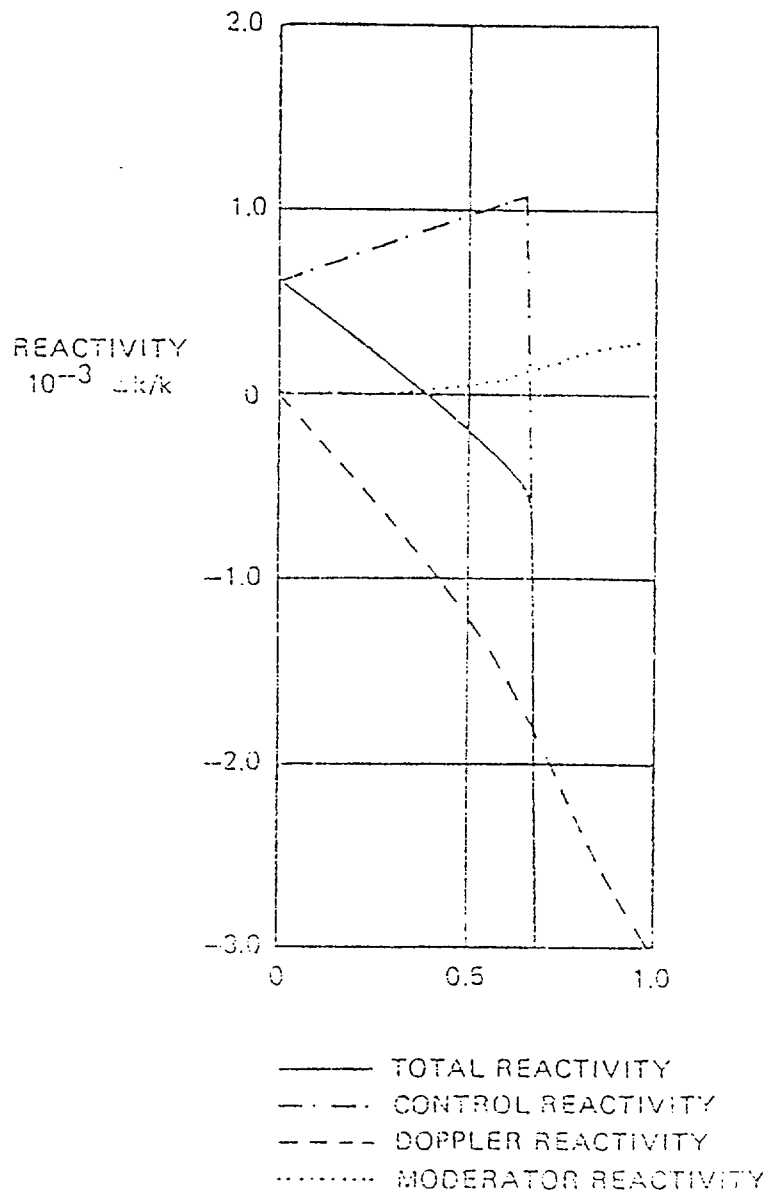


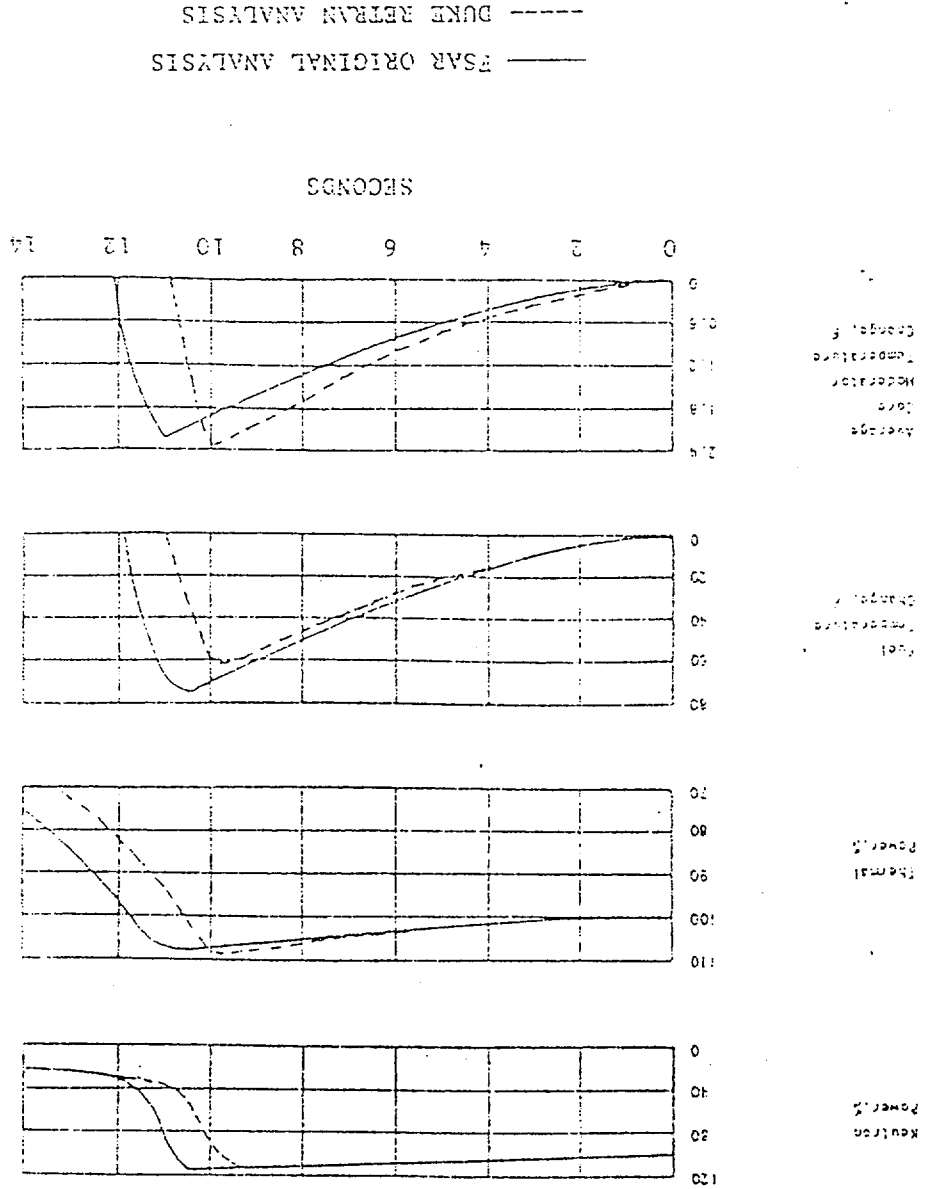
Figure 4-2. (PSAR Figure 14-2)

Q. 5. Paragraph 8.3.3. Rod Withdrawal Accident at Rated Power Operation

Give the variation of the reactivity as in 4. above.

A. 5. The reactivity response of the rod withdrawal accident at rated power simulation performed by B&W and used in the original FSAR analysis is not available. In order to respond to the question a similar analysis was performed by Duke Power Company using the RETRAN code and matching as accurately as possible the modeling assumptions of the original analysis. Figure 5-1, a revised FSAR Figure 14-9, shows the comparison between the original analysis (solid lines) and the new analysis (dashed lines). No attempt was made to match the results of the original analysis, the intent being to match the assumptions and initial conditions. The similarity between the results of the two analyses supports the conclusion that the reactivity response of the new analysis shown in Figure 5-2 is representative of the original analysis.

Figure 5-1 (FSAR Figure 14-9)



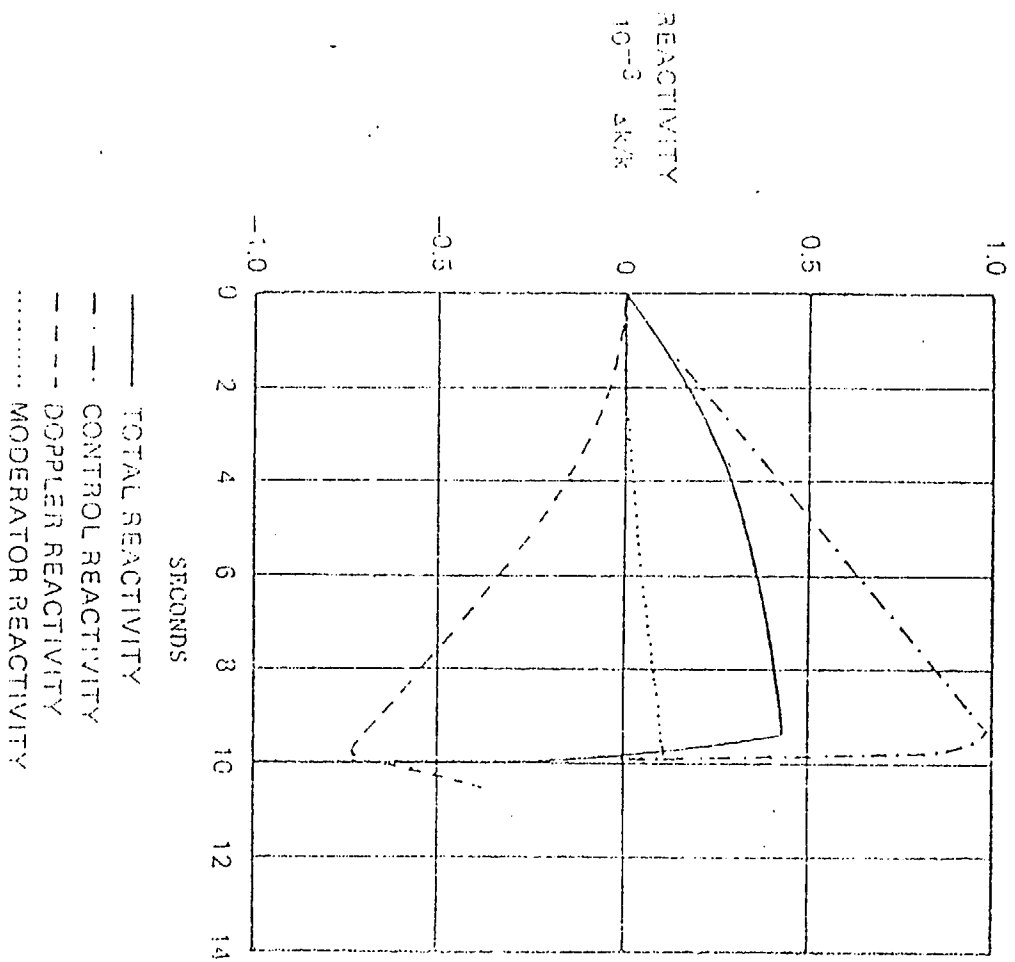


Figure 5-2 (FSAR Figure 14-9)

Q. 6. Paragraph 8.3, Discussion of Individual Accidents

Have the computer codes used in accident analysis (summarized in Appendix A) been updated and revised since the Oconee FSAR was issued? If so, would the general conclusions of the accident analysis change if the analysis was to be performed with the updated codes? Justify your conclusion.

A. 6. The computer codes summarized in Appendix A of NRS-1001 are primarily the nuclear, thermal, and thermal-hydraulic analysis codes intended for the reload core design. All the codes necessary for accident analyses are not included in that appendix.

The analysis of the loss of coolant accident was revised since the issuance of the Oconee FSAR using updated codes. BAW-10103 represents this revised analysis. Although many of the other accidents have not been reanalyzed utilizing updated codes, it is believed that the general conclusions of the existing analyses would not change if the analysis was repeated utilizing state-of-the-art computer codes. This conclusion is based on the premise that the earlier computer codes employed generally conservative modeling compared to the more accurate modeling utilized in current computer codes. Furthermore, the input parameters and assumptions employed in establishing the plant models have the dominant influence on accident consequences.

As discussed in the report, the safety analysis review performed during reload design involves a thorough review of the input data and assumptions used in the accident analyses and a comparison to the values generated by the reload design. The goal of the review is to verify that the reload design values remain bounded by the accident values and thus confirm that the safety analyses remain valid.

Q. 7. Paragraph 8.3.4. Moderator Dilution Accident

"Additional Analysis" is claimed to demonstrate complete protection during refueling operations. Give more information of this analysis.

A. 7. The "Additional Analysis" referred to is summarized in FSAR Section 14.1.2.4.2, the last paragraph on page 14-9. This paragraph is reproduced below.

During refueling or maintenance operations when the reactor closure head has been removed, the sources of dilution water makeup to the letdown storage tank--and therefore to the reactor coolant system--are locked closed, and the high pressure injection pumps are not operating. At the beginning of core life when the boron concentration is highest, the reactor is about 9.5 per cent $\Delta k/k$ subcritical with the maximum worth rod stuck out. To demonstrate the ability of the reactor to accept moderator dilution during shutdown, the consequences of accidentally filling the letdown storage tank with dilution water and starting the high pressure injection pumps have been evaluated. The entire water volume from the letdown storage tank could be pumped into the reactor coolant system (assuming only the coolant in the reactor vessel is diluted), and the reactor would still be 4.9 per cent $\Delta k/k$ subcritical.

Q. 8. Paragraph 8.3.6. Loss of Coolant Flow

It is stated that the hot channel power peak augmentation factors, fuel densification, and rod bow effects are not expected to change for the reloads; however, it is not stated how this conclusion has been arrived at.

- A. 8. Hot channel power peak augmentation factors are associated with the mechanical design of the fuel assembly. The mechanical design is not normally modified in the reload design process. The fuel assembly design for Oconee has a history of very few modifications, none significantly affecting mechanical or nuclear performance. For example, the hot channel factors which account for the effect of statistical uncertainty in parameters such as enrichment, fuel rod loading, and geometry on the fuel rod heat flux and heat generation rate, remain valid for all fuel manufactured within the specified tolerances in these parameters.

The presently accepted treatment of the fuel densification effect on minimum DNBR analysis is the use of densified fuel stack length for calculating the heat flux. The original analysis was based on an initial fuel density of 92.5%, which produced the maximum stack length reduction compared to the subsequent reload fuel batches consisting of higher density fuel. For each reload, values of the densified heat flux are evaluated in the thermal hydraulic design analysis section of the reload report.

The effect of fuel rod bowing, dependent on the fuel assembly mechanical design and burnup, is explicitly factored into the thermal-hydraulic design of the reload core. The reactor protection system setpoints necessary for DNBR protection are established to provide the necessary margin to account for the effect of fuel rod bowing, as discussed in Sections 4.3 and 6.10 of NFS-1001.

Q. 9. Paragraph 8.3.9, Steam Line Failure

It is stated in the accident description that continued feedwater flow in the affected steam generator, combined with excessive heat removal and primary cool down the reactor may experience "a return to low power levels." There is not quantification of this power level, its potential consequences, or measures and actions for the return of the reactor to subcritical. Under what conditions is there a minimum of rod worth which could have the most adverse effects?

A. 9. The answers to these questions may be found in the Oconee FSAR, Chapter 14 and Supplement 3. However, a brief response summarizing the FSAR material follows.

A number of cases involving a variety of secondary system behavior during a steam line break are evaluated in the FSAR. Cases involving failure to isolate the affected steam generator, excessive feedwater addition due to malfunction in the feedwater control function, or of the auxiliary feedwater in addition to the continuing feedwater to the affected steam generator predict a return to power (1% FP, 3% FP, 35% FP, respectively) for a brief period of time. In each case, the reactor is returned to a subcritical condition by the action of the ECCS (high pressure injection, core flood tank and low pressure injection) within 350 seconds. The return to power situations are calculated to occur with the conservative assumption of the minimum tripped rod worth associated with the minimum shutdown margin specified in the Technical Specifications and considering the highest-worth rod to be stuck out.

Q. 10. Supplement 2, Figure 4-1 and Paragraph 3.1.1.1.

Figure 4-1, Supplement 2 appears to contradict the statement in paragraph 3.1.1.1 that reads:

"NON-fuel cross sections with the exception of burnable poison assemblies and control rods are also generated using EPRI-CELL. Cross sections for burnable poison assemblies and control rods for use in diffusion theory calculations are generated by matching reaction rates between the diffusion theory code PDQ07 and CPM (a collision probability code)."

Give a more detailed description of the procedure for control rod and burnable poison cross section generation and the use of burnable poison cross sections in PDQ07-HARMONY depletion calculations.

A. 10. While there appears to be a contradiction both statements have merit. The ARMP procedure for generation of burnable poison cross sections was developed from CPM and PDQ07 calculations. The procedure however needs only EPRI-CELL and PDQ07 calculations to use it. Detailed description of the procedure can be found in the "Advanced Recycle Methodology Program System Documentation, September 1977." Part I Chapter 6 Section 4.2 describes the development of the procedure using CPM and PDQ07 while Section 4.3 describes the procedure using EPRI-CELL and PDQ07.

The procedure for developing control rod cross sections is described in Part I Chapter 6 Section 3.4 of the "Advanced Recycle Methodology Program System Documentation, September 1977."

Q. 11. Supplement 2, Paragraph 3.2, Comparison of ARMP PDQ07 to Cold Criticals.

The two-dimensional simulation of the cirticals has not been performed at Duke nor with PDQ07, yet it was concluded that the results would have been identical with the PDQ07 results. Justify the above conclusion.

A. 11. The cold criticals have been simulated with PDQ07. The results have been published in Part I Chapter 2, Rev. 1 of the ARMP System Documentation. This work was performed under EPRI Research Project 11S-1.

These benchmark calculations use standard ARMP methodology, standard ARMP codes (EPRI-CELL, NUPUNCHER, PDQ07) and Duke Power also uses these codes and methodology. Therefore, if the calculations had been performed at Duke Power the results would have been identical.

- Q. 12. Supplement 2, paragraph 3.4, Conclusions.

The conclusions for the calculated results of the peak power are not tenable. There is no reason why the diffusion theory estimation by PDQ07 of the local radial peaking should be more conservative than those calculated with transport theory codes, or the measured values. This result must be regarded as fortuitous. For example (Fig. 3-4), many fuel assembly maxima were underpredicted by PDQ07. Justify the conclusion that PDQ07 will always be conservative in peak power predictions and present physical arguments for this justification.

- A. 12. In Section 3, PDQ07's ability to conservatively predict the assembly local radial is addressed. In Figures 3-2, 3-3, and 3-4, it was shown that the maximum local radial as calculated by PDQ07 was conservative with respect to the measured or transport theory calculated values for three completely different lattice conditions. Each of these figures show the pin-wise power distributions within a single fuel assembly.

In Figures 3-2, 3, 4, the eight highest measured (or EPRI-CPM calculated) pin powers were selected. The means and standard deviations of the (calculated-measured) difference were tabulated for all three groups together, and by each group (by Figure) individually.

In these samples, the mean was taken as the sample mean with the true standard deviation unknown. Then 95% confidence limits of the true mean were determined by:

$$\bar{D}_{U,L} = \bar{D} \pm \frac{t(.025, n-1) * S(D)}{\sqrt{n}}$$

Table 1 displays the results of this analysis.

Table 1

95% Confidence Level Estimates of the C-M
Radial Local Means

Figure	n	\bar{D}	S (D)	\bar{D}_U	\bar{D}_L
3-2	8	.0070	.01739	.0215	-.0075
3-3	3	.02225	.01268	.0329	.0116
3-4	3	.0105	.008767	.0178	.0032
3-2, 3, 4	24	.01325	.01445	.0194	.0071

A. 12. cont'd.

Since $\bar{D} > 0.0$ for all four sample groups, it is concluded that PDQ07 would overpredict the mean radial local of the highest power pins within an assembly. Furthermore, using 95% confidence limits estimates, PDQ07 over-predicts the mean radial local in the lower 2.5% interval ($\bar{D}_L > 0.0$) for three of the four cases considered.

Besides the observations in Chapter 3 of Supplement 2, the Oconee fuel assembly employs a uniform lattice with a small interassembly water gap. A water hole's area is only as large as that of a fuel rod so that thermal flux peaking is minimized. Likewise, even at cold conditions, the nominal water gap between assemblies is only 12% of a pin pitch.

Thermal physics constants are standardly calculated using the Mixed Number Density (MND) procedure. Thermal absorption and fission constants are products of their respective 2200 m/sec cross sections and the cell average velocity (relative to 2200 m/sec). Thermal diffusion constants are treated in a similar fashion.

Thermal reaction rates in PDQ07 are proportional to the magnitude of the thermal flux. When excess thermalization occurs, e.g., near a water hole, MND cross sections conservatively yield higher thermal reaction rates than conventional cross sections.

This conservatism of the MND method is shown in Figure 1. Here a comparison was made of MND and conventional PDQ07 pin powers relative to EPRI-CPM. The data source for the MND PDQ07 and EPRI-CPM assembly simulation was Figure 3-4 of Supplement 2. It was shown that for the eight maximum pin powers, MND cross sections yielded a mean percent difference of .99%; while the conventional cross section PDQ07 had a nonconservative mean of -.31%.

The statistics presented in Supplement 2 justify use of a radial ONRF of 1.03 for unrodded fuel cycles. We have suggested use of 1.05 which allows approximately two percent conservatism for any local pin peak uncertainties.

The above statistics, physical geometry, and modeling procedures support the conclusion that no additional uncertainty is needed on the radial local peak. However, a 2% conservatism is built into the 1.05 radial ONRF we propose using.

A.12

FIGURE 1

PERCENT DIFFERENCE COMPARISON OF PIN POWERS

REFERENCE CALCULATION: EPRI-CPM

CODE USED	PDQ07	PDQ07	EPRI-CPM
MODEL	1/4 ASS'Y	1/4 ASS'Y	1/4 ASS'Y
X-SECTIONS	MND	CONV	CPM
%FP	100	100	100
PPMB	0.0	0.0	0.0

IT							
-0.79	.29	MND PDQ07					
-1.58	-.59	CONV PDQ07					
-0.30	0.0 ^⑥	X					
-.10	-.96	X					
-.40	.98	.85 ^①	2.45 ^⑤				
.20	.69	-.38	.94				
-.40	.98	1.04 ^③	1.76 ^①	X			
.40	.79	-.28	-.19	X			
-.30	.10 ^⑧	X		1.13 ^④	.58 ^⑦		
.30	-.58	X		-.56	-.48	.41	
-.82	.30	-.29	.60	-.21	-.84	-1.28	
.21	.40	-.78	.50	.41	.21	0.0	
-1.25	-.94	-.52	-.73	-1.05	-1.38	-1.61	-1.52
.10	.21		.31		0.0	-.11	-.11

*NOTE: PIN #1 IS THE PEAK LOCAL RADIAL,
#2 - THE SECOND HIGHEST PIN, ETC.

- Q. 13. Supplement 2, paragraph 4.2, Oconee Fuel Cycle Simulation.

It appears that the EPRI-NODE-P almost consistently under-predicts the assembly peak power for cycles 2 and 3. Justify the conclusion in paragraph 4.3 that the EPRI-NODE-P "yielded consistently good power distributions..."

- A. 13. Conclusions about power distributions are reached in view of the global behavior of EPRI-NODE-P. The Cycle 3 data was shown in Section 4 of Supplement 2 only for illustrative purposes since the measured data was not considered benchmark quality as the other four cycles.

The derived total ONRF from chapter 5 was 1.10 for rodged cycles. Only 6% of the products of the ONRF and calculated peak exceeded the cycle 2 measured peaks. Therefore, based on a 95/95 criterion, the agreement was judged good.

- Q. 14. Supplement 2, Figure 4-2 through 4-127.

The EPRI-NODE-P calculated power distributions for the first four cycles of operation of Oconee 1 consistently underpredicted the relative power in assembly H-8, often by more than 10%. Is the reason for this anomaly known?

- A. 14. Yes. It is current Duke design practice to perform only one radial power normalization at approximately 25 EFPD. The normalization is referenced to a two-dimensional discrete pin model PDQ07 power distribution.

The normalization is performed such that there is good radial power agreement in both the central nine (H-8 included) and the peripheral assembly regions. Since only the internal leakage factor, g_h , was adjusted for the central nine, agreement of the central nine as a whole was addressed rather than H-8 specifically. This method yielded radial differences of 5% or less early in each cycle for H-8 as shown by Figures 4-4, 4-41, and 4-87. Assembly K-9 in Cycle 3 had a 20% larger radial at BOC than H-8, therefore the central nine normalization gave a more accurate agreement with a more limiting assembly. Cycles 1, 2, and 3 were all rodged cycles, and therefore rod interchanges severely changed the radial power shape. A radial power renormalization to PDQ07 after the rod interchange would have significantly improved radial and peak agreement.

The reactors at Oconee will soon all be operated in the unrodged mode and so only the statistics for Cycles 4 and 5 are representative of future design calculations.

In Cycle 4, the largest radial power difference for H-8 was 3.3%. In Cycle 5, differences of up to 10% were seen. However, H-8 was a low power assembly, and K-9 was the assembly of concern. Good agreement was shown between assemblies K-9 and also H-9 throughout this cycle.

The only other method of assuring less than 5% power difference to H-8 would have been to apply a K_{eff} multiplier. Such an ad hoc method of normalization is contrary to Duke design practice.

Q. 15. Supplement 2, paragraph 5.2, Normality Test Results.

All data sets have been used with the assumption of normal distribution, yet some have failed the normality test. Justify the use of the data sets as normal.

A. 15. The D' test for normality is a very rigorous test, and in Table 5-1 of Supplement 2 it was shown that nine of 16 individual and grouped data sets passed the normality criteria outright - with a 5% level of significance.

Table 1 below presents the percent differences by which the other seven data sets missed the D' percentage point cutoff values for normality. Of these seven, four data sets were combinations of individual nonnormal datasets which in turn, carried inherent near-normality into the larger sets.

Table I

Nearly Normal Data Sets

<u>Cycle</u>	<u>Type</u>	<u>N</u>	<u>Percent Difference from Cutoff</u>	<u>Figure</u>
1	Radial	308	-2.16%	5-11
1,2	Radial	455	-1.75%	5-21
1,2,4,5	Radial	730	-1.56%	5-23
1	Peak	377	- .26%	5-16
3	Peak	211	-3.67%	5-19
1,2	Peak	612	-1.38%	5-24
1,2,4,5	Peak	1027	-1.72%	5-26

The argument presented in paragraph 5.2 was that although certain distributions did not pass the normality test criteria, an ocular inspection of the histograms indicated that, for engineering purposes, normality would be a reasonable approximation of these distributions. This is further supported by Table I above.

It should also be noted that cycle 4, cycle 5, and cycle 4 & 5 radial and peak power data sets passed the normality test. These unrodded cycles are typical of future Ocone reload designs.

DUKE POWER COMPANY
POWER BUILDING
422 SOUTH CHURCH STREET, CHARLOTTE, N. C. 28242

WILLIAM O. PARKER, JR.
VICE PRESIDENT
STEAM PRODUCTION

TELEPHONE: AREA 704
373-4083

January 28, 1981

Mr. Harold R. Denton, Director
Office of Nuclear Reactor Regulation
U. S. Nuclear Regulatory Commission
Washington, D. C. 20555

Attention: Mr. R. W. Reid, Chief (40)
Operating Reactors Branch No. 4

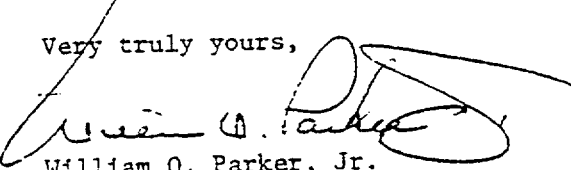
Subject: Oconee Nuclear Station
Docket Nos. 50-269, -270, -287
Oconee Reload Design Methodology Technical Report

Dear Sir:

Please find attached Revision 2 to the Reload Design Methodology Technical Report (NFS-1001) for the Oconee Nuclear Station. Only those pages which have been changed from Revision 1 are provided in Attachment 1. Please replace the corresponding pages of the subject report with the newly revised pages of Attachment 1. It should be noted that Section 4 of the report is revised in its entirety.

In addition, Attachment 2 provides supplemental responses to Duke Power's submittal of November 13, 1980, which responded to the Staff's questions of October 16, 1980, concerning the subject report.

Very truly yours,


William O. Parker, Jr.

FTP:pw
Attachments

bcc: P. M. Abraham
N. A. Rutherford
R. H. Clar
H. T. Snead
Master File OS-801.01

K. S. Canady
R. L. Gill
R. M. Gribble
J. L. Jones
Section File OS-801.01

DUKE POWER COMPANY
OCONEE NUCLEAR STATION

Attachment 2

Supplement to Duke Responses of November 13, 1980
to NRC Questions of October 16, 1980

Questions 11 and 12

- Re Q. 11 NRC reviewer would like a copy of the work performed under EPRI Research Project 118-1.
- Re A. 11 Enclosed is a copy of the EPRI-CELL Criticals Benchmarking portion of Project 118-1. Figures 6-5 and 6-6 of 118-1 correspond to Figures 3-2 and 3-3 in Supplement 2 of NFS-1001.

Advanced Recycle Methodology Program
System Documentation

Research Project 118-1

EPRI-CELL Criticals Benchmarking

October 30, 1978

Prepared for:

Electric Power Research Institute
3412 Hillview Avenue
Palo Alto, CA 94304

Principal Investigators

W. J. Eich (NAI)*
M. L. Kennedy (NAI)
R. D. Mosteller (Science Applications, Inc.)

EPRI Project Manager

B. A. Zolotar

Prepared by:

Nuclear Associates International Corporation
6003 Executive Boulevard
Rockville, MD 20852

With revisions by:
Electric Power Research Institute

* Current affiliation: Electric Power Research Institute
Palo Alto, CA 94303

TABLE OF CONTENTS

<u>Section</u>	<u>Title</u>	<u>Page</u>
1	OVERVIEW	2-1
2	ANALYTIC PROCEDURE	2-2
3	PRINCIPAL UO ₂ RESULTS	2-5
4	PRINCIPAL MO ₂ RESULTS	2-9
5	SUPPLEMENTARY INFORMATION AND OTHER RESULTS	2-11
6	LARGE-SCALE MOCK-UP RESULTS	2-18
E	REFERENCES	E-1

effect, however, adds several tenths of a percent in reactivity to very watery lattices but such are so far from reactor conditions that their analysis lacks most practical relevance.) Finally, the two items of input required for the simulation of grain heterogeneities have been entered for the MO_2 cases.

Box 3 of Figure 2-1 signifies the non-depletion EPRI-CELL (GAM/THERMOS) run which produces printed output (Box 4) and, by option, the few PDQ-7 input cards containing the macroscopic few group EPRI-CELL output in Table Set Format (Box 5). These cards are part of the input to a "one-dimensional" radial plane PDQ-7 - Box 7 (one mesh in the Z-direction with zero current boundaries). Another item of input is the axial buckling, B_2^2 , (Box 6) which has generally been measured. If this buckling was not available in the literature, then it has been accurately estimated from measured critical water heights and reflector savings measured in similar lattices. Since the criticals analyzed in the course of this Program have been restricted to arrays having relatively high moderator heights, dependence of the final value of k_{eff} (Box 8) is quite minimal on axial buckling uncertainty. Another item of input to these PDQs is a set of (four fast group) reflector constants which were developed to match the results of multigroup transport (P3) calculations⁴. These critical analyses could as validly have been conducted with 3 fast groups *mutatis mutandis*⁵ but the effort had been initiated before the installation of the collapsed broad group edits. The Mixed Number Density model is implicit in the core and reflector thermal group constants used in these PDQ calculations.

The approach used in analyzing large-scale mock-up experiments differs in some respects from the procedure discussed above. That approach is described in more detail in Section 6 of this Chapter.

SECTION 6LARGE-SCALE MOCK-UP RESULTS6.1 Introduction

Figure 6-1 schematically illustrates the calculational process followed in the analysis of five large-scale mock-ups. The procedure is basically similar to the approach described in Section 2 of this chapter for critical lattices. There are three principal differences between the two methodologies:

- (1) the large-scale mock-ups were analyzed for the verification of existing ARMP libraries and procedures rather than to aid in the development of the system
- (2) the mock-ups were sufficiently heterogeneous that two-dimensional rectangular diffusion theory calculations were required in place of one-dimensional radial calculations
- (3) separate EPRI-CELL calculations were required for different parts of lattices--fuel pins, water holes, and burnable poison pins

These mock-ups are of special interest because they permit accurate determination of the worth of burnable poison rods (BPR's). Heretofore, BPR contributions to reactivity in PWR's have been subsumed into core analyses which integrate a number of additional effects, such as control rod worth, Xenon worth, Doppler defect, and soluble boron worth. These mock-ups, however, determine the BPR worth up to 9 percent $\Delta\rho$ by means of straightforward soluble boron substitution. Furthermore, these particular BPR's have a boron loading which is approximately 70 percent heavier than that for PWR assemblies of any current design. The agreement achieved with the experimental data therefore uniquely validates the ARMP representation of burnable poisons and, in addition, further substantiates the benchmarking of EPRI-CELL against critical experiments, which is described in the preceding sections of this chapter.

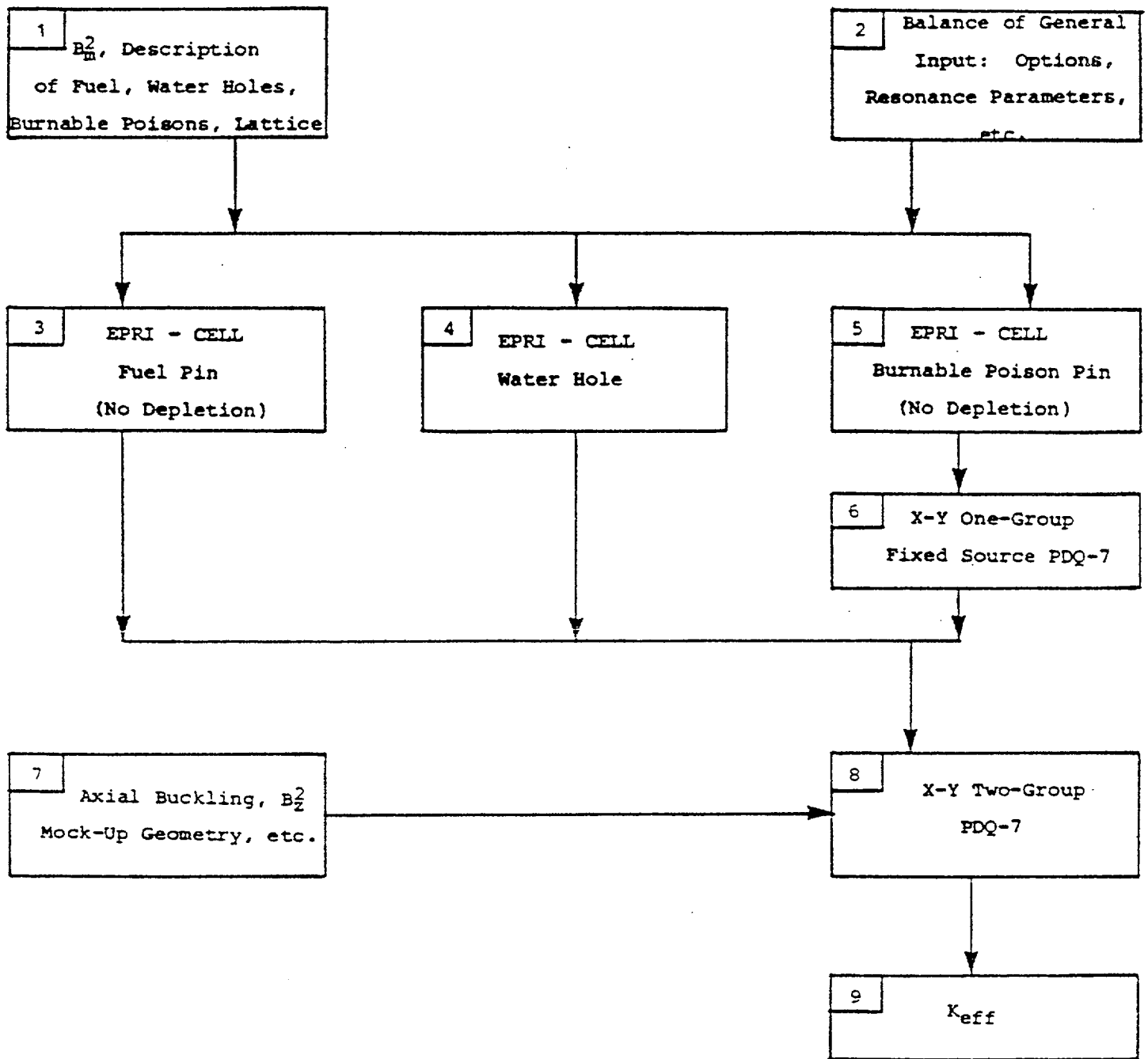


FIGURE 6-1 Flow Chart for Large-Scale Mock-Up Analysis

6.2 Description of Experiments²¹

The experimental configuration employed in these critical mock-ups is shown in Figure 6-2. The subassembly regions indicated there are fictitious in the sense that there is no structural material in the active region of the geometry and that there is no physical significance to the subassembly boundary. A subassembly region, however, does correspond to a 15 x 15 assembly in size and configuration. The outer buffer region was comprised only of fuel pins and borated moderator, but the contents of the subassembly regions were rearranged from case to case and the soluble boron concentration was adjusted until a multiplication factor of 1.0007 was achieved. The subassembly configurations for the different cases, or "loads," are summarized in Figure 6-3. All locations other than those indicated are fuel cells.

The fuel pins and burnable poison rods are described in Table 6-1. Unlike normal fuel pins, these pins are clad with aluminum. The BPR's are unclad cylinders of pyrex glass which have a much higher boron content than normal BPR's. Water holes contain nothing but borated water, and moderator characteristics are summarized in Table 6-1, as well. All measurements were performed at room temperature and pressure, with a moderator height of 145 cm.

For the loadings of interest in this study relative power densities were obtained for one octant of the central subassembly. These measurements were made at the midplane of the active height, using a sodium iodide (thallium activated) scintillation counter to count collimated fission-product gamma rays from activated fuel rods.

The five loadings considered here allow direct determination of BPR worth by the method of soluble boron substitution. In load 1 the subassemblies contain a uniform lattice of fuel pins, and the central region is identical to the buffer. In loads 2 and 3, 17

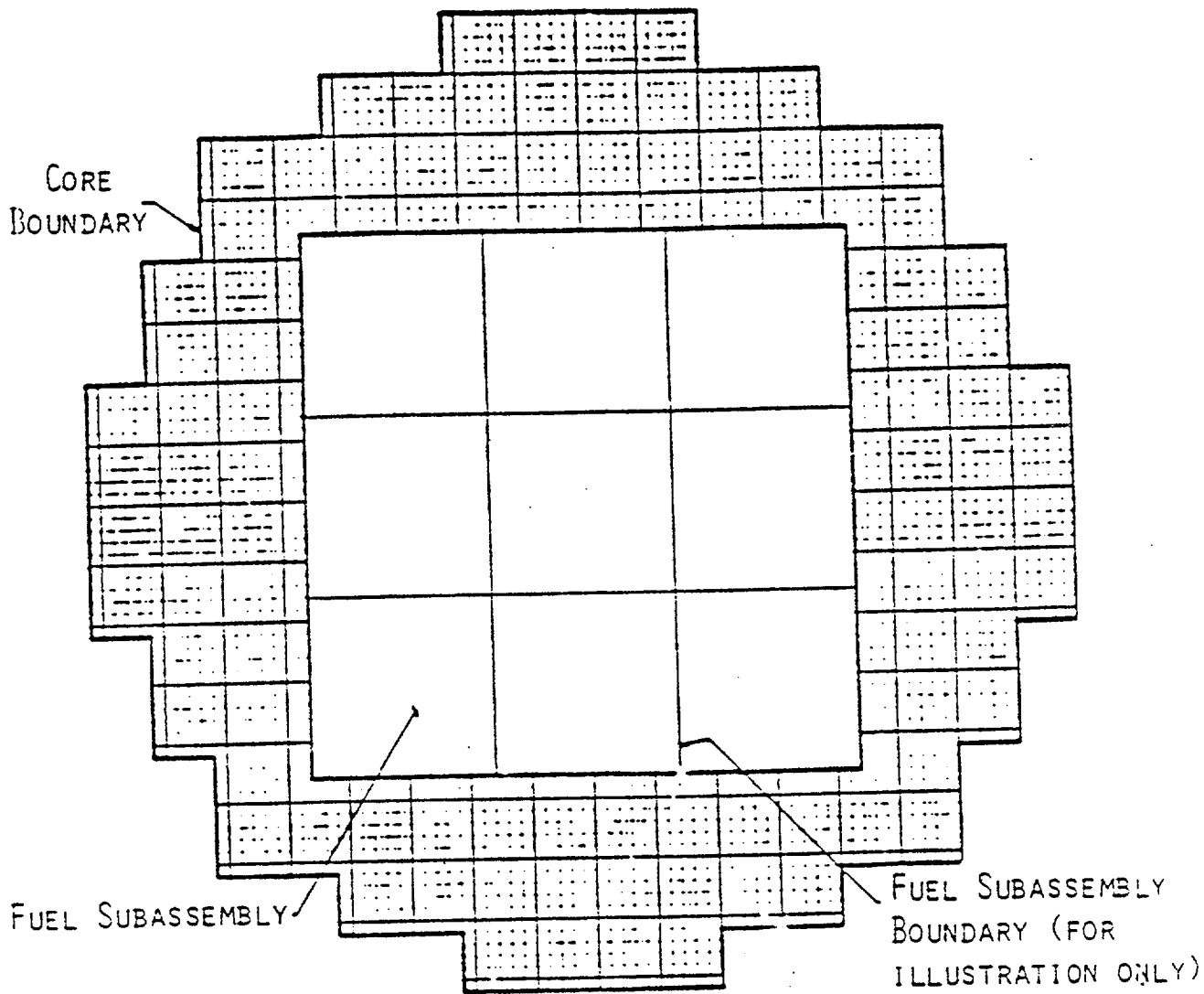
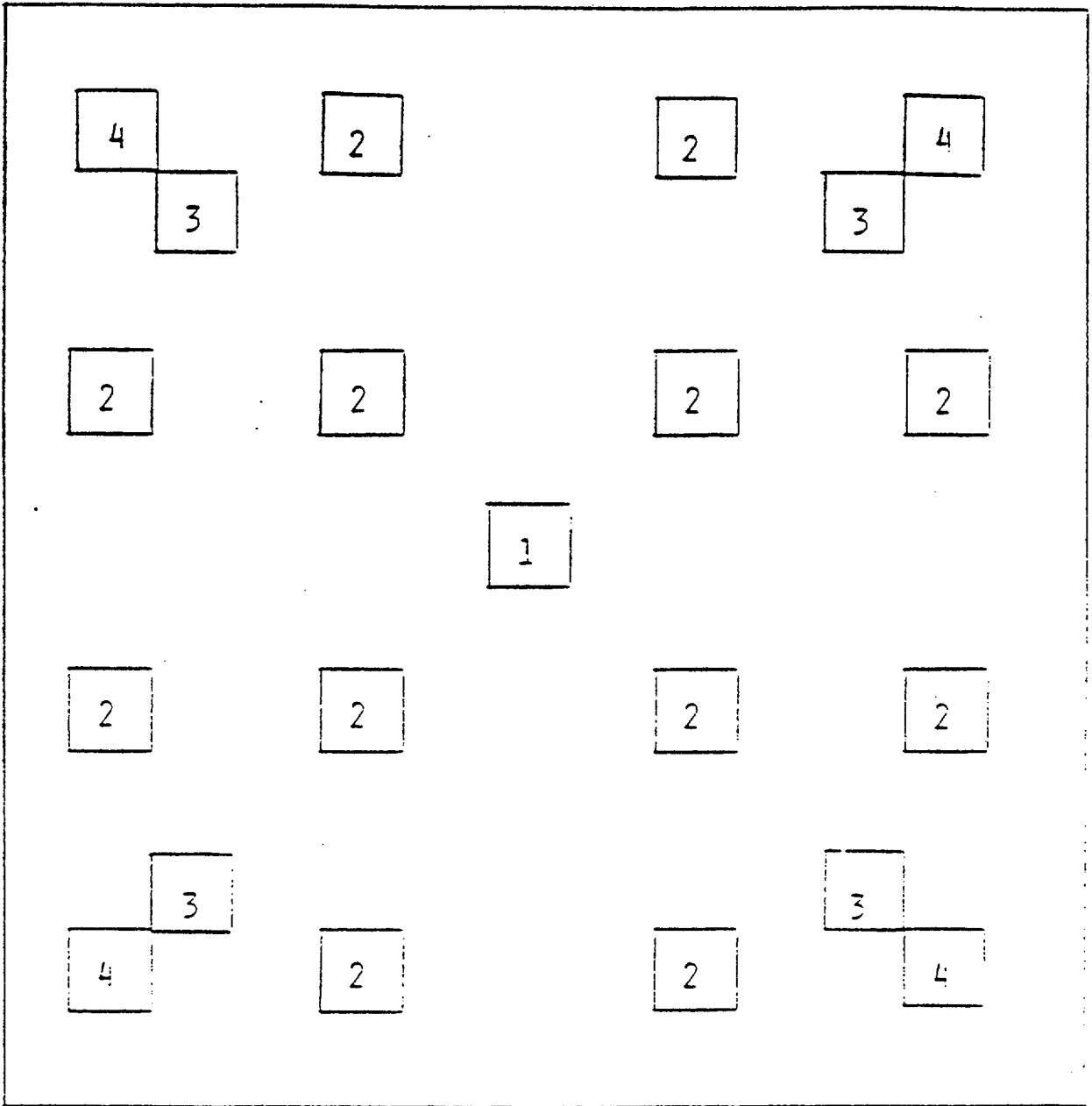


FIGURE 6.2 Geometry for Large-Scale Mock-Up Experiments



	<u>LOAD 1</u>	<u>LOAD 2</u>	<u>LOAD 3</u>	<u>LOAD 4</u>	<u>LOAD 5</u>
LOCATION 1	FUEL	WATER	WATER	WATER	WATER
LOCATIONS 2	FUEL	WATER	WATER	POISON	POISON
LOCATIONS 3	FUEL	WATER	FUEL	POISON	FUEL
LOCATIONS 4	FUEL	FUEL	WATER	FUEL	POISON

FIGURE 6-3 Subassembly Configurations

TABLE 6-1

PHYSICAL CHARACTERISTICS OF PINS AND MODERATOR

Fuel Pin

Enrichment, w/o	2.459, \pm .002
Pellet Material	UO ₂
Pellet Density, g/cm ³	10.24 \pm .04
Pellet Diameter, cm	1.0297 \pm .0013
Active Fuel Length, cm	153.34 \pm .89
Clad Material	6061 Aluminum
Clad Thickness, cm	.0813 \pm .0025
Clad Outer Diameter, cm	1.2060 \pm .0015
Fuel Pin Pitch, cm	1.636 \pm .003

Burnable Poison Rod

Poison Material	Pyrex Glass
Poison Density, g/cm ³	2.244 \pm .008
Poison Diameter, cm	1.170 \pm .001
Boron Content, w/o	3.919 \pm .002
Poison Length, cm	188.0 \pm .1
Clad	None

Moderator

Water Density, g/cm ³	.9978
Water Temperature, °C	21 \pm 1
Soluble Boron Content, ppm	
Load 1	1511 \pm 3
Load 2	1335.5 \pm 3
Load 3	1335.5 \pm 3
Load 8	794 \pm 3
Load 9	779 \pm 3

fuel pins have been removed from each of the subassemblies, leaving borated water in their place. In both loads the subassemblies are octant symmetric, but the water hole locations are slightly different. In loads 8 and 9 the same fuel pins have been removed as in loads 2 and 3, respectively, but BPR's have been inserted in their place everywhere except in the central location of each subassembly. Comparison of results from loads 2 and 8 and from loads 3 and 9 therefore provides a value for the BPR worth in terms of the change in the soluble boron concentration.

6.3 Analytical Procedure

Loads 1, 2 and 8 first were simulated with the standard ARMP PWR procedures described in Part I, Chapter 6 of this documentation, following the process indicated in Figure 6-1. It is to be emphasized that only the standard procedures were used -- more detailed treatments normally employed during benchmarking against critical experiments, such as four energy groups and four mesh spaces per pin cell side in the two-dimensional PDQ calculation, were not needed because of the very low leakage of all these configurations.

This approach produces very good agreement with the experimental data for loads 1 and 8 but not as good for load 2. In the ARMP procedure, a four-group fine-mesh correction is applied to the multiplication factor when water holes are present (see Part I, Chapter 8, Section B), but the discrepancy in the result for load 2 is somewhat beyond the range of the recommended correction factor for operating PWR's. On the other hand, the water density in these mock-up experiments is about 50% greater than under normal operating conditions, and so the higher soluble boron density can produce a larger reactivity discrepancy.

Because the leakage from these mock-up experiments is quite low, a change in group structure would have very little effect and so only a fine-mesh correction is needed. A finer mesh spacing, two

mesh spaces per pin cell side rather than one, was selected and the two-dimensional calculations for loads 1, 2, and 8 were re-run.

As Figures 6-4, 6-5, and 6-6 illustrate, this change produced a significantly better value for the multiplication factor for load 2 and left the multiplication factors for loads 1 and 8, which were already in good agreement with the experimental data, essentially unchanged. (The convention adopted in these Figures is that water holes are represented by an "X" and that BPR's are represented by a "+".) In load 1, no non-fuel locations are present and so no correction is necessary. In load 8, the BPR parameterization itself, which preserves the reaction rate predicted by EPRI-CELL by adjusting the PDQ thermal MND absorption cross section for the BPR, produces a BPR worth which is mesh independent.

Calculations also have been performed for loads 3 and 9, and the results are presented in Figures 6-7 and 6-8, respectively.

Once this mesh change was made in PDQ-7, the ARMP system produced excellent agreement with the measured data from all five loads. No additional modification of any of the ARMP procedures was needed, and it should be emphasized that this one change was necessitated by the high density of the moderator, relative to normal operating conditions. EPRI-CELL therefore has been shown to describe accurately the neutronic behavior of BPR's, even when they are as heavily loaded as the ones in these experiments.

1.026	1.025	1.022	1.018	1.013	1.005	.997	.986
1.026	1.025	1.022	1.018	1.013	1.005	.996	.986
	1.024	1.021	1.017	1.012	1.004	.996	.985
	1.024	1.021	1.017	1.012	1.004	.996	.985
		1.019	1.015	1.009	1.002	.993	.983
		1.019	1.015	1.009	1.002	.993	.983
			1.011	1.005	.998	.989	.979
			1.011	1.005	.998	.989	.979
				1.000	.992	.984	.973
				1.000	.991	.984	.973
					.985	.976	.966
					.985	.976	.966
						.968	.958
						.968	.957
							.947
							.947

Relative Pin Power in Central Subassembly

	K_{EFF}	K_{∞}	M^2
EXPERIMENT	1.0007	-	-
ARMP, STANDARD	.9999	1.0182	35.64
ARMP, FINER MESH	.9998	1.0179	35.64

ARMP, STANDARD
ARMP, FINER MESH

FIGURE 6-4 Comparison of Results for Load 1

X	1.072	.993	.968	.992	.993	.948	.951
	1.085	1.010	.985	.978	.978	.957	.934
	1.085	1.004	.979	.973	.976	.955	.933
	1.033	1.040	1.002	1.013	1.062	.993	.970
	1.075	1.074	1.033	1.028	1.050	.998	.940
	1.058	1.076	1.016	1.011	1.054	.986	.939
	X	1.080	1.082	X	1.035	.930	
		1.087	1.087		1.036	.947	
		1.088	1.089		1.043	.944	
		1.056	1.108	1.096	.999	.894	
		1.096	1.122	1.102	1.003	.939	
		1.069	1.117	1.099	.992	.937	
			X	1.073	.974	.942	
				1.056	.959	.925	
				1.050	.955	.925	
				.982	.941	.940	
				.995	.936	.914	
				.983	.934	.916	
				.939	.919	.890	
				.917	.905	.896	
				.918	.908	.899	

Relative Pin Power in Central Subassembly

	K_{EFF}	K_{∞}	M^2
EXPERIMENT	1.0007	-	-
ARMP, STANDARD	1.0052	1.0240	35.24
ARMP, FINER MESH	1.0018	1.0205	35.25

EXPERIMENT
ARMP, STANDARD
ARMP, FINER MESH

FIGURE 6-5 Comparison of Results for Load 2

X	1.102	.986	1.003	1.015	1.005	1.045	1.079
	1.114	.998	.990	.996	1.005	1.046	1.087
	1.120	.996	.991	.998	1.004	1.046	1.085
	.995	.907	.961	.943	.924	1.027	1.061
	.999	.899	.924	.931	.914	.993	1.077
	1.011	.890	.938	.945	.904	1.003	1.078
			.864	.864		.961	1.044
			.851	.855		.945	1.070
			.844	.845		.932	1.072
			.878	.820	.896	1.007	1.045
			.839	.816	.855	.994	1.090
			.860	.813	.851	1.005	1.092
					.931	1.053	1.093
					.926	1.067	1.123
					.914	1.070	1.121
					1.028	1.095	1.147
					1.021	1.115	1.153
					1.030	1.116	1.150
						1.118	1.151
						1.155	1.178
						1.152	1.174
							1.158
							1.196
							1.191

Relative Pin Power in Central Subassembly

	K_{EFF}	K_{∞}	M^2	
EXPERIMENT	1.0007	-	-	EXPERIMENT ARMP, STANDARD ARMP, FINER MESH
ARMP, STANDARD	.9993	1.0234	35.52	
ARMP, FINER MESH	.9998	1.0234	35.54	

FIGURE 6-6 Comparison of Results for Load 8

X	1.061	.985	.979	.988	.977	.950	.948
	1.086	1.006	.979	.973	.976	.955	.933
	1.030	1.033	.996	1.004	1.036	.993	.940
	1.060	1.076	1.015	1.009	1.052	.985	.938
	X	1.063	1.055	X	1.043	.937	
		1.057	1.052		1.022	.927	
		1.014	1.034	1.080	.997	.931	
		1.021	1.017	1.063	.990	.937	
		.997	1.095	.997	.951		
		1.012	1.059	.986	.933		
		X	1.023	.953			
			1.028	.932			
		.961	.936				
		.963	.917				
		.912					
		.901					

Relative Pin Power in Central Subassembly

	K_{EFF}	K_{∞}	M^2	EXPERIMENT ARMP, FINER MESH
EXPERIMENT	1.0007	-	-	
ARMP, FINER MESH	1.0022	1.0209	35.25	

FIGURE 6-7 Comparison of Results for Load 3

X	1.107	1.003	1.016	1.011	1.011	1.058	1.072
	1.144	1.016	1.011	1.016	1.019	1.058	1.097
	1.013	.901	.961	.958	.931	1.036	1.070
	1.032	.908	.959	.965	.919	1.014	1.088
			.882	.900		.954	1.056
			.875	.880		.940	1.076
			.932	.968	.925	.993	1.055
			.941	.949	.897	1.003	1.086
				.956	.960	1.018	1.082
				.956	.903	1.010	1.094
						.996	1.096
						.961	1.010
						1.045	1.094
						1.055	1.127
							1.105
							1.153

Relative Pin Power in Central Subassembly

	K_{EFF}	K_{∞}	M^2
EXPERIMENT	1.0007	-	-
ARMIP, FINER MESH	.9997	1.0235	35.54

EXPERIMENT
ARMIP, FINER MESH

FIGURE 6-8 Comparison of Results for Load 9

17. V.O. Uotinen, et al., "Lattices of Plutonium-Enriched Rods in Light Water--Part I: Experimental Results," Nucl. Tech., 15, 257 (1972).
18. H. Windsor and R. Goldstein, "Analysis of Lattices Containing Mixed-Oxide Fuel in Particulate Form," Trans. Am. Nucl. Soc., 15, 107 (1972).
19. Askew, et al., op cit.
20. Hellens, op cit.
21. M.N. Baldwin and M.E. Stern, "Physics Verification Program -- Part III, Task 4, Summary Report," BAW-3647-20 (1971).

- Re Q. 12 Additional justification is required to support the conclusion that PDQ07 conservatively predicts maximum pin powers.
- Re A. 12 Nuclear reactor cores are modeled in two dimensions at Duke Power Company using the PDQ07 code. A discrete pin geometry and two neutron energy group Mixed Number Density (MND) EPRI-CELL physics constants are used.

In the following figures, hot full power (HFP) PDQ07 and CASMO individual pin powers are presented from quarter-assembly calculations. These calculations were performed at beginning-of-life with no xenon; at this time pin power peaking is most severe. The enrichments used are typical of future reloads at Oconee. A variety of soluble boron concentrations and burnable poison (BP) weight percents (B_4C) were used. Also, water filled control rod guide tubes (CRGT) were used. All assemblies contained an instrument tube (IT). Table 1 identifies the five cases.

TABLE 1

<u>Case</u>	<u>U-235 w/o</u>	<u>Absorber</u>	<u>PPM-Boron</u>
1	3.08	1.0 w/o B_4C	500
2	3.08	1.0 w/o B_4C	1000
3	3.38	.2 w/o B_4C	1000
4	3.38	CRGT	1000
5	3.08	CRGT	0

In evaluating pin powers, the CASMO code solves the transport equation in two dimensions and seven neutron energy groups¹. PDQ07 used only two energy groups in evaluating the diffusion equation. Therefore, the Duke PDQ07 model was tested not only by a higher order neutronics method, but also by more neutron energy groups.

In all five cases it is shown that PDQ07 predicts accurately and conservatively each assembly's maximum pin power. PDQ07 also predicted the same location of the maximum pin for each case as CASMO.

For pin powers equal to or greater than 1.000, pinwise powers usually agree within 1%. The CRGT cases, however, show PDQ07 to be up to 2% more conservative.

Therefore it is concluded from these comparisons, as well as those in NFS-1001 Supplement 2, that the two group MND PDQ07 accurately and conservatively predicts the maximum pin power within an assembly over a wide range of moderator and fuel temperatures, enrichments, soluble boron concentrations, and BP loadings.

1. These CASMO calculations were run using 69 energy groups in the microregion calculation.

FIGURE 1
 QUARTER ASSEMBLY PINWISE POWERS - CASE 1

CODE	PDQØ7	CASMO	_____
K-INF	1.1419	1.1421	_____
U-235 w/o	3.08	3.08	_____
PPMB	500	500	_____
B-4-C w/o	1.0	1.0	_____

IT							
1.044 1.050	1.009 1.012	CASMO PDQØ7					
0.992 0.993	0.970 0.973	BP					
0.982 0.977	0.974 0.966	0.952 0.952	0.956 0.948				
0.981 0.975	0.973 0.965	0.952 0.952	0.946 0.947	BP			
0.986 0.980	0.967 0.968	BP	0.959 0.960	0.971 0.973	1.000 0.994		
1.003 1.000	0.997 0.992	0.981 0.986	0.997 0.994	1.010 1.007	1.024 1.022	1.041 1.043	
1.035 1.036	1.033 1.034	1.031 1.033	1.035 1.038	1.043 1.046	1.054 1.058	1.068 1.076	1.096 1.109

FIGURE 2
 QUARTER ASSEMBLY PINWISE POWERS - CASE 2

CODE	PDQØ7	CASMO	_____
K-INF	1.0938	1.0930	_____
U-235 w/o	3.08	3.08	_____
PPMB	1000	1000	_____
B-4-C w/o	1.0	1.0	_____

IT							
1.043 1.049	1.009 1.012	CASMO PDQØ7					
0.992 0.993	0.971 0.974	BP					
0.983 0.978	0.975 0.967	0.953 0.954	0.958 0.950				
0.982 0.976	0.975 0.966	0.953 0.954	0.948 0.949	BP			
0.986 0.981	0.968 0.969	BP	0.960 0.961	0.972 0.974	1.000 0.994		
1.003 0.999	0.997 0.993	0.982 0.987	0.997 0.994	1.010 1.006	1.023 1.020	1.039 1.040	
1.034 1.035	1.032 1.033	1.030 1.032	1.034 1.036	1.042 1.045	1.052 1.056	1.065 1.073	1.092 1.105

FIGURE 3
 QUARTER ASSEMBLY PINWISE POWERS - CASE 3

CODE	PDQØ7	CASMO	
K-INF	1.1891	1.1876	
U-235 w/o	3.38	3.38	
PPMB	1000	1000	
B-4-C w/o	0.2	0.2	

IT							
1.037 1.043	1.013 1.023	CASMO PDQØ7					
0.994 0.993	1.002 1.004	BP					
0.984 0.976	0.988 0.988	0.999 1.002	0.995 1.007				
0.982 0.972	0.986 0.986	0.999 1.003	1.003 1.014	BP			
0.984 0.975	0.995 0.994	BP	1.002 1.011	0.999 1.001	0.990 0.988		
0.988 0.980	0.992 0.991	1.001 1.002	0.994 0.996	0.991 0.986	0.990 0.983	0.995 0.989	
1.007 1.002	1.008 1.005	1.009 1.008	1.008 1.007	1.008 1.004	1.009 1.006	1.015 1.015	1.037 1.042

FIGURE 4
 QUARTER ASSEMBLY PINWISE POWERS - CASE 4

CODE	PDQØ7	CASMO	
K-INF	1.2210	1.2170	
U-235 w/o	3.38	3.38	
PPMB	1000	1000	
B-4-C w/o	CRGT	CRGT	

IT							
1.024 1.028	1.011 1.029	CASMO PDQØ7					
0.990 0.989	1.028 1.031	CRGT					
0.980 0.971	0.996 1.006	1.041 1.050	1.030 1.063				
0.977 0.966	0.994 1.004	1.042 1.052	1.058 1.080	CRGT			
0.978 0.968	1.019 1.017	CRGT	1.046 1.062	1.028 1.030	0.983 0.985		
0.971 0.960	0.985 0.988	1.020 1.017	0.992 0.999	0.974 0.968	0.962 0.949	0.958 0.942	
0.980 0.967	0.983 0.975	0.988 0.983	0.984 0.977	0.977 0.966	0.972 0.959	0.974 0.961	0.993 0.984

FIGURE 5
 QUARTER ASSEMBLY PINWISE POWERS - CASE 5

CODE	PDQØ7	CASMO	_____
K-INF	1.3272	1.3267	_____
U-235 w/o	3.08	3.08	_____
PPMB	0	0	_____
B-4-C w/o	CRGT	CRGT	_____

IT							
1.026 1.030	1.013 1.031	CASMO PDQØ7					
0.992 0.993	1.030 1.032	CRGT					
0.981 0.974	0.998 1.009	1.043 1.051	1.033 1.065				
0.978 0.969	0.996 1.006	1.044 1.053	1.060 1.080	CRGT			
0.979 0.970	1.019 1.016	CRGT	1.047 1.061	1.028 1.029	0.982 0.985		
0.971 0.960	0.985 0.988	1.020 1.016	0.992 0.999	0.974 0.968	0.960 0.948	0.956 0.941	
0.979 0.966	0.982 0.974	0.987 0.982	0.982 0.976	.975 1.964	0.969 0.956	0.970 0.958	0.989 0.979

DUKE POWER COMPANY
POWER BUILDING
422 SOUTH CHURCH STREET, CHARLOTTE, N. C. 28242

WILLIAM O. PARKER, JR.
VICE PRESIDENT
STEAM PRODUCTION

March 18, 1981

TELEPHONE: AREA 704
373-4033

Mr. Harold R. Denton, Director
Office of Nuclear Reactor Regulation
U. S. Nuclear Regulatory Commission
Washington, D. C. 20555

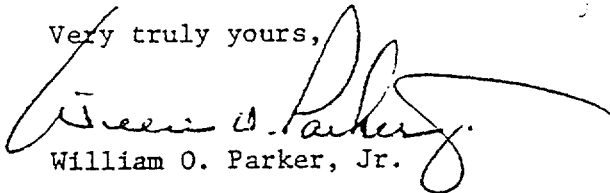
Attention: J. F. Stolz, Chief
Operating Reactors Branch No. 4

Subject: Oconee Nuclear Station
Docket Nos. 50-269, -270, -287
Oconee Reload Design Methodology Technical Report

Dear Sir:

My letter of November 13, 1980 provided Duke Power Company's responses to ~~the Staff's questions~~ concerning the subject report. Attached are revised responses to Questions 4 and 11 which were addressed by that letter. These responses have been revised to provide additional clarification, as requested informally by the Staff on March 16, 1981.

Very truly yours,



William O. Parker, Jr.

FTP:pw
Attachment

bcc: P. M. Abraham
K. S. Canady
N. A. Rutherford
R. L. Gill
J. L. Jones

R. H. Clark
H. T. Snead
G. B. Swindlehurst
Section File OS-801.01

4159

Q. 4. Paragraph 8.3.2 Start-up Accident

Give the variation of the total (and its components) reactivity for the start-up accident for the first 10 seconds after the accident initiation, (these would complement Fig. 14-1 and 14-2 of the Oconee FSAR Rev. 16).

- A. 4. The approach taken in the review of FSAR transient analyses as an integral part of the reload design methodology is discussed in Section 8 of NFS-1001. For each FSAR analysis the main parameters of interest have been identified and documented in the FSAR. In order to assure that a reload core is in conformance with the assumptions in the analysis, it is necessary to determine that the parameters associated with the reload core are bounded by the parameters assumed in the FSAR. If this criterion is met, it can be concluded that the existing FSAR analysis remains valid for the reload core.

Question 4 requests additional information for the start-up accident concerning the variation of the components of the reactivity response. These parameters are an intermediate output of the analysis whose response is indicated by other documented parameters such as power level, but are not normally included in the analysis documentation. However, the components of the reactivity response are determined by the parameters which are reviewed and shown to be within the bounds of the FSAR analysis. The reactivity response determined by those parameters remains valid until the value of a parameter is no longer bounded for a reload core. The safety review methodology of Section 8 assures the identification of all pertinent reload core parameters affecting the reference safety analysis, confirmation of the validity of the reference safety analysis for the reload core, and the resolution of any non-conservative parameter.

In order to respond to the question, the variation of the total reactivity and its components were calculated from the results presented in FSAR Figures 14-1 and 14-2, utilizing the analysis assumptions specified in the FSAR. The variation of the total reactivity during a startup accident is the sum of three reactivity effects. The withdrawal of the control rod banks adds positive reactivity which causes the neutron power level to increase and raise the average core temperature. The increase in fuel temperature causes a negative reactivity feedback due to the negative Doppler coefficient. The increase in power level increases heat transfer from the fuel to the coolant, resulting in an increase in moderator temperature. This causes a positive reactivity feedback since a positive beginning of cycle moderator coefficient is assumed. The transient response is primarily determined by the rate of positive reactivity addition from the withdrawal of rods, and the Doppler feedback which slows or terminates the nuclear excursion. The moderator feedback has a smaller effect. Figures 4-1 and 4-2 show the variation of the reactivity consistent with FSAR Figures 14-1 and 14-2 respectively. It should be noted that these figures do not represent the first 10 seconds of the transients, considering that the initial conditions are $10E-9$ rated power and 1% k/k subcritical. Figures 4-1 and 4-2 illustrate the time interval of greatest interest during the transient, Figure 4-1 is the same scale as Figure 14-1, and Figure 4-2 is the first one second of the response in Figure 14-2. For both transients the reactivity addition for the first 10 seconds following initiation of rod withdrawal would only cause a reduction in the subcriticality margin.

- Q. 11. Supplement 2, Paragraph 3.2, Comparison of ARMP PDQ07 to Cold Criticals.

The two-dimensional simulation of the criticals has not been performed at Duke nor with PDQ07, yet it was concluded that the results would have been identical with the PDQ07 results. Justify the above conclusion.

- A. 11. The cold criticals have been simulated with PDQ07. The results have been published in Part I Chapter 2, Rev. 1 of the ARMP System Documentation. This work was performed under EPRI Research Project 118-1.

These benchmark calculations use standard ARMP methodology, standard ARMP codes (EPRI-CELL, NUPUNCHER, PDQ07) and Duke Power also uses these codes and methodology. Duke Power Company has been actively involved in developing in-core fuel management capability since 1969. Currently in the Nuclear Fuel Services Section, there are a total of nine employees with a cumulative thirty-two (32) man-years of PDQ experience. The level of individual experience ranges from one to nine years, and includes experience with Combustion Engineering, Westinghouse, and Babcock & Wilcox core design calculations. Therefore, Duke Power considers that if it had performed these benchmark calculations, the results would have been identical.

44

DUKE POWER COMPANY

POWER BUILDING

422 SOUTH CHURCH STREET, CHARLOTTE, N. C. 28242

WILLIAM O. PARKER, JR.
VICE PRESIDENT
STEAM PRODUCTION

June 16, 1981

TELEPHONE: AREA 704
373-4083

Mr. Harold R. Denton, Director
Office of Nuclear Reactor Regulation
U. S. Nuclear Regulatory Commission
Washington, D. C. 20555

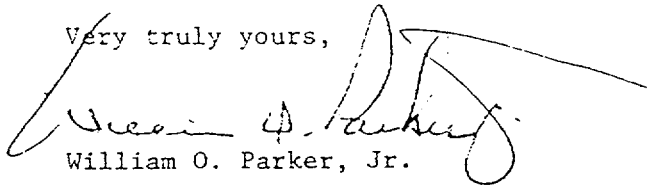
Attention: Mr. J. F. Stolz, Chief
Operating Reactors Branch No. 4

Re: Oconee Nuclear Station
Docket Nos. 50-269, -270, -287

Dear Sir:

In response to your letter dated June 2, 1981 requesting additional information regarding Technical Report NFS 1001, "Reload Design Methodology," please find the attached responses in Attachment 1 of this submittal. Attachment 2 transmits Revision 4 of Technical Report 1001, "Reload Design Methodology."

Very truly yours,



William O. Parker, Jr.

JLJ:scs

Attachments

- bcc: w/o Attachment 2
- K. S. Canady
- N. A. Rutherford
- R. L. Gill
- R. C. Futrell
- P. M. Abraham
- R. H. Clark

- R. M. Gribble
- J. E. Smith
- R. T. Bond
- T. B. Owen
- ✓ Section File OS-801.01

ATTACHMENT 1

DUKE POWER COMPANY
OCONEE NUCLEAR STATION

Response to NRC Letter of June 2, 1981

Question 492.1 (Section 6.7)

Provide a more detailed discussion on how the core outlet pressure - reactor outlet temperature curves are determined.

Response

The core outlet pressure - reactor outlet temperature curves (P-T Safety Limits, Figure 6.2) are determined by varying core outlet pressure and core inlet temperature using CHATA Command Routines 1 and 2 (CR 1/2). Using the equivalent two channel model, described in Section 6.6, core inlet temperature is varied at a constant pressure (one inlet temperature value per CHATA run) until the inlet temperature that yields a hot channel minimum DNBR of 1.4326 at that pressure has been determined. This single limiting combination of reactor coolant pressure and inlet temperature is then used to calculate the corresponding reactor vessel outlet temperature, using a simple reactor vessel heat balance.

This process is repeated over a range of pressures, typically 1800, 1900, 2000, 2100, 2200, and 2300 psia. For each of these pressures, a limiting inlet temperature is determined and a corresponding reactor outlet temperature is calculated. Finally, the resulting P-T Safety Limits are plotted for each allowable combination of operating reactor coolant pumps.

Question 492.2 (Section 6.8.2)

The method used to determine the Maximum Allowable Peaking (MAP) factor was to vary the hot channel power until the limiting DNBR was reached. Babcock and Wilcox varies the radial peaking factor rather than the power. Demonstrate that the Duke method is an acceptable and equivalent method when compared to the Babcock and Wilcox method.

Response

The Duke method is identical to the Babcock and Wilcox method; further, the operation of CHATA Command Routine 8 prohibits such a variation in this procedure. In addition to this response, it may also be helpful to review Reference 10 of NFS-1001, specifically page 10-3 and Appendix H, which describe the CHATA Command Routines.

The MAP curves are generated using CHATA Command Routines 1 and 8 (CR 1/8) and the equivalent two channel model described in Section 6.6. (This two channel model contains an average channel (Command Routine 1) that represents the overall core and a hot channel (Command Routine 8) that is "driven" by the average channel's pressure drop.

Command Routine 8 (CR8) accepts the average channel (CR1) pressure drop as a boundary condition, and varies hot channel flow and percent over power in the hot channel until the criteria of dP and minimum DNBR are satisfied in the hot channel.

The hot channel in CR8 is a single rod; therefore, for this single rod, over-power is functionally equivalent to pin peak. Usually the pin power input

data field in the CR8 hot channel model is set equal to the core overpower fraction (for example 1.12) such that CR8 will output the allowable pin peak directly.

Question 492.3 (Section 6.8.2)

More information is needed on the generic DNBR curves or MAP curves.

Item 1: Provide a detailed discussion of how the curves are developed.

Response

MAP curves are developed using the equivalent two channel model described in Section 6.6 and further described in Duke's response to question 492.2, above. CHATA Command Routines 1 and 8 are used for MAP analyses.

Maximum allowable total peaking (MAP) limits are determined both for RPS DNB offset limits and for "operational" DNB offset limits. These two types of MAP curves are described in the response to Item 2 of this question.

CHATA Command Routines 1 and 8 are used to vary (in a series of hundreds of separate computer analyses) the axial flux shape peak and axial peak location. One computer run is required for each combination of axial peak and axial peak location, for example, an axial peak of 1.7 at 80% of the active fuel length. CHATA CR 1/8 is run such that the average channel model (CR1) calculates and transmits the dP boundary condition to the hot channel (CR8). The hot channel model then determines the maximum rod power (peak) and the hot channel flow that satisfy the dP and DNBR boundary conditions.

The inputs to CR 1/8 for MAP analyses are core operating conditions (temperature, pressure, power, and average channel flow), average and hot channel geometries, hydraulic characteristics, average channel pin power (pin peak = 1.0), and a specific axial flux shape to be assessed. To develop a set of MAP curves, axial flux shape is varied from an axial peak of 1.1 to 2.0, with the location of the axial peak varying from the bottom to top of the active fuel length in increments of 10 percent of active fuel length. Output from the hot channel model (CR-8) is the allowable hot channel overpower fraction (functionally equivalent to pin peak for this single rod model). The output pin peak is then multiplied by the axial peak to yield the maximum allowable total peak for the flux shape being analyzed.

Item 2: State the differences between the RPS DNB offset curves and the DNB operational offset curves.

Response

Two types of MAP curves are developed. One type is used for the RPS DNB offset limits. Multiple subsets of RPS MAP limits are determined, one subset for each allowable combination of operating reactor coolant pumps. The second type of MAP curves is used for DNB operational offset limits.

RPS MAP curves are determined at two separate operating conditions (temperature and pressure) for each allowable combination of operating reactor coolant

Table 492.3-1

MAP Analysis Input Operating Conditions

4 Pump Operation

High Temperature

Core Power Level = 112% Rated
T RV outlet = 619F

*Pcore = 2063 psia (typical)

MDNBR = 1.4326

Low Pressure

Core Power Level = 112% Rated
* Tcore inlet = 544F (typical)

Pcore = 1800 psia

MDNBR = 1.4326

3 Pump Operation

High Temperature

Core Power Level = 87.2% Rated
T RV outlet = 619F

*Pcore = 2065 PSIA

MDNBR = 1.4326

Low Pressure

Core Power Level = 87.2% Rated
* Tcore inlet = 542 (typical)

Pcore = 1800 psia

MDNBR = 1.4326

2 Pump Operation

High Temperature

Core Power Level = 59.4% Rated
T RV outlet = 619F

* Pcore = 1870 psia

MDNBR = 1.4326

Low Pressure

Core Power Level = 59.4% Rated
* Tcore inlet = 552F (typical)

Pcore = 1800 psia

MDNBR = 1.4326

* Pcore is that pressure which results in a MDNBR = 1.4326 with a RV outlet temperature at the high temperature setpoint.

* Tcore inlet is that temperature that results in a MDNBR = 1.4326 with a pressure at the low pressure setpoint.

Table 492.3-2

Operational MAP Input Operating Conditions

The following operating conditions describe the additional set of MAP curves that are developed at 4 pump conditions and are overlaid with the RPS MAP curves to form the operational MAP curves.

Core Power Level = 102% Rated*

T_{core inlet} ≅ 557.2F (includes +2°F error)

P_{core} = 2135.0 psia (includes -65 psi error)

MDNBR ≅ 2.38 (B&W-2)*

*NOTE: The maximum allowable total peak resulting from these constraints is the same as the maximum allowable peak that results from an analysis performed at 112% power and a DNBR of 2.05.

Question 492.4 (Section 7.3.1)

In determining the reactor protection system P-T set points, the applicant stated that the RCS high pressure trip set point was 2356 psig. In the Technical Specifications for Oconee Units 1, 2, and 3, the high pressure trip is at 2300 psig. Correct this discrepancy.

Response

The current value for the high pressure trip set point is indeed 2300 psig. This discrepancy will be corrected in the next revision of the report on the following pages:

- 1) Paragraph 2, page 7-0
- 2) Table 7-1, page 7-16
- 3) Figure 7-4, page 7-20

Question 492.5 (Section 7.3.1)

Provide the values that are used to error adjust the P-T set point curve. How are these numbers obtained?

Response

The error-adjustment of the P-T set point curve is the same as for previous Oconee reload designs. The error-adjustment for temperature is $+1^{\circ}\text{F}$. This conservatively accounts for the maximum temperature error in the instrumentation string. The pressure measurement error is ± 30 psi which is added to the minimum pressure difference between the core outlet and the pressure tap on the hot leg, $\Delta P = +30$ psi. The net error-adjustment for pressure is 0 psi.

Question 492.6 (Section 7.3.2)

On page 7-10 reference is made to the flux/flow ratio ratio calculated in Section 6.8. The flux/flow ratio is calculated in Section 6.9. Correct this discrepancy.

Response

This editorial correction will be in the next revision of the report.

Question 492.7 (Section 7.3.2)

Provide a reference for the 6.5 percent full power error-adjustment factor used in setting the RPS power-flow imbalance.

Response

The 6.5 percent full power error-adjustment is the same as for previous Oconee reload designs and is discussed in the B&W Topical Report, "RPS Limits and Set-points", BAW-10121, on page 5-13. Although this report is based on the 205 class plant, this factor is the same for the Oconee Units (see Technical Specifications 2.3 and 4.1).

Amendment 2

NRC Safety Evaluation Report

RLG



RECEIVED
UNITED STATES
NUCLEAR REGULATORY COMMISSION
WASHINGTON, D. C. 20555

AUG 1 1981 July 29, 1981

Dockets Nos. 50-269, 50-270 DUKE POWER CO.
and 50-287 REGULATION & LICENSING

Mr. William O. Parker, Jr.
Vice President - Steam Production
Duke Power Company
P. O. Box 33189
422 South Church Street
Charlotte, North Carolina 28242

Dear Mr. Parker:

The staff has completed the review of Technical Report NFS-1001, "Oconee Nuclear Station Reload Design Methodology" which was submitted by letter dated April 23, 1979 and revised by letters dated May 20, 1980, January 28, April 22 and June 16, 1981. The results of our review are contained in the enclosed Safety Evaluation.

We have found the revised report to be an acceptable method of performing reload design calculations for future Oconee Nuclear Station, Units 1, 2 and 3 reloads.

If you have any questions on this subject, please contact me.

Sincerely,

Philip C. Wagner

Philip C. Wagner, Project Manager
Operating Reactors Branch #4
Division of Licensing

Enclosure:
Safety Evaluation

cc w/enclosure:
See next page

Duke Power Company

cc w/enclosure(s):

Mr. William L. Porter
Duke Power Company
P. O. Box 33189
422 South Church Street
Charlotte, North Carolina 28242

Office of Intergovernmental Relations
116 West Jones Street
Raleigh, North Carolina 27603

Oconee County Library
501 West Southbroad Street
Walhalla, South Carolina 29691

Honorable James M. Phinney
County Supervisor of Oconee County
Walhalla, South Carolina 29621

U. S. Environmental Protection Agency
Region IV Office
ATTN: EIS COORDINATOR
345 Courtland Street, N.E.
Atlanta, Georgia 30308

Mr. Francis Jape
U.S. Nuclear Regulatory Commission
Route 2, Box 610
Seneca, South Carolina 29678

Mr. Robert B. Borsum
Babcock & Wilcox
Nuclear Power Generation Division
Suite 420, 7735 Old Georgetown Road
Bethesda, Maryland 20014

Manager, LIS
NUS Corporation
2536 Countryside Boulevard
Clearwater, Florida 33515

J. Michael McGarry, III, Esq.
DeBevoise & Liberman
1200 17th Street, N.W.
Washington, D. C. 20036



UNITED STATES
NUCLEAR REGULATORY COMMISSION
WASHINGTON, D. C. 20555

SAFETY EVALUATION BY THE OFFICE OF NUCLEAR REACTOR REGULATION
OF THE RELOAD DESIGN METHODOLOGY
TECHNICAL REPORT NFS-1001
FOR THE
DUKE POWER COMPANY
OCONEE NUCLEAR STATION, UNITS NOS. 1, 2 AND 3
DOCKETS NOS. 50-269, 50-270 AND 50-287

1.0 Introduction

Duke Power Company (DPC) submitted Technical Report NFS-1001, "Oconee Nuclear Station Reload Design Methodology" for NRC review on April 23, 1979 (Reference 1a). The report contains information pertaining to the design of core reloads for the Oconee Units 1, 2 and 3, and includes fuel design, mechanical and thermal-hydraulic design, Technical Specification and accident analysis review, and core physics parameters.

By letter dated May 20, 1981 (Reference 1b), DPC submitted Revision 1 to NFS-1001 which revised the original submittal in its entirety and included two supplements on comparison of predicted and measured physics parameters in addition to providing supplemental and clarifying information. Additional revisions (2, 3 and 4) were submitted by DPC on January 28, April 22, and June 16, 1981 (References 1c, 1d and 1e) to incorporate additional or clarifying information requested by the staff.

2.0 Summary of Report

Technical Report NFS-1001 describes the reload design methodology for the Oconee Nuclear Station. The topics included deal with nuclear fuel cycle

design, Technical Specifications, transient and accident analysis, the development of core physics parameters, fuel design and thermal-hydraulic analyses. All of the above are analytical procedures with the objective of designing a reload in a manner that the reactor can be operated at its power level within the specified safety margins for a given number of full power days. The nuclear fuel cycle design employs EPRI-CELL, NUPUNCHER and PDQ07 for the calculation of cross sections, assembly constants and quarter core power distributions, local pin peaking, and reactivity as a function of burnup. Finally, the results are processed by EPRI-FIT and SUPERLINK for EPRI-NODE-P which produces three dimensional information on power distribution, rod worths, etc. The Technical Specifications reflect certain Limiting Safety System Settings (LSSs), and Limiting Conditions of Operation (LCOs) which are established on the basis of nuclear and thermal-hydraulic characteristics and the applicable transient and accident analyses. The limits refer to DNBR, linear heat generation rate, pressure-temperature regions of operation, power imbalance and centerline fuel melt limits.

The accident analysis section considers the safety analysis of postulated transient and accidents and is designed to demonstrate that the reactor is able to mitigate such events and that the calculated consequences are acceptable. Considerations of importance in the accident analysis are: values of pertinent plant parameters, performance of the assumed mitigating systems and the analytical methods. Analysis is presented for: startup accidents, uncompensated operating reactivity changes, rod withdrawal at rated power, moderator dilution, cold water injection, loss of coolant flow, stuck or dropped control rods, loss of electric power, steam line failure, steam generator tube failure, fuel handling accident, rod ejection, and loss of coolant.

The development of core physics parameters is based on measurements performed on Oconee Unit 1 Cycles 1-5 and were compared to analytical values obtained with the EPRI-NODE-P code. The measured parameters include critical boron concentration at hot, zero power (HZZ) and hot, full power (HFP), control rod worths, ejected rod worths (using boron swap, rod swap and rod drop) and isothermal temperature coefficients. Comparison of calculated and measured values was used to estimate adequacy of the calculated procedures in predicting core physics parameters. Lastly, the benchmarking of the EPRI-NODE-P is described with the measured assembly powers, local radial power peaking comparisons, statistical analysis and the fitting procedure used.

Two sections of the report address reload aspects of the fuel design's material features, as apart from physics or thermal-hydraulic concerns: (1) Section 2.0 Fuel Design and (2) Section 4.0 Fuel Mechanical Performance. In the Fuel Design section, brief descriptions are provided of the fuel pellets, fuel rods, and fuel assembly design. As noted in the Fuel Mechanical Performance section, design analyses that envelope the operation of current fuel designs have been completed by the fuel vendor, and the approach taken by Duke Power Company for a specific fuel cycle (reload) design is to compare that design against the enveloping design analysis. The information contained in Section 4.0, therefore, is intended to (1) describe the types of comparisons that must be made to justify a fuel cycle design without reanalysis and (2) provide some detail concerning the types of analyses that must be performed if required by either the fuel cycle design or changes in the fuel design itself.

Section 6.0 of the report addresses the thermal-hydraulic design. A thermal-hydraulic analysis must be performed in conjunction with a reload when there is a change in fuel design, a change in the input assumptions of earlier analyses or a change in regulatory criteria. The general criterion for thermal-hydraulic performance is that no damage due to critical heat flux takes place during normal operations or anticipated transients. The thermal-hydraulic analyses, therefore, establishes the maximum permissible core power and power distribution for various operating conditions and the permissible combination of core outlet pressure and reactor outlet temperature to ensure that a minimum departure from nucleate boiling ratio (DNBR) of 1.30 or greater can be maintained.

3.0 Evaluation

3.1 Core Physics Evaluation

The fuel cycle design section is divided into preliminary and final fuel cycle design. The design process is initiated with the generation of the necessary cross sections using EPRI-CELL for each of the subassemblies. They are then put into the proper tabular form by NUPUNCHER and inputted to PDQ07 which solves the diffusion-depletion problem in one, two, or three dimensions. The PDQ07 results are processed by EPRI-FIT and SUPERLINK and are input to EPRI-NODE-P which yields three dimensional power distribution, rod worths etc. The objective of this phase of the analysis is to estimate cycle lifetime, power peaking and number, and enrichment of fuel assemblies. The final fuel cycle design phase aims at optimizing the placement of the burned and fresh assemblies, control rod grouping, and burnable poison assemblies. At this point, the design must meet several criteria; radial pin peak power, moderator temperature

coefficient, maximum pellet burnup, shutdown margin and ejected rod worth at HZP and HFP. The control rod worths are calculated for operation at either the "rods in" or "rods out" mode, for several groupings, shutdown margin, ejected and dropped rod. The power distribution is calculated for the assemblies and the rods and ascertained that they meet the requirements such as the ones on linear heat generation rate and centerline melting.

The reactivity coefficients are calculated including Doppler, moderator temperature, and power and power defect. The boron related parameters, i.e., boron critical concentrations at beginning of cycle (BOC) and end of cycle (EOC) for HZP and HFP and various rod positions are computed. Finally, xenon worths and the kinetics parameters are calculated.

The technical specifications are developed for safe reactor operation under applicable transient and accident analyses. Those affected by the reload design and within the interest of this review are core safety limits emanating from or involving core physics parameters. The allowable total peaking factor is determined from the ratio of the center fuel melt linear heat rate limit over the product of the average linear heat rate times the fraction of rated power. This peaking factor is then increased by (a) the nuclear uncertainty factor of 1.075, (b) spacer grid effect factor of 1.026, (c) radial local power peaking factor, (1.10, typical value), (d) an engineering hot channel factor of 1.014, and (e) a densification power spike factor depending on core location. From the above factors limiting safety settings have been developed for the Reactor Protection System (RPS).

The transient and accident evaluation was a systematic analysis of all postulated accidents. The accidents considered were:

- (a) Uncompensated operating reactivity changes: on the basis of a Doppler coefficient of $-1.17 \times 10^{-5} \Delta K/K/^{\circ}F$ and moderator temperature coefficient $0.5 \times 10^{-4} \Delta K/K/^{\circ}F$ at the BOC it was concluded that no safety limits would be exceeded.
- (b) Start-up accident: during which it is assumed that a control rod is inadvertently withdrawn. Assuming total control rod worth of $10\% \Delta K/K$ and the parameters of (a) above it is concluded that the overpower limit of 112% applicable in this case is not exceeded.
- (c) Rod withdrawal at rated power: the analysis in this case was carried out under the same assumptions as (b) above and the result indicated that the reactor power and pressure will remain within acceptable limits.
- (d) Moderator dilution accident: occurs when the boron concentration of the coolant make up flow is less than the concentration of the primary coolant. With power and pressure assumptions as in (c) above and reactor minimum shutdown margin of $1\% \Delta K/K$ it is estimated that no safety limits will be exceeded.
- (e) Cold water injection accident, i.e., the abrupt introduction of cold water was treated assuming conservative values of EOC Doppler coefficient of $-1.3 \times 10^{-5} \Delta K/K/^{\circ}F$ and a moderator coefficient of $-3.0 \times 10^{-4} \Delta K/K/^{\circ}F$. The minimum value of 1.3 for DNBR is not exceeded.

- (f) Loss of coolant flow; which could be caused by loss of power or be due to mechanical damage to one or more coolant pumps. Assuming a Doppler coefficient of $-1.2 \times 10^{-4} \Delta K/K/^{\circ}F$, moderator temperature coefficient of $-0.5 \times 10^{-4} \Delta K/K/^{\circ}F$, coolant flow of 352,000 gpm, radial local power peaking factor 1.783 and axial peaking of 1.50 the criterion of 1.3 minimum DNBR for loss of power or 1.0 for mechanical failure are not violated.
- (g) Control rod misalignment accident, could cause significant distortion of power distribution and result in excessive local power peaking. The requirement of 1% $\Delta K/K$ shutdown margin prevents exceeding 1.3 minimum of DNBR. The coefficients are assumed as in (e) above.
- (h) Loss of electrical power will cause a reactor trip on overpower-overpressure after loss of load. This accident is the same as the analysis in the FSAR.
- (i) Steam line failure, when the heat sink is essentially assumed to be lost; assuming Doppler coefficient of $-1.2 \times 10^{-5} \Delta K/K/^{\circ}F$, moderator temperature coefficient of $-3.0 \times 10^{-4} \Delta K/K/^{\circ}F$ and available scram worth of 3.46% $\Delta K/K$, the potential radioactivity release is within 10 CFR 100 limits.
- (j) Steam generator tube failure has been analyzed in the FSAR. The analysis is valid for the reload.
- (k) Fuel handling accidents are the same as those presented and analyzed in the FSAR.
- (l) Rod ejection accident would result in rapid reactivity insertion. Assuming conservative parameter values for BOC and EOC it is shown that no safety limits are exceeded.

- (m) The loss of coolant accident consequences are primarily dependent on the size of the break. Reactor trip and injection of borated water will limit the consequences of the LOCA. The criteria for this accident are set forth in 10 CFR 50.46 and it is shown not to be exceeded.

Development of Physics Parameters, is based upon PDQ07 and EPRI-NODE-P depletion calculations and are used to predict startup and cycle physics parameters. The comparison of calculated and measured values from Cycles 1-5 of Oconee Unit 1 confirm the adequacy of the calculational procedure. This procedure, based on EPRI-NODE-P was benchmarked with measured assembly powers and local radial peaking factors. Adequate statistical analyses and fitting procedures were discussed and documented.

The predictive capability of EPRI-NODE-P was confirmed with comparisons to measured data from Oconee 1, Cycles 1 to 5. The predictive capability discussed in the report refers to measurements before the calculation. In this manner there was assurance of the correct input. The comparisons were presented by means of the differences of measured and calculated data and their corresponding standard deviation. Calculated and measured power distributions were statistically combined to derive 95/95 Observed Nuclear Reliability Factors (ONRF) for EPRI-NODE-P calculations.

Local radial peaking factor reliability analysis involved cold criticals as well as simulated hot full power condition comparisons. The codes PDQ07, CASMO, and CPM were used. The comparisons indicated that there was a conservative overprediction of the peak pin powers for both the cold and hot criticals.

Three-dimensional Oconee simulations were performed using the EPRI-NODE-P in quarter core configurations. Auxiliary calculations were performed by CPM, EPRI-CELL and PDQ07/HARMONY. K_{eff} , critical boron concentration, power distributions and reactivity coefficients were calculated as a function of operating conditions and depletion. The results of these calculations were compared to extensive measured data from Oconee 1, Cycles 1-5.

The differences of the measured from the calculated value of a parameter were treated as on a normal distribution. On this assumption the Observed Nuclear Reliability Factor (ONRF) were calculated, for the rodged, unrodged, and combined cycles. For the unrodged cycle the radial and total ONRFs were found to be 1.03 and 1.04 respectively. However, for consistency with B&W values and for increased conservatism they are to be taken as 1.05 and 1.075 respectively. Finally, normality tests for the differences are shown.

The following is a brief description of the physics related codes. (Use the following abbreviations: MG = multigroup, 2D = two dimensional, 3D = three dimensional, TT = transport theory, DT = diffusion theory, DP = depletion.)

- CASMO: MG, 2D, TT for DP calculations.
- DELAY: Computes delayed neutron fractions decay constants, neutron lifetime and reactivity vs period.
- EPRI-CELL: Computes fuel cell neutron spectrum dependence on space and burnup.
- EPRI-CPM: MG, 2D, collision probability for PWR DP.
- EPRI-FIT: A PDQ07 editor.
- EPRI-NODE: 3D, computes K_{eff} , power, flow, temperature, and fuel exposure distributions. Accounts for part length rods and can be used for fuel management.
- EPRI-NUPUNCHER: Cross section preparation.
- EPRI-PDQ07: MG, 2D, and 3D, DT, DP.
- EPRI-SHUFFLE: File manager and editor for PDQ07.

The report NFS-1001 has been reviewed within the guidelines provided by the Standard Review Plan, Section 4.3 and the applicable parts of Section 15, i.e., 15.4.1, 2, 3, 7, and 8. Sufficient information is provided in the report to permit a knowledgeable person to ascertain that the methods and techniques used are satisfactory and the data employed are adequate. On the basis of our review we concluded that Technical Report NFS-1001 may be referenced in licensing actions by the Duke Power Company for the physics calculations for the Oconee Nuclear Power Station reloading procedures. We recommend that the Duke Power Company continue to perform periodic reevaluations of the reload methodology to provide continuing assurance of model applicability.

3.2 Fuel Design Evaluation

Our review of Section 2.0 and 4.0 of Technical Report NFS-1001 was performed in conformance with the design limits and acceptance criteria used in the Safety Evaluation of the Oconee FSAR. In addition, we examined the Technical Report Sections to determine if the same fuel performance parameters and concerns were addressed there as in the original Oconee FSAR. Those parameters and issues included fission gas release, fuel rod dimensional changes, corrosion or irradiation effects of mechanical properties, fretting, seismic disturbances, temperature gradients, and cladding stress and strain.

As noted in Section 2.0 of the report, the fuel design consists of (a) fuel assembly design (material selection, fuel rod lattice, and fuel rod number specification); (b) spacer grid design (number of grids, material selection and fuel assembly end fittings); and (c) fuel rod design (rod dimensions, cladding type and dimensions, pellet density and dimensions, design of fuel stack spacers, fuel stack length, fuel rod fill gas pressure and composition, and specified tolerances on fuel rod design parameters). The fuel pellet radius is stated to be such that the cladding plastic strain will not exceed one percent. The fuel rod internal volume is said to be designed to maintain the internal pin pressures below the primary system pressure at temperatures greater than 425°F for Conditions I and II operation, and all rods are to be pre-pressurized with helium to aid heat transfer, to prevent cladding collapse, and to avoid hydrogen contamination. Thus, the criteria (one percent cladding strain, fuel pin pressure less than system pressure, and no creep collapse) are consistent with the Oconee FSAR acceptance criteria and the current Standard Review Plan criteria, as well, and are, therefore, acceptable.

It is stated in report Section 4.0 Fuel Mechanical and Thermal Performance that differences in the reload fuel design (from previous design analyses) must be assessed in regard to cladding creep collapse, cladding stress and strain, fuel pin temperature, and fuel pin pressure. These parameters are all consistent with the parameters listed above for the Oconee FSAR. Individual subsections of report Section 4.0 address cladding collapse, cladding strain analysis, cladding stress analysis, fuel pin pressure analysis, linear heat rate capability, power spike model, and rod bow calculations.

With respect to creep collapse, the CROV computer code (Ref. 2) is said to be used to calculate ovality changes in the fuel rod cladding due to thermal and irradiation creep and is used to perform the fuel rod creep analysis when required. CROV predicts the conditions necessary for collapse and the resultant time to collapse. CROV is a reviewed and approved code, and its use for these purposes is acceptable. Among the inputs to the CROV code, however, are the internal pin pressures and cladding temperatures, which were stated to be calculated by TACO 2 (Ref. 3). TACO 2 is still under review and has not yet been approved. Thus, at the time of the submittal of the Oconee 3 Cycle 7 reload analysis, a reanalysis of the cladding creep-down and collapse may be

required, using an approved code such as TAFY 3 (Ref. 4)* or TACO (Ref. 5)** for input to CROV. To demonstrate acceptability, the maximum expected residence time of any fuel rod during the cycle should be less than the number of effective full power hours required for cladding collapse, as calculated by the approved codes. By letter dated June 16, 1981 (Ref. 1e) the licensee committed to use the approved TACO Code until the TACO2 Code is approved by the staff.

A generic strain analysis is said to have been completed by the fuel vendor, again using TACO 2. The same restrictions and requirements apply to its use in this application as those listed above for the cladding collapse calculation.

The cladding stress analysis is stated to be bounded by a design analysis that uses Section III of the ASME boiler and pressure vessel code as a guide in classifying the stresses into various categories, assigning appropriate limits to those categories, and combining those stresses to determine stress intensity. Although as stated in the report, reanalysis should not be required for standard mark B fuel assembly reloads (because the stress analysis "is very conservative"), each new fuel cycle design will be assessed in terms of cladding stress, taking into account such parameters as cladding O.D., I.D., and thickness, pellet diameter and

* TAFY-3 is acceptable provided peak rod exposures do not exceed 42 GWd/mtU.

** TACO is acceptable provided the approved version of the code is used (see reference 5).

density, and initial pre-pressure within the fuel rods. This is consistent with standard industry practice and is, therefore, acceptable. The limits for (a) fuel cladding stresses and (b) stress intensity value of the primary membrane stresses are also consistent with industry practice and are, therefore, acceptable for the same reason. Inasmuch as (a) the methods used to calculate and to combine worst case compressive loads with other loads and to analyse worst core tensile loads, as described in the technical report, are conservative, (b) the limits for cladding stresses and stress intensity are consistent with present industry practice, and (c) ovality bending stresses, flow induced vibration, and differential fuel rod growth stresses are also addressed, we conclude that the technical report provides an adequate description of cladding stress limits and methods of calculation and that the Duke reload methodology for cladding stresses is acceptable.

For the fuel pin pressure analysis, the report indicates that the same parameters as listed earlier for the cladding stress calculation are used, along with one additional parameter, pin power history versus burnup. The pin pressure analysis is said to be performed using TACO 2, which as noted earlier, is an unapproved code. Therefore, a reanalysis will be required using an approved code, if the Oconee 3 Cycle 7 reload analysis is submitted prior to approval of TACO 2. Similarly, the linear heat rate to melt (LHRTM) analysis may have to be redone because it was also performed with TACO 2.

As indicated in Section 4.8 of the technical report, the NRC rod bowing correlation is used by Duke Power in the reload design. We conclude, therefore, that the effect of rod bowing on DNBR will be appropriately accounted for up to the maximum burnup assumed in the technical report (33,000 MWd/t).

Based on our evaluation of the information provided in Technical Report NFS-1001 and in discussions held with representatives of Duke Power Company, we conclude that reasonable assurance has been provided that the Duke reload methodology is appropriately conservative with respect to the mechanical and thermal aspects of fuel performance in the reload design, and is, therefore, acceptable.

3.3 Thermal-Hydraulics Evaluation

The thermal-hydraulic analysis establishes the maximum permissible core power level and power distribution and the permissible combination of core outlet pressure and temperature to ensure that the minimum departure from nucleate boiling ratio (MDNBR) of 1.30 is not violated during steady-state operation or during anticipated transients. This criterion of 1.30 will prevent core damage for the types of operations mentioned above.

The DNBR is calculated using the Babcock and Wilcox Critical Heat Flux (CHF) correlation BAW-2. The minimum DNBR limit of 1.30 assures that there is a 95% probability at a 95% confidence of not experiencing DNB. However, the effects of rod bowing on DNBR must be accounted for in the form of a penalty applied to the MDNBR.

The rod bow penalty has an initial value of 11.2%. The staff has given a 1% credit due to a flow area reduction factor included in the thermal hydraulic analysis. Thus a penalty of 10.2% is applied to the MDNBR. This results in a MDNBR of 1.4326. This penalty is only applicable for burnups less than or equal to 33,000 MWD/MTU. If an increase in burnup is desired the applicant must submit a change to the Technical Specifications to provide for a modified rod bow penalty.

The methodology used in the steady-state analysis determines the maximum allowable pressure-temperature operating limits at 112% overpower and a set of generic DNBR curves. These curves show the allowable pressure-temperature matchups which ensure that the minimum DNBR is not violated.

The approach used in generating the curves is to determine the core mass flow rate and core inlet temperature for each operating condition. Once the core flow rate is known the core wide flow distribution is determined using the CHATA computer code. CHATA determines the assembly flow by varying this flow until each assembly has the same pressure drop and the total of the assembly flows equals the core flow. The core is modeled on an eighth-core symmetric basis and the primary output is the hot assembly flow.

The major input parameters used by CHATA are core flow effective for heat transfer, individual fuel assembly geometries, form loss coefficients, the radial peaking distribution, the 1.5 design cosine axial flux shape, and the core operating conditions.

The core flow rate is a limiting parameter in the thermal-hydraulic analysis. The Technical Specifications for the Oconee Units list the system flow rate for four pump operation as 374,880 GPM or 106.5% of the original design flow rate. This value is obtained from the lowest value of flow rate measurements and a downward adjustment of measurement uncertainty, and is acceptable. However,

reactor coolant flow reduction may occur in future cycles due to system degradation such as plugging of steam generation tubes. Therefore, the coolant flow rate listed in the Technical Specifications must be evaluated to ensure that it is the minimum acceptable flow rate needed to obtain adequate cooling. The core bypass flow is also cycle dependent. Its value depends on the number of orifice rods and burnable poison rod assemblies. A value of 8.10% is given as a typical value in this report.

The isothermal flow distribution is assumed to be relatively flat with a maximum deviation of 5% for 4 pump flow conditions. The hot assembly is assumed to receive only 95% of the total nominal assembly flow based on the assumption given above. Those values were approved in the design review of the Oconee Units (Ref. 7).

The flow maldistribution factors are considered by the use of an additional form loss coefficient located at the entrance of the hot assembly.

Once the hot assembly flow rate is known a hot assembly/hot channel analysis is performed. The hot assembly is that fuel assembly which has the highest radial peaking factors. This assembly is not an individual fuel assembly but is the intersection of four 1/4 assemblies.

The hot assembly flow rate, calculated in the CHATA analysis, is input into the TEMP code. The calculations performed by TEMP account for energy interchange between channels at each calculational increment. Mass interchange between subchannels is not included in this model. The minimum DNBR and hot channel flow rates are the outputs of importance from this analysis and are

used to establish the equivalent hot channel model discussed below. The minimum DNBR for 112% overpower analysis is the reference design DNBR. The output from this analysis is used as input in the hot channel analysis. The hot channel is that subchannel which has the highest single pin peaking factors.

The hot channel factors used in the hot assembly/hot channel analysis are listed in Table 1. A comparison of these hot channel factors and those used in the Cycle 5 and 6 Oconee Unit 3 reloads is included.

An equivalent two channel model is used for all subsequent parametric analyses. This model contains a hot channel (the results from the TEMP analysis) and an average channel. The CHATA code is used to model these two channels. The hot channel contains all the conservatisms used in TEMP. An engineering hot channel factor on enthalpy rise, $F\Delta h$, is applied in the CHATA analysis. This factor is used to match the CHATA hot channel with the TEMP hot channel. The $F\Delta h$ value is varied until the MDNBR calculated by CHATA equals the TEMP MDNBR. The average channel serves as a driver of the hot channel. This parametric analysis will be used to determine the pressure-temperature core protection safety limits and the generic DNBR curves.

The pressure-temperature safety limits are obtained by using the equivalent two channel model. For a given outlet pressure the inlet temperature is varied until the MDNBR of 1.4326 has been determined. Using a reactor vessel heat balance, the reactor vessel outlet temperature, for the given pressure and inlet temperature, is determined. This process is repeated for a series of different pressures, typically 1800, 1900, 2000, 2100, 2200, and 2300 psia.

The results of these calculations are the temperature-pressure points corresponding to the MDNBR of 1.4326. This analysis is performed for a combination of 4-, 3- and 2-pump cases. The most limiting type of operation is 4-pump operation. This is the same method used by Babcock & Wilcox.

The generic DNBR curves are used to determine the power-power imbalance limits based on the DNBR criterion. How the power-power imbalance limits are calculated is discussed in the SER for Section 7.2 "Technical Specifications." This report deals only with the method used to calculate the generic DNBR curves. For each series of axial peaking factors the parametric hot channel analysis uses axial power shapes which are a series of smooth curves whose peak can be specified at various distances up the channel. The Technical Report states that the power shapes used were smooth cosine curves. The licensee explained, during subsequent discussions, that the curves were derived from a polynomial without tails. The staff concludes that the use of these flux shapes in the thermal-hydraulic design is acceptable.

The power input of each channel is increased until the limiting DNBR is obtained. The maximum allowable total peak for a specified axial peak and its location are then determined. The final results of this analysis are two sets of generic DNBR curves or Maximum Allowable Peaking (MAP) curves. One generic DNB curve is used for DNB operational offset limits and the other is used for Reactor Protection System offset limits. Finally, the actual power shapes which yielded the lowest DNBR are input into the hot channel code to confirm the conservatism of the corresponding smoothed curves used in the development of the generic DNBR curves.

The thermal-hydraulic analysis used to determine the generic DNBR curves utilized two additional hot channel factors on local heat flux. A penalty of 1.026 was incurred to increase calculated axial powers since flux depression at the spacer grids is neglected and the ratio of the total nuclear uncertainty (1.075) to the radial nuclear uncertainty (1.05) resulted in a penalty of 1.024. These additional penalties increased the value of Fq'' from 1.014 to 1.065.

The reactor to flow setpoint is used to initiate a reactor trip. The trip ensures that the MDNBR of 1.4326 is not violated during loss of one or more pumps. The coastdown analysis assumes the loss of two pumps because it is possible that the loss of one coolant pump may not be detected by the reactor protection system, and therefore, the reactor will not immediately trip. Since a two pump coastdown is more conservative than the one pump coastdown, and for a loss of four pumps the reactor trips immediately; the two pump coastdown is the most limiting.

The RADAR code is used for the transient analysis to assure that the 1.4326 MDNBR is not violated during the transient. The initial conditions are the results from the steady-state thermal-hydraulic analysis. The power-flow setpoint is determined by varying the time of reactor trip following the loss of two RC pumps until the minimum ratio (Flux/flow) required to maintain the MDNBR of 1.4326 has been determined.

Our review of the thermal-hydraulic design of the Duke reload methodology included the CHF correlation, the computer codes used, the method of combining the codes, the peaking factors used, the method of determining pressure-temperature core protection safety limits and the method of generating the generic DNBR curves.

The staff has previously approved the BAW-2 CHF correlation (Ref. 16) and the TEMP computer code. The use of the BAW-2 CHF correlation in a subchannel analysis performed by CHATA is still under staff review. Also, the CHATA computer code is being reviewed by the staff. However, the CHATA code with the BAW-2 correlation has been used in the thermal-hydraulic design of Babcock & Wilcox reactors and found to be acceptable for preliminary design approval by the staff (Refs. 11 and 12). Based on these previous approvals and the current advanced status of our CHATA review, the staff concludes that the use of the BAW-2 correlation in a CHATA subchannel analysis and the use of CHATA are acceptable in this analysis. Any limitations resulting from our completion of the CHATA review will be compensated for by appropriate operating restrictions; however, none are anticipated.

The method of combining the CHATA core wide analysis and the TEMP hot assembly/hot channel analysis; the equivalent two channel analysis; and the initial conditions, from the TEMP steady-state analysis, for the RADAR transient analysis are acceptable based on our preliminary review of CHATA. Once again any limitations identified during completion of the CHATA review will be appropriate by compensated for by operating restrictions.

The values and use of the peaking factors, both local and total, can be easily verified in either the Oconee FSAR or approved B&W topical reports. Therefore, the staff concludes that their use in the Oconee Reload Methods is acceptable. The peaking factors F_q , F_q'' and F_A , and the design radial-local peaking factor, have all been approved by the staff in the Oconee Units SER (Ref. 21). The reactor flow of 106.5% and the bypass flow of 8.10% were approved in the Cycle 6 reload but can vary from reload to reload; therefore, the staff can not give a generic approval to these items.

In summary, the staff concludes that the methodology used by Duke is an acceptable means of performing the thermal-hydraulic analysis necessary for a reload with the limitations discussed above. If any of the parameters are changed such as the DNBR penalty for rod bow, the licensee should justify the use of these new numbers in their thermal-hydraulic analysis. If the DNBR penalty is changed, the licensee should insert into the basis of the technical specifications any generic or plant specific margin that has been used to offset the reduction in DNBR due to rod bow and identify the source and reference previous staff approval of each generic margin.

Table 1

Thermal-Hydraulic Design Comparisons

	Cycle 5 Unit 3	Cycle 6 Unit 3	Reload Methodology
Reactor Coolant Flow % Design	106.5	106.5	106.5
Core Bypass Flow % Total	10.4	8.10	8.10
Ref. Design radial-local power	1.71	1.71	1.71
Hot Channel Factors:			
Enthalpy Rise	1.011	1.011	1.011
Heat Flux	1.014	1.014	1.014
Flow Area	0.98	0.98	0.98
Min. DNBR w/o Densification Penalty	1.4326	1.4326	1.4326
CHF Correlation	BAW-2	BAW-2	BAW-2

The P-T limits are used to determine the core outlet pressure - vessel outlet temperature conditions which will ensure a MDNBR of 1.30 when other pertinent parameters are at their design limit (maximum or minimum). The design MDNBR of 1.4326 was calculated for 4-pump operation at 112% overpower. The SER for Section 6 tells how the DNBR-core outlet pressure - vessel outlet temperature curves are generated. These curves used a DNBR of 1.4326 as their parameter and were generated for 4-, 3- and 2-pump operation. These curves serve as the basis of the Tech. Spec. P-T limits.

Since the curves were generated for DNBR of 1.4326, the staff concludes that the method used to determine the Tech. Spec. P-T limits is conservative and therefore, acceptable.

The method used to determine the Power-Power Imbalance limits is to first perform a maneuvering analysis which generates the power distribution in the core for various design conditions and various times in the cycle. The calculated maximum total peaking factors of each assembly are increased by a radial uncertainty factor of 1.05, and a radial-local factor, and the resulting adjusted peak is compared to the allowable peaking factor for that axial peaking factor and axial peak location. The DNBR margin is then calculated for each assembly in the 1/4-core, and then the MDNBR margin in the core for each power distribution is determined.

Finally the axial offset limits that correspond to the acceptable DNBR margin are determined. The licensee stated that these limits "are determined in a manner similar to that used to establish the center fuel melt limited offset limits." The staff has reviewed this methodology and concludes that the methodology used to determine the power-power imbalance limits is acceptable for preliminary design considerations.

The RPS P-T trip setpoints are derived by error adjusting the P-T core safety limits generated in Section 7.2.1 and also considering the high RCS pressure, low RCS pressure, and high RCS outlet temperature setpoints.

First the high RCS pressure setpoint (2300 psig), the low RCS pressure setpoint (1800 psig) and the high RCS temperature setpoint (619 F) are identified on the Core Safety P-T Limit Curve. The locus of P-T points constrained by the high RCS pressure trip, low RCS pressure trip, and high RCS temperature is determined using the trip points and the P-T safety curve discussed in Section 6 and 7.2-1. The pressure-temperature points are adjusted to account for the difference between core pressure and the RCS pressure at the measurement location and for errors in measurements. The net error adjustment for pressure is 0 psi and the error-adjustment for Temperature is +1 F. The temperature adjustment accounts for the maximum temperature error in the instrumentation string. The pressure measurement error is +30 psia which is added to the difference between the hot leg and core outlet, $P = +30$ psi. Therefore, the net error-adjustment is 0 psi.

The staff has reviewed this method and compared it with the method used by Babcock and Wilcox. Based on our review and the fact that the Duke method is comparable to the Babcock and Wilcox method, the staff concludes that the Duke method is an acceptable method. However, Duke should supply adequate justification to show that the error-adjustments do not change for each reload.

The power-flow-imbalance trip setpoint is the value of reactor power at which a RPS trip should occur. The trip should occur whenever the combinations of power, flow and their uncertainties produce values of power and flow which result in the design MDNBR during a flow transient and whenever the combination of power, imbalance, and their uncertainties correspond to the core safety limits on power imbalance.

This setpoint is determined by first calculating the maximum power/flow or flux/flow ratio. This calculation is described in the SER on Section 6. The ratio is then reduced by an error adjustment factor. This factor accounts for noise in the RPS flow signal and other electronic errors in RPS flow instrumentation. Next, an error adjustment factor of 6.5% FP is used to adjust the power level limit and the imbalance limit. The 6.5% adjustment factor is comprised of a 4% FP allowance for neutron flux error, 2% FP allowance for the calorimetric error, and 0.5% FP allowance for any setpoint error. The error adjustment factor for imbalance is a function of the imbalance limit and power level limit and is used to account for the uncertainty in the measurement of axial imbalance by the out-of-core detector system.

Finally, a set of curves are produced which envelop the allowable operation. The curves are flux/flow setpoints for 4-, 3-, and 2-pump operation.

The staff has reviewed the method used to determine the Flux/Flow setpoint and compared it with the method used by Babcock and Wilcox. Based on our review and comparison the staff concludes that it is an acceptable method.

4.0 Conclusion

The staff has reviewed Technical Report NFS-1001, "Oconee Nuclear Station Reload Design Methodology", as revised through Revision 4 (References 1a, 1b, 1c, 1d and 1e) and has concluded, based on the considerations and approval of the individual issues discussed above, that the use of this methodology is an acceptable means of performing reload design calculations for future Oconee Nuclear Station Units 1, 2 and 3 reloads.

Dated: July 29, 1981

References

1. a) William O. Parker, Jr. (Duke Power Company) letter to H. R. Denton (NRC), April 23, 1979.
b) William O. Parker, Jr. letter to H. R. Denton, May 20, 1980.
c) William O. Parker, Jr. letter to H. R. Denton, January 28, 1981.
d) William O. Parker, Jr. letter to H. R. Denton, April 22, 1981.
e) William O. Parker, Jr. letter to H. R. Denton, June 16, 1981.
2. "Program to Determine In-Reactor Performance of B&W Fuels - Cladding Creep Collapse," Babcock and Wilcox report BAW-10084P, Rev. 1, October 1976.
3. Y. A. Hsii, et al, "TACO-2: Fuel Pin Performance Analyses," Babcock and Wilcox Company Report BAW-10141P, January 1979.
4. C. D. Morgan and H. S. Kao, "TAFY - Fuel Pin Temperature and Gas Pressure Analysis," Babcock and Wilcox Company Report BAW-10044, May 1972.
5. "TACO - Fuel Pin Performance Analysis," Babcock and Wilcox Company Report BAW-10087P-A, Rev. 2, August 1977.
6. "Rules for Construction of Nuclear Power Plant Components," ASME Boiler and Pressure Vessel Code, Section III, 1977.
7. Oconee Nuclear Station, Units 1, 2, and 3 Final Safety Analysis Report Docket Nos. 50-269, 50-270 and 50-287.
8. J. M. Alcorn, R. H. Wilson, "CHATA-Core Hydraulic and Thermal Analysis," BAW-10110, Rev. 1, May 1977.
9. C. D. Morgan, H. C. Cheatwood, and J. R. Gloudemans, "RADAR-Reactor Thermal and Hydraulic Analysis During Reactor Flow Coastdown," BAW-10069, July, 1973.
10. "TEMP-Thermal Enthalpy Mixing Program" BAW-10021, April, 1970.
11. D. F. Ross, Jr., (AD for Reactor Safety, DSS) to D. B. Vassallo, (AD for LWRs, DPM) Memorandum, "BSAR-205 SER Input," May 25, 1977.
12. D. F. Ross, Jr., (AD for Reactor Safety, DSS) to D. B. Vassallo, (AD for LWRs, DPM) Memorandum, "Midland 1 and 2 - Round 2 Questions," September 28, 1978.
13. Oconee Unit 3, Cycle 5 - Reload Report BAW-1522, Babcock & Wilcox, March, 1979.

14. Oconee Unit 3, Cycle 6 - Reload Report BAW-1634, Babcock & Wilcox, August, 1980.
15. L. S. Rubenstein (AD for Core and Containment Systems, DSI) to T. M. Novak, (AD for Operating Reactors, DL), Memorandum, "CPB Thermal-Hydraulic SE Input on Oconee, Unit 3, Reload Safety Analysis", Feb. 2, 1981.
16. D. F. Ross, Jr., (AD for Reactor Safety, DSS) to R. C. Young (Ad for LWRs), Memorandum, "Topical Report Evaluation - BAW-10000, Correlation of Critical Heat Flux in a Bundle Cooled by Pressurized Water", March 2, 1976.
17. Midland Plant, Units 1 and 2 Final Safety Analysis Report, Docket Nos. 50-329, 50-330.
18. D. F. Ross, Jr., (AD for Reactor Safety, DSS) to D. B. Vassallo (AD for LWRs, DPM), Memorandum, "Evaluation of the Effect of a Change in the Flow Maldistribution Factor on DNB for Babcock and Wilcox 205 Fuel Assembly Plants (Reissued)," May 23, 1978.
19. H. A. Hassan, et al., "Power Peaking Nuclear Uncertainty Factors," BAW-10119-P-A, February, 1979.
20. "Safety Evaluation Report of the Duke Power Company Oconee Nuclear Power Station Unit 1" Docket 50-269 U. S. Atomic Energy Commission, December 29, 1970.
21. "Safety Evaluation of the Oconee Nuclear Power Station Units 2 and 3" Docket 50-270; 50-287, U. S. Atomic Energy Commission, July 6, 1973.

Supplement 1

Supplement 1 - Deleted

Supplement 2

Supplement 2 - Deleted